Universität für Bodenkultur Wien
University of Natural Resources
and Life Sciences, Vienna

Doctoral Dissertation

Biogeographical dynamics of plant taxa and climate-landscape history of the Eurasian steppe belt: Genes documenting history

submitted by

Anna Seidl, MSc

in partial fulfilment of the requirements for the academic degree

Doktorin der Bodenkultur (Dr.nat.techn.)

Vienna, March 2022

Supervisor:

Univ.Prof. Dipl.Geograph Dr. Karl Georg Bernhardt
Institute of Botany

Affidavit

I hereby declare that I have authored this dissertation independently, and that I have not used any assistance other than that which is permitted. The work contained herein is my own except where explicitly stated otherwise. All ideas taken in wording or in basic content from unpublished sources or from published literature are duly identified and cited, and the precise references included. Any contribution from colleagues is explicitly stated in the authorship statement of the published papers.

I further declare that this dissertation has not been submitted, in whole or in part, in the same or a similar form, to any other educational institution as part of the requirements for an academic degree.

I hereby confirm that I am familiar with the standards of Scientific Integrity and with the guidelines of Good Scientific Practice, and that this work fully complies with these standards and guidelines.

City, date Anna SEIDL *(manu propria)*

Acknowledgement

The research presented in this doctoral dissertation was conducted within the framework of the project “Biogeographical dynamics of plant taxa and climate-landscape history of the Eurasian steppe belt: Genes documenting history”, funded by the Austrian Science Fund (project number: I 3002-B25). As a result of this work, two papers addressing the biogeography and history of *Kraschenninnikovia* have already been published. Another paper on *Adonis vernalis* is in preparation.

Zuerst möchte ich Karl Georg Bernhardt für die Möglichkeit danken, diese Arbeit anzufertigen. Auch Karin Tremetsberger gebührt mein herzlicher Dank für die intensive und engagierte Betreuung. Danke für Deine Geduld und Vertrauen. Auch dem ganzen Steppenteam und allen Kollegen im Feld möchte ich meinen Dank entsenden für zahlreiche Exkursionen, Aufsammlungen und rege Diskussionen. Besonders möchte ich hier Karl Georg Bernhardt, Nikolai Friesen, Alexander Ivanovich Shmakov, Polina V. Veselova, Herbert Hurka, Barbara Neuffer, Oyuntsetseg Batlai und Karin Tremetsberger für die Organisation und Durchführung von Exkursionen erwähnen, die den Grundstein für die Arbeit legten.

Herzlichen Dank auch an Alexandra Elbakyan.

Ich bin sehr dankbar meiner Familie und Nikolai, die mir den Rücken gestärkt und freigehalten haben, damit diese Arbeit auch ein Ende finden kann. Ein Dank auch an meine Schwester Elisabeth, der ich sagen möchte, dass es sicher auch wo anders ein Zitat für “mehr Bier” gibt und man nicht die große Schwester damit beauftragen muss, das extra in einer Veröffentlichung zu erwähnen. Ich freue mich unendlich darauf mit meinem Papa Wurzeln zu ziehen und Kulturen zum Blühen zu bringen.

Es war immer eine Freude, Wissenschaftliches und Privates mit meinen lieben Bürokolleginnen Julia und Inga zu teilen.

Danke an alle für diese wunderbare gemeinsame Zeit.

Table of content

Abstract

The aim of this work is to shed light on the evolutionary history of the Eurasian steppe belt using the genetic “fingerprints” of two different steppe plants. For this purpose, the relatively old species *Krascheninnikovia ceratoides*, which is widespread in large parts of the dry steppe of the Northern Hemisphere, and the younger steppe species *Adonis vernalis*, which has a smaller distribution area in the western part of the Eurasian steppe belt and prefers more humid steppe habitats, were chosen. We tried to obtain leaf samples from five individuals per population in our collections, covering the entire distribution range of the respective species. The DNA of the samples was extracted and sequenced. Sequences of individual gene segments were used to estimate the time frame of diversification within the species. Genotyping-by-sequencing, a technique in which 100 base pair long fragments are sequenced from random locations of the genome, was used to determine the geographic origin of the species and the relationships between populations. According to my results, *Krascheninnikovia*, like the first steppe habitats, originated in Central Asia and spread from there across the steppe. *Adonis vernalis*, on the other hand, originated in Europe and probably migrated from there in the already widespread steppe to the east, and within Europe. The repeated transgression of the Caspian Sea has left traces in the genetic information of the individuals of *Krascheninnikovia*: The results in this study suggest that the species survived east and west of the flooded area and that the individuals later came back into contact. While *Krascheninnikovia* seems to have benefited from the changing climate in the Pleistocene, *Adonis vernalis* probably lost large parts of its range. The evolution of the steppe is thus partly reflected in the genetic information of its inhabitants.

Kurzfassung

Das Ziel dieser Arbeit ist, die Entstehungs- und Entwicklungsgeschichte des Eurasischen Steppengürtels anhand des genetischen „Fingerprints“ von zwei unterschiedlichen Steppenpflanzen zu beleuchten. Dazu wurde zum einen die relativ alte Art *Krascheninnikovia ceratoides* gewählt, die in weiten Teilen der trockenen Steppe der nördlichen Halbkugel verbreitet ist und zum anderen die jüngere Steppenart *Adonis vernalis*, die ein kleineres Verbreitungsgebiet im westlichen Teil des Eurasischen Steppengürtels aufweist und feuchtere Steppenhabitate bevorzugt. Wir haben versucht, bei unseren Aufsammlungen Blattproben von fünf Individuen pro Population zu erhalten und dabei das gesamte Verbreitungsgebiet abzudecken. Die DNA der Proben wurde extrahiert und sequenziert. Mit Hilfe einzelner Genabschnitte wurde der Zeitrahmen der Diversifizierung innerhalb der Art abgeschätzt. Mit Hilfe von „Genotyping-by-sequencing”, einer Technik, bei der 100 Basenpaare lange Fragmente von zufälligen Orten des Genoms sequenziert werden, wurde der geographische Ursprung der Art und die Verwandtschaftsverhältnisse zwischen den Populationen ermittelt. Laut meinen Ergebnissen entstand *Krascheninnikovia* wie auch die ersten Steppenhabitate in Zentralasien und breitete sich von dort in der Steppe aus. *Adonis vernalis* hingegen entstand in Europa und migrierte von dort aus in der bereits verbreiteten Steppe unter anderem nach Osten und innerhalb Europas. Die wiederholte Transgression des Kaspischen Meeres hat Spuren in der genetischen Information der Individuen von *Krascheninnikovia* hinterlassen: Die Ergebnisse in dieser Arbeit lassen darauf schließen, dass die Art östlich und westlich des überschwemmten Gebiets überlebt hat und die Individuen später wieder in Kontakt gekommen sind. Während *Krascheninnikovia* anscheinend im Pleistozän vom wechselnden Klima profitiert hat, verlor *Adonis vernalis* wahrscheinlich große Teile seines Verbreitungsgebiets. Die Entwicklung der Steppe wird somit teilweise in der genetischen Information seiner Bewohner widergespiegelt.

1. Introduction

The natural vegetation of up to one third of Earth's terrestrial surface are grasslands and grass-dominated habitats (White, Murray and Rohweder, 2000; Blair and Briggs, 2014). Grasslands are heterogeneous and provide a habitat to various plants and animals, including humans. Not only are the open grasslands (savannas) of Africa thought to be home to the first *Homo* species (Reed, 1997; Groucutt *et al.*, 2015), but these biomes have also provided food through agricultural use and livestock rearing since the Neolithic (White, Murray and Rohweder, 2000). Grassland products such as food, fibre and fuel are used daily by all people today. However, due to sometimes massive direct and indirect anthropogenic impacts such as agricultural expansion and climate change, grasslands are now under threat, and protection and restoration would be necessary to keep the habitat as it was (Solomon *et al.*, 2007; B. Chen *et al.*, 2014; Li *et al.*, 2018; Ren and Zhou, 2018). Some of the most threatened ecosystems on Earth are temperate grasslands (Sala *et al.*, 2000; Hoekstra *et al.*, 2005). In the dry nemoral zone or temperate semi-arid region, the natural grassland is called steppe (Walter, 1968).

General abiotic features in this area are cold winters, hot summers, and an annual precipitation of 200-400 mm, most of which falls in summer (Hurka *et al.*, 2019; Pfadenhauer and Klötzli, 2020). The main steppe areas in the world are the Eurasian steppe, the North American prairies and the Pampa/Patagonian steppe in South America (Pfadenhauer and Klötzli, 2020). The Eurasian steppe belt is the largest steppe region in the world (Walter, 1968, 1974; Hurka *et al.*, 2019; Pfadenhauer and Klötzli, 2020)**.**

The Eurasian steppe belt extends in the northern hemisphere from the Amur (eastern China) to the Pannonian Basin (Hungary). Exclaves exist in Central Europe and in Northern Asia. At the Altai Mountains, the Eurasian steppe divides into a Mongolian Chinese and a Euro-Siberian part. Both parts differ in their floristic composition, climate, and edaphic factors. The Asian monsoon causes later precipitation in Mongolia and China than west of the Altai Mountains, which is an effective barrier to the low-pressure system and summer cyclones of Central Asia. Chernozem is common in the Euro-Siberian steppe, while it is rare in the Mongolian Chinese steppe (Hurka *et al.*, 2019).

As a contact zone between the two parts of the Eurasian steppe, the Altai Mountains are of particular interest. The Altai Mountains serve as a refuge for various species and provide a range of different habitats. During the Pleistocene, it may have hosted some temperate forest species, while today relicts of Pleistocene biota find a refuge there (Pavelková Řičánková, Robovský and Riegert, 2014; Hais *et al.*, 2015; Hurka *et al.*, 2019).

In general, steppes can be divided into three broad groups in a physiognomic approach: Forest and meadow steppes (also called long or tall grass steppes), short grass steppes and desert steppes. In the Eurasian steppe, the overall steppe types differ according to moisture and edaphic factors and can range from forest to desert formations along the precipitation gradient, from a meadow-like tallgrass steppe with tree or forest islands to shortgrass steppes, semi-deserts and desert formations. The transitions between types are fluid, and within the same climatic zone different types may occur due to differences in precipitation on southern or northern slopes, limited water availability due to soil properties, steep slopes and intensity of grazing or general land use (Smelansky and Tishkov, 2012; Erdős *et al.*, 2018; Hurka *et al.*, 2019).

The wettest steppe formation is the forest steppe, which usually occurs in the transition zone between (closed) forest and dry steppe, forming a macromosaic of meadow steppe and tree or forest islands (Walter and Breckle, 1986; Erdős *et al.*, 2018; Hurka *et al.*, 2019). It is found in Eastern Europe, Western Siberia, China and eastern North America (Werger and van Staalduinen, 2012; Hurka *et al.*, 2019;

Pfadenhauer and Klötzli, 2020). Forest steppes provide a diverse habitat and host a large variety of species (Erdős *et al.*, 2018).

The plants that occur in meadow steppes are hygrophytic or mesophytic and can reach heights of up to 1.5 m. Species richness, evenness, coverage, total biomass (especially above ground), and productivity are high (Smelansky and Tishkov, 2012). The first flowering plants of the year appear in April, such as *Adonis vernalis*, *Pulsatilla patens* and *Carex humilis*. In June, *Filipendula vulgaris*, *Hypochaeris maculata*, *Phlomoides tuberosa*, *Salvia pratensis* and C3 grasses such as *Stipa pennata*, *Calamagrostis epigejos*, *Bromus erectus*, *Dactylis glomerata* and *Koeleria macrantha* often dominate the overall picture. In August, most of the plants have dried up. The tall grass steppes of China in eastern and north-eastern Inner Mongolia consist of *Leymus chinensis* and various Asteraceae (like *Hypochaeris ciliata*, *Syneilesis aconitifolia*, *Ligularia*), Fabaceae (*Lathyrus quinquenervius*, *Trifolium lupinaster*, *Lespedeza*), Rubiaceae (*Galium verum*), Rosaceae (*Sanguisorba officinalis*), Ranunculaceae (*Thalictrum minus*, *Delphinium grandiflorum*) and tall geophytes (*Hemerocallis*, *Lilium*, *Veratrum*). In North America, tall grass prairies are found as a transition from oak-hickory forests and west of the forest steppe zone as a distinct formation. In the cold and dry north (Canada), C3 grasses such as *Elymus smithii*, *E. lanceolatus*, *Koeleria macrantha* and *Hesperostipa spartea* are dominant, while in the warmer and more humid south C4 grasses like *Andropogon gerardi*, *Panicum virgatum* and *Sorghastrum nutans* are dominant (Pfadenhauer and Klötzli, 2020).

The short grass steppe, also called true or dry steppe, has a coverage of 50 to 80 %, which is lower than in tall grass steppes and consists mostly of xero-mesophytic and xerophytic plants (Smelansky and Tishkov, 2012; Pfadenhauer and Klötzli, 2020). Short grass steppes are mainly used for livestock; they are usually unsustainable as arable land due to aridity, low soil fertility and widespread salinization (Smelansky and Tishkov, 2012). Clump grasses with xerophytic characteristics such as hairiness, well-developed cuticle and grey colouration of the plant parts dominate. Small hemicryptophytes, chamaephytes and geophytes may grow among the clump grasses. The plants can grow up to 1 m high. In Eurasia, mainly *Stipa* and *Festuca*, *Koeleria*, *Poa* and *Elymus* are present. In Eastern Europe and Western Siberia, various *Stipa* species are found together with *Festuca*. In the southern short grass steppes, *Artemisia* and *Cleistogenes* are characteristic, occurring mainly in desert steppes, as are some Chenopodioideae like *Kraschenninnikovia ceratoides*. In short grass steppes, many geophytes of the genera *Tulipa*, *Gagea*, *Ornithogalum* and *Iris* and therophytes occur. In Central Asia, short grass steppes are common in forest-steppe regions and south of them. Grasses such as *Agropyron cristatum*, *Festuca lenensis*, *Koeleria macrantha*, *Cleistogenes squarrosa* and *C. songorica* and *Stipa* are found here, but almost no geophytes or therophytes. In Eurasia, *Carex*, *Dontostemon*, *Goniolimon*, *Potentilla*, *Orostachys* and *Oxytropis* are common. In North America, the short grass prairies are restricted to the warm and arid southwestern region. *Bouteloua aristidoides*, *Bouteloua dactyloides*, *Aristida longiseta*, *Hilaria jamesii*, *Sporobolus cryptandrus*, *Elymus smithii*, *Koeleria macrantha*, *Hesperostipa comata* and *Artemisia frigida* are widespread here. The composition depends on the frequency of fires, the weather and the intensity of grazing. The transition between tall and short grass prairie is called mixed grass prairie, which contains two layers, tall grasses and short forbs and dwarf shrubs. In the Southern Hemisphere, there are short grass steppes with clump grasses, *Stipa*, *Bromus*, *Poa* and *Rytidosperma* taxa as well as geophytes and hemicryptophytes and dwarf shrubs (at steep slopes) (Pfadenhauer and Klötzli, 2020).

Desert steppes form the transition to semideserts and have an annual precipitation of less than 200 mm. Short grasses (10 to 20 cm) and dwarf shrubs and subshrubs dominate with a coverage of less than 50% (Smelansky and Tishkov, 2012; Pfadenhauer and Klötzli, 2020). Desert steppes are mostly used as pastures for seasonal grazing (Smelansky and Tishkov, 2012). In South Kazakhstan, these steppe formations consist of *Stipa orientalis*, *S. lessingiana*, *Psathyrostachys juncea*, *Artemisia* and therophytes such as *Erophila* and *Alyssum*, while in Central Asia *Stipa caucasica* and *S. tianschanica* dominate the formation. Short or annual taxa of *Artemisia* and of Chenopodiaceae as well as

Reaumuria songarica and dwarf shrubs of the genus *Caragana* are common (Pfadenhauer and Klötzli, 2020).

Other steppe types occur on a smaller scale, e.g. special mountain steppes such as the high mountain cryophytic cold steppe in the Altai Mountains, where mountain steppes and alpine tundra grasslands are in direct contact under extreme continental dry conditions (Smelansky and Tishkov, 2012).

1.1. Evolution of the steppe

After the first land plants appeared in the middle Cambrian to early Ordovician (Morris *et al.*, 2018), the carbon dioxide (CO_2) concentration in the atmosphere dropped rapidly (Lenton *et al.*, 2012). The globally warm and humid climate changed to a regionally cold and arid one. This may have been caused by the formation of the supercontinent Pangea, which had strong continentality in the inner regions and glaciers in the mountains of the Southern Hemisphere (Parrish, 1993; Pfadenhauer and Klötzli, 2020). First forests appeared. Thereafter, rising temperatures, drought and atmospheric CO_2 concentrations favoured the development of gymnosperms, which were better adapted to drought than ferns (Pfadenhauer and Klötzli, 2020). During the Jurassic, Pangea began to break up into Laurasia and Gondwana. The two continents were separated by the Tethys Ocean, which acted as a migration barrier and caused the flora of the two landmasses to develop differently (Hurka *et al.*, 2019). During the Cretaceous, Gondwana split into Africa and South America. The Indian subcontinent separated and collided with Asia during the Paleogene, leading to the uprise of the Tibetan plateau. Plate tectonic activity led to the destruction of the western Tethys in the late Eocene and the formation of Paratethys (Dietz and Holden, 1970; Hurka *et al.*, 2019). Laurasia split into two continents: North America and Eurasia (Dietz and Holden, 1970). Although the two landmasses separated about 120 Mya (million years ago), contact between the floras persisted into the Tertiary through land bridges such as Beringia, leading to floristic similarities (Tiffney, 1985; Pfadenhauer and Klötzli, 2020).

During the Cretaceous, CO_2 concentration and temperature increased, giving an advantage to the better adapted angiosperms (Barron *et al.*, 1995; Crane, Friis and Pedersen, 1995; Magallón and Castillo, 2009; Hay, 2017). It was not until the beginning of the Tertiary that angiosperms spread massively, colonising the world and pushing other species into niches (Crane, Friis and Pedersen, 1995; Pfadenhauer and Klötzli, 2020).

To understand the distribution of vegetation today, the last 65 Myr (million years; Cenozoic era, Paleogene, Neogene and Quaternary) are particularly important, during which mountains rose, dramatic cooling occurred, cumulating in the Pleistocene ice ages, Antarctica glaciated and the increasing influence of humans during the Holocene shaped the appearance of the landscape and vegetation. The era started with a warm climate caused by high CO_2 and methane levels (Beerling and Royer, 2011). Today's polar ice deserts and tundra had a nemoral to subtropical flora with trees such as *Betula*, *Juglans*, and *Taxodium* (Hamilton, 1968; Basinger, Greenwood and Sweda, 1994). Since the Eocene, almost continuous cooling set in. The concentration of CO_2 in the atmosphere also decreased (Liu *et al.*, 2009; Beerling and Royer, 2011; Zhou *et al.*, 2019). Steppe formation presumably began in the Paleogene/early Miocene in Central Asia (Hurka *et al.*, 2019 and literature cited therein) and spread westwards in the middle to upper Miocene. In the middle Eocene, east Central Asian steppe desert was inhabited by halophytic and xerophytic shrub vegetation, with broad leaved forest and other angiosperms being more common than Asteraceae, Poaceae and Chenopodioideae (Barbolini *et al.*, 2020).

Although grasses have been present in the dry and open habitats of Central Asia since at least the Eocene, widespread dispersal only occurred from the middle Miocene onwards, showing a gap between species diversification and ecological spread (Barbolini *et al.*, 2020).

In the early Miocene, most of the Eurasian continent was covered with forests, while Central Asia had a drier environment (Ivanov *et al.*, 2011). Aridity in Eurasia increased during the middle Miocene (Utescher *et al.*, 2007). As cooling continued and precipitation became more seasonal and continental, the landscape opened up and forests were replaced by woodlands and grasslands (Bredenkamp, Spada and Kazmierczak, 2002; Strömberg, 2011; Hurka *et al.*, 2019).

A continuous steppe belt was present in the Pliocene (Eronen *et al.*, 2009, 2010). The forest steppe was widespread in south-eastern Europe and western Siberia. In the arid region of Middle and Central Asia, there was a treeless steppe (Hurka *et al.*, 2019). Numerous cold-warm cycles occurred during the Pleistocene, as shown by oxygen isotope studies of marine sediments (Cohen and Gibbard, 2019). Significant glaciation of the Northern Hemispheric began at the start of the Pleistocene.

As a large amount of water was bound as ice during glaciations, the aridity of the overall climate increased. During the ice ages, the Northern Hemisphere had massive glaciers, with ice-free areas due to the lack of precipitation in central and eastern Siberia (Farmer and Cook, 2013). The Beringia street, also ice-free, was exposed as a result of lowered sea levels and formed a land bridge between Asia and North America, facilitating the migration of plants and animals (Elias and Brigham-Grette, 2013). The high mountains of the Northern Hemisphere were covered with ice (Farmer and Cook, 2013; Hurka *et al.*, 2019).

During the cool glacial periods, steppes spread at the expense of forests, while forests recolonised these areas during the warmer interglacial periods (Frenzel, 1968). The range of plants growing in steppe and semi-desert formations expanded and contracted accordingly (Tarasov *et al.*, 2000). Today's steppe exclaves are possibly relicts of a larger distribution area during the glacial periods.

These repeated contractions and expansions of forest or steppe formations have had serious consequences for the affected taxa: In Europe, arctic-alpine disjunction (Muster and Berendonk, 2006: *Pardosa saltuaria* (wolf spider); Schmitt and Hewitt, 2004: *Zygaena exulans* (moth); Stevanović *et al.*, 2009) has developed. Some taxa persisted as ice age steppe relicts (*Adonis vernalis*) or tundra relicts (*Kraschenninnikovia ceratoides*, *Betula nana*); profound fragmentation of the Tertiary flora occurred, with many species becoming extinct in Europe but not in barrier-free Central Asia and North America (Pfadenhauer and Klötzli, 2020). In North America and Eurasia, a mass extinction of megafauna occurred, possibly due to rapidly changing climate and vegetation, as well as human influence through hunting and disease. In Europe, remnants of the once more or less continuous *Artemisia*-Chenopodioideae cold steppe (tundra-steppe) belt (Frenzel, 1968; Hurka *et al.*, 2019) are now found in extrazonal exclaves as well as in artificial, man-made exclaves of steppe species (Hejcman *et al.*, 2013; Dengler *et al.*, 2014). It is hypothesized that some trees existed in Europe even during glacial phases (Willis, Rudner and Sümegi, 2000; Willis and Vanandel, 2004). Depending on the potential tree coverage, the dispersal of steppe species could have been limited. With only a few patches of trees, colonization of the European exclaves would have been possible through a stepwise migration. Such migration has been assumed, for example, for the steppe plant *Iris aphylla* L. in Europe (Wróblewska and Brzosko, 2006; Wróblewska, 2008). Alternatively, with denser tree cover and only few suitable habitats, exclaves could have been colonized by long-distance dispersal, as assumed for some southern European Pleistocene relict species (e.g., *Microcnemum coralloides* (Loscos & J.Pardo) Font Quer (Kadereit and Emre Yaprak, 2008)).

Some important landscape structures that might have affected the ability of steppe plants to migrate within their suitable habitat during the ice ages were permanent, such as the Altai Mountains in Russia and Mongolia, or the Khangai Mountains of central Mongolia (Caves Rugenstein *et al.*, 2014). On the other hand, transitory large bodies of water in the area south of the Ural Mountains, caused by the transgressions of the Caspian Sea during the ice ages, might have prevented the migration of steppe plants for a limited time only (Dolukhanov *et al.*, 2009; Tudryn *et al.*, 2013; Yanina *et al.*, 2018; Hurka *et al.*, 2019).

During the Holocene, the range of the steppes shifted again, caused by climate change and increased anthropogenic influence: anthropogenic meadows emerged (Feurdean *et al.*, 2015), agriculture and migration changed the species composition of the formations. Human influence destroyed parts of the steppe, e.g., through agriculture, and led to secondary steppes, e.g., through deforestation, possibly resulting in a subdivision and expansion of the steppe belt. Often, natural steppe biomes are only preserved in nature reserves, on steep or inaccessible slopes, on the edge of fields and next to roads (Tomescu, 2000; Wick, Lemcke and Sturm, 2003; Magyari *et al.*, 2010; Novenko *et al.*, 2016; Cheng *et al.*, 2020).

As the largest steppe region in the world (Walter, 1968, 1974; Hurka *et al.*, 2019; Pfadenhauer and Klötzli, 2020) with diverse habitats, the Eurasian steppe belt represents an interesting and ecologically important study area that has experienced a number of range shifts and been affected by climate change.

To study and trace the history of the Eurasian steppe belt, one can investigate its inhabitants. For species that were affected by the repeated range shifts of their habitat, effects should be detectable at the genomic level. In order to study and compare different aspects of steppe history, two species with different histories and habitats were selected: on the one hand, a relatively young thermophilic study species with a preference for meadow steppes, *Adonis vernalis*, and on the other hand, an older eurythermal species found in dry steppes and semi-deserts, *Krascheninnikovia ceratoides*.

1.2. Krascheninnikovia

The goosefoot genus *Krascheninnikovia* Gueldenst. (Chenopodioideae) is represented by a single species, *Krascheninnikovia ceratoides* (L.) Gueldenst., which inhabits shortgrass steppes, desert steppes and semi-deserts of the Holarctic temperate region with extensions into the subtropical region throughout the Northern Hemisphere (Heklau and Röser, 2008; Heklau and von Wehrden, 2011; Pfadenhauer and Klötzli, 2020). The main distribution of *K. ceratoides* subsp. *ceratoides* largely corresponds to the Irano-Turanian floristic region (Takhtajan, 1986), but its entire range extends far beyond. It is broad, extending in Asia from Mongolia and northern China in the east to the southern Volga and Don regions (European Russia) in the west (Figure 1A). To the south, it extends to the Himalayas and Iran. West of this continuous distribution, there are small and isolated exclaves in Anatolia (Turkey), Europe (Austria, Romania, Spain, and Ukraine) and North Africa (Egypt and Morocco). *Krascheninnikovia ceratoides* subsp. *lanata* occurs in shortgrass prairies, dry scrublands and semi-deserts in central and western Canada, the USA and Mexico (Heklau and von Wehrden, 2011). The distribution of the species reflects the extent of dry grassland regions.

Central Asia has been considered the centre of diversification of *Krascheninnikovia* due to (1) the elevated number of populations and the abundance of individuals (Braun-Blanquet and Bolòs, 1957), (2) the high and variable degree of ploidy, with di-, tetra-, and hexaploid individuals occurring in the same population (Rubtsov *et al.*, 1989); in contrast to the exclusively tetraploid Western European populations or the diploid and tetraploid North American populations (Castroviejo and Soriano, 1990; Sainz Ollero, Múgica and Arias Torcal, 1996; Domínguez *et al.*, 2001; eFloras, 2008), and (3) the high morphological variation of the Central Asian populations, which in several cases has led to errors in the identification and description of new species, resulting in a complicated taxonomy and a large number of synonyms of *K. ceratoides* (Rechinger, 1963; Komarov, 1964; Täckholm, 1974; Welsh *et al.*, 1987; Davis, 1988; Castroviejo and Soriano, 1990; Tutin *et al.*, 1993; Heklau, 2006; eFloras, 2008). Heklau et al. (2008) analysed almost the entire range of putative *Krascheninnikovia* species based on genetic and morphologic differences, which did not segregate into separate linages, but remained unresolved as a polytomy (*K. arborescens*, *K. eversmanniana*, *K. lenensis* and *K. lanata*). Today, *Krascheninnikovia* is thought to constitute a single species with two subspecies, the Eurasian

K. ceratoides subsp. *ceratoides* and the North American *K. ceratoides* subsp. *lanata* (Pursh) Heklau (Heklau and Röser, 2008).

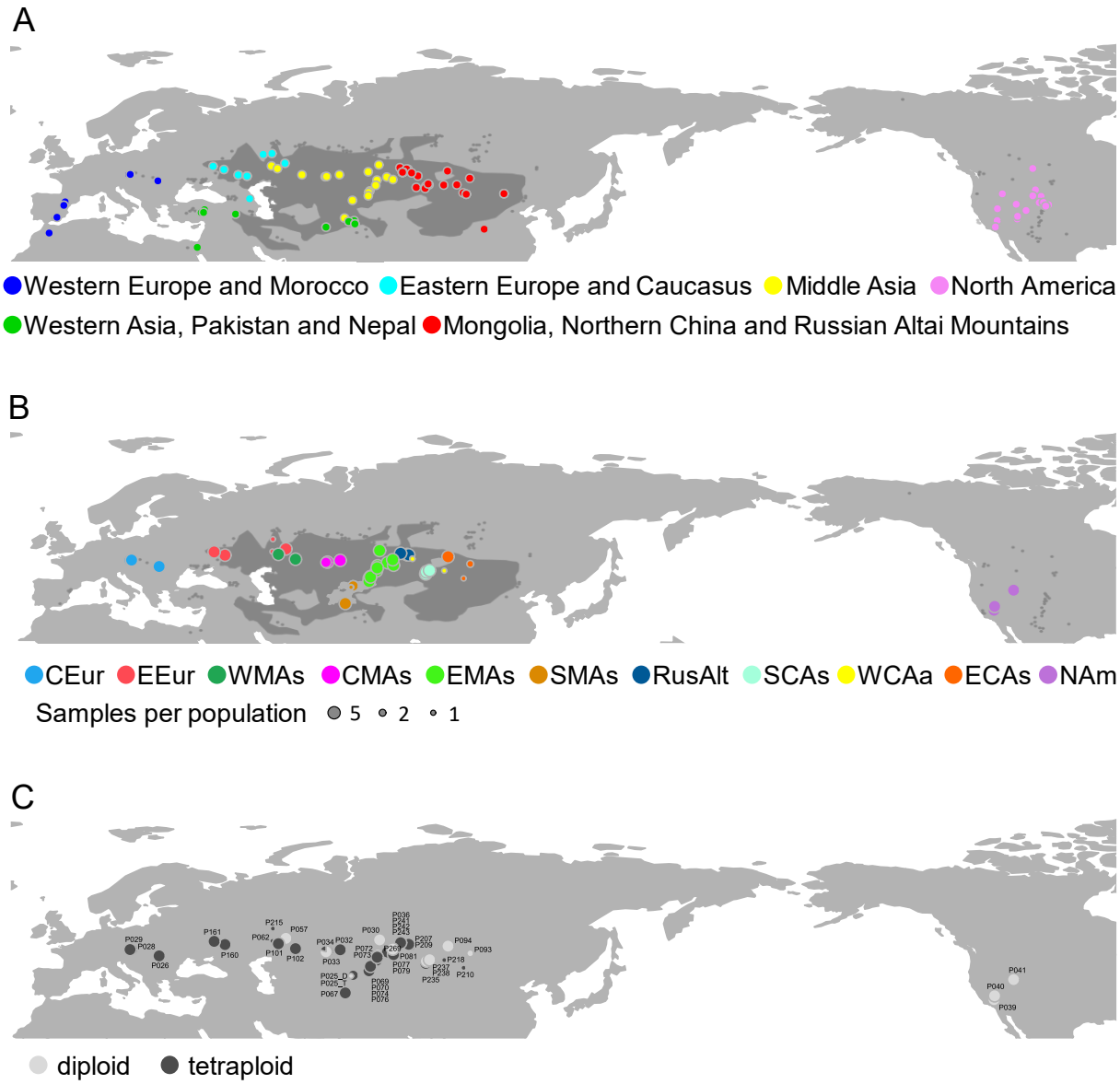

Figure 1: Distribution map and population sampling of *Krascheninnikovia ceratoides*. Up to five individuals per population were used, as indicated by dot size in B and C. A) Single locus sampling. The colour coding indicates the assigned geographical region of the population following Brummitt (2001). B) Genotyping-by-sequencing (GBS) sampling. The colour coding indicates the assigned geographical region of the population following Brummitt (2001) (CEur = Central Europe; EEur = Eastern Europe; WMAs = West Middle Asia; CMAs = Central Middle Asia; EMAs = East Middle Asia; SMAs = South Middle Asia; RusAlt = Russian Altai; SCAs = South Central Asia; WCAs = Western Central Asia; ECAs = East Central Asia; NAm = Northern America). C) The ploidy is indicated by colour: diploid (grey) and tetraploid (black).

Krascheninnikovia ceratoides subsp. *ceratoides* comprises (former) *Krascheninnikovia arborescens* (Losinsk.) Czerep. (Inner Mongolia to North China: Gansu, Jilin, Liaoning, Sichuan), *K. ceratoides* (L.) Gueldenst. (Far East, north-eastern Egypt, Spain), *K. compacta* (Losinsk.) Grubov (China: Gansu, Qinghai, Xinjiang), *K. eversmanniana* (Stschegl. ex Borshch.) Grubov (Kazakhstan, Mongolia, China: Xinjiang), *K. intramongolica* (H.C.Fu, J.Y.Yang & S.Y.Zhao) Z.Y.Zhu, C.Z.Liang & W.Wang (Inner Mongolia), *K. latens* J.F.Gmel., *K. lenensis* (Kuminova) Tzvelev (west and east Siberia), *K. longipilosa* (C.P.Tsien & C.G.Ma) G.L.Chu, *K. pungens* (Popov) Czerep. (Afghanistan, Uzbekistan). In Russian, the

common name of *Krascheninnikovia* is 'Teresken', as a general name for all species and subspecies of the genus *Krascheninnikovia*.

The putative species *K. compacta*, *K. longipilosa* (or *K. compacta* subspecies *longipilosa*), *K. ceratoides*, *K. eversmanniana* and *K. arborescens* have been distinguished on the basis of floral tube, leaf shape and general growth form, with the size ranges of the attributes mostly in the range of those of *K. ceratoides* (eFloras, 2008). As reviewed in Heklau and Röser (2008), Grubov (1999) has recognized only three species for Central Asia: *K. compacta* (prostate growth), *K. eversmanniana* (round or weakly cordate leaf base and short unfused part of the bracteoles of the female flowers) and *K. ceratoides* (cuneate or narrowed leaf base and the unfused part of the bracteoles longer than in *K. eversmanniana*), while *K. arborescens* was considered a synonym of *K. ceratoides*. Aktaeva (1973) also reduced *K. eversmanniana* to a synonym of *K. ceratoides*.

Former *K. lanata* (Pursh) A.Meeuse & A.Smit is distributed in western North America. Although the leaves are comparatively narrow and long with stellate leaf hairs, the flower and inflorescence characteristics are not consistently different from the Eurasian species *K. ceratoides*. Therefore, *K. lanata* has been proposed to be a subspecies of *K. ceratoides* (Heklau and Röser, 2008).

The classification of *Krascheninnikovia* changed frequently, resulting in a variety of scientific names. Former names of *K. ceratoides* subsp. *ceratoides* are *Achyranthes papposa*, *Axyris ceratoides*, *Blitum arborescens*, *Ceratoides arborescens*, *Ceratoides compacta*, *Ceratoides compacta* var. *longipilosa*, *Ceratoides eversmanniana*, *Ceratoides intramongolica*, *Ceratoides latens*, *Ceratoides lenensis*, *Ceratoides orientalis*, *Ceratoides papposa*, *Ceratoides pungens*, *Ceratospermum papposum*, *Diotis ceratoides*, *Diotis ferruginea*, *Eurotia arborescens*, *Eurotia ceratoides*, *Eurotia compacta*, *Eurotia eversmanniana*, *Eurotia ferruginea*, *Eurotia lanata*, *Eurotia lenensis*, *Eurotia prostrata*, *Eurotia pungens*, *Krascheninnikovia arborescens*, *Krascheninnikovia compacta*, *Krascheninnikovia compacta* var. *longipilosa*, *Krascheninnikovia eversmanniana*, *Krascheninnikovia intramongolica*, *Krascheninnikovia latens*, *Krascheninnikovia lenensis*, *Krascheninnikovia longipilosa*, *Krascheninnikovia pungens*, *Saltia papposa* (Imperatorskaia akademiia nauk, 1771; IPNI, 2020).

Within the Chenopodioideae, the genera *Krascheninnikovia*, *Axyris* and *Ceratocarpus* form the group of Axyrideae. The stellate hairs probably once originated within the Amaranthaceae, in the common ancestor of *Ceratocarpus*, *Axyris* and *Krascheninnikovia* (Heklau and Röser, 2008). The Asian genus *Axyris* comprises six annual species (Suchorukow, 2005): in northern and north-western Central Asia, *Axyris amaranthoides* L., *A. hybrida* L., *A. prostrata* L. and *A. sphaerosperma* Fisch. & C.A.Mey. are common, while in Korea *A. koreana* Nakai (Nakai, 1939) and in the central Caucasus *A. caucasica* (Sommier & Levier) Lipsky (Sommier & Levier, 1894; Il'in, 1936) are found. The Eurasian genus *Ceratocarpus* consists of two annual species, *C. arenarius* L. (south-eastern Europe to Central Asia) and *C. utriculosus* Bluket (Caucasus Mountains to Middle and Central Asia) (Il'in, 1936; Tzvelev, 1996; Grubov, 1999).

Krascheninnikovia ceratoides is a long-lived xeromorphic shrub with a growth height of 0.1 to 2 m, depending on the habitat (Walter and Breckle, 1986). Plants of *K. ceratoides* can reach an age of about 300 years (Steshenko, 1956), with the time of first reproduction being about 25 years (Zalenski and Steshenko, 1957). The plants appear to be grey in colour due to their dense cover of dendroid stellate hairs and simple, unbranched hairs. The flat leaf blades are linear to narrowly lanceolate to ovate, with entire margins, and truncate, cuneate, rounded, or subcordate at the base. The flowers are unisexual, the plants can be monoecious or dioecious. The male flowers form an interrupted spike or a subcapitate inflorescence with glomeruled, ebracteate flowers. These consist of four basally connate perianth segments, which are ovate or elliptic, membranous and abaxially hairy; and four stamens with oblong anthers and linear, exserted filaments. The female flowers are sitting single or paired axillary, enclosed by two hairy bracteoles, that are connate in the lower part, compressed to slightly keeled, with four hornlike tips; a perianth is absent, the female flowers consist only of an ovary with a short style and two elongated stigmas (eFloras, 2008; Heklau and Röser, 2008).

The bractlets surrounding the ovate and compressed fruit and the utricle are densely covered with long hairs, which may facilitate wind dispersal. *Krascheninnikovia ceratoides* is thought to outcross (Barnes, 2009). This eurythermal species tolerates a wide range of hot and cold temperatures and altitudes: it grows at sea level (e.g., in the lowlands of Kazakhstan) and at altitudes of 4,500–4,800 m in the southern part of its range, such as in the Pamir and Ladakh mountain ranges (Walter and Breckle, 1986; Hartmann, 1997).

Chromosomal variations exist in *K. ceratoides* throughout its range. Diploids with $2n = 18$ chromosomes have been reported from the Ural Mountains in western Russia through Kazakhstan and Kyrgyzstan to Mongolia and China (Zakharjeva and Soskov, 1981; Kurban, 1984; Rubtsov *et al.*, 1989; Yan *et al.*, 1989; Yang *et al.*, 1996; Seidl *et al.*, 2020, 2021). Tetra- and/or hexaploids ($2n = 36$ and 54) have been reported from Kazakhstan (Zakirova, 1999), the Russian Altai Mountains (Lomonosova and Krasnikov, 1993), Tajikistan (Zakharjeva and Soskov, 1981), China (Kurban, 1984; Yan et al., 1989; Yang et al., 1996), Kyrgyzstan (Rubtsov et al., 1989), Armenia (Takhtajan, 1990) and Iran (Ghaffari et al., 2014). A mixed population of di-, tri-, tetra-, penta- and hexaploids ($2n = 18$, 27, 36, 45 and 54) has been reported from Kyrgyzstan (Rubtsov et al., 1989). Central European and Mediterranean populations have been found to be tetraploid (Austria: (Dobeš, Hahn and Morawetz, 1997); Spain: (Castroviejo and Soriano, 1990); (Sainz Ollero, Múgica and Arias Torcal, 1996; Domínguez *et al.*, 2001)). In North America, diploid and tetraploid populations have been found (eFloras, 2008).

In Asia, the plant is used as firewood and fodder. Its overuse led to dwindling populations and consequently soil degradation. This phenomenon has been termed *Teresken syndrome* after the common name for *Krascheninnikovia* in Russian: Teresken (Kraudzun, Vanselow and Samimi, 2014; Vanselow and Samimi, 2014). In North America, it is used as fodder for livestock in winter ('winterfat') (Smoliak and Bezeau, 1967; Waldron *et al.*, 2010).

The disjunct distribution pattern of *K. ceratoides* subsp. *ceratoides* has long intrigued researchers (Willkomm and Lange, 1870; Braun-Blanquet and Bolòs, 1957; Costa Tenorio, Morla-Juaristi and Sáinz-Ollero, 2000). It was hypothesized that *K. ceratoides* subsp. *ceratoides* may have spread from Asia to Europe by a pre-Quaternary (Miocene or Pliocene) stepping-stone migration (de Bolòs, 1951; Braun-Blanquet and Bolòs, 1957; Sainz Ollero, Múgica and Arias Torcal, 1996; Costa Tenorio, Morla-Juaristi and Sáinz-Ollero, 2000). The disjunct populations could also be the result of recent migration and/or long-distance dispersal during the Pleistocene, as has been proposed for vicariant distributions in other plants and animals (e.g., insects, (Ribera and Blasco-Zumeta, 1998); *Microcnemum coralloides*, (Kadereit and Emre Yaprak, 2008); *Smilax aspera*, (C. Chen et al., 2014); *Cheirolophus*, (Vitales et al., 2014)). This hypothesis is also supported by recent phylogeographic studies, which suggest that some southern European plants previously thought to be 'Tertiary' relicts may in fact be the result of recent (Quaternary) dispersal and speciation events (e.g., *Microcnemum coralloides*, (Kadereit and Emre Yaprak, 2008); *Krascheninnikovia ceratoides* in Spain, (Perez-Collazos and Catalan, 2007); *Ferula loscosii*, (Pérez-Collazos et al., 2009); Ruppiaceae, (Triest and Sierens, 2014)). A more recent introduction of the plant by humans as fuel and fodder would also be a possible explanation (Willkomm and Lange, 1870; Costa Tenorio, Morla-Juaristi and Sáinz-Ollero, 2000). Colonisation of North America by *K. ceratoides* from Asia via the Bering Strait has also been proposed (Heklau and Röser, 2008), but this hypothesis has not yet been tested by biogeographical analysis.

In *Krascheninnikovia*, inter-simple sequence repeat (ISSR) population genetic assays have been used to investigate genetic structure and diversity of Iberian and Chinese populations and guide the conservation of those threatened and scarce populations (Perez-Collazos and Catalan, 2007; Wang et al., 2015). Internal transcribed spacer (ITS) data has been used to support taxonomic studies of the genus (Heklau and Röser, 2008). Based on ITS, rbcL and atpB-rbcL spacer, the phylogeny of the Chenopodioideae was calculated with a focus on Atripliceae (Kadereit et al., 2010).

Due to its distribution and age, *Krascheninnikovia ceratoides* (L.) Gueldenst. (Chenopodioideae) is a particularly suitable object to shed light on the formation of dry steppes and semi-deserts.

1.3. *Adonis vernalis*

Adonis vernalis is a member of the family Ranunculaceae. The most recent common ancestor of *A. vernalis* and its next relative, *A. villosa*, originated in Asia (Lindhuber, 2020). *Adonis vernalis* and *A. volgensis* differentiated about 2.66 Mya at the border between Neogene and Quaternary (Lindhuber, 2020). In contrast to *Krascheninnikovia ceratoides*, *A. vernalis* is only distributed in the Euro-Siberian part of the Eurasian steppe belt and prefers rather mesic habitats. *Adonis vernalis* occurs in western Asia, southern Siberia and the Pontic-Pannonian region, with scattered occurrences in Europe (Meusel *et al.*, 1978) (Figure 2). The thermophilic species grows in a wide array of habitats, including open forests, forest-steppe, mesic steppe, forest clearings and dry meadows, mostly on calcareous soil (Poluyanova and Lyubarskii, 2008). It grows in colline to montane altitudes, ranging from sea level (e.g. in Romania) to 1,600 m (in Spain).

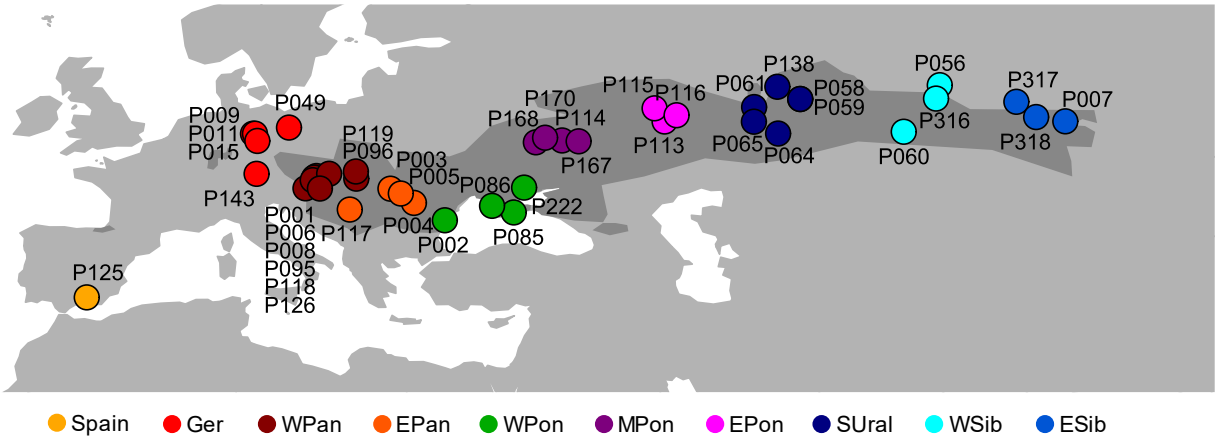

Figure 2: Distribution map and population sampling of *Adonis vernalis*. The distribution area is marked in grey. Up to five individuals per population were used. The colour coding indicates the assigned geographical region of the population following Brummitt (2001) (Spain; Ger = Germany; WPan = Western Pannonian; EPan = Eastern Pannonian; WPon = Western Pontic; MPon = Middle Pontic; EPon = Eastern Pontic; Sural = Southern Ural; WSib = Western Siberia; ESib = Eastern Siberia).

The perennial herbaceous plant is hemicryptophytic, usually unbranched and reaches a height of 10 to 40 cm. The leaves are pinnatisect and their position at the stem alter. *Adonis vernalis* flowers early in the year, from April to June, with showy yellow flowers. The apical flower has a diameter of four to eight centimetres. The numerous carpels develop into nutlets after pollination, which sit densely at the receptacle. Ripe, dry fruits fall out of the receptacle (barochory). The nutritious elaiosomes of the nutlets attract ants, which then disperse the seeds (myrmecochory) (Fokuhl, 2008). Pollination is mainly carried out by insects such as dipterans, coleopterans, heteropterans and hymenopterans (Denisow, Wrzesien and Cwener, 2014).

The pronounced rhizome, which can be up to 1 m deep in the soil, functions as storage organ from which shoots are formed during growth. This vegetative propagation usually leads to the characteristic patches of clones (Gostin, 2011; Denisow, Wrzesien and Cwener, 2014). *Adonis vernalis* is diploid with 16 chromosomes (Bara, Rugina and Bara, 2003). Because of its striking yellow flowers, it is sometimes used as an ornamental plant in the garden. The poisonous plant has also been used as a medicine against heart diseases due to its content of cardiac glycosides (Büchner *et al.*, 1965; Sokolova, Lovkova and Buzuk, 2007), but due to its complicated dosage, its use is discouraged today.

Synonyms of *Adonis vernalis* are *Adonanthe vernalis* (L.) Spach, *Adoniastrum vernale* (L.) Schur, *Adonis davurica* Ledeb. ex Rchb., *A. helleborus* Crantz, *A. parviflora* Janka ex Nyman, *A. pratensis* Ledeb., *Anemone consiligo* Baill. and *Chrysocyathus vernalis* (L.) Holub (IPNI, 2020). *Adonis volgensis* Steven ex DC. (or *A. wolgensis* Steven, synonyms *A. marschalliana* Andrz. ex Besser, *A. ruthenica* Stapf, *Chrysocyathus volgensis* (Steven) Holub, *A. apennina* Pall., *Adonanthe volgensis* Chrtek & Slavíková) is

a close relative of *A. vernalis*. A potential hybridization between both species is hypothesised. There are herbarium vouchers described as hybrids as well (Metlesics, 1969).

While the biogeographical history of *Kraschenninnikovia ceratoides* has not been studied so far, *A. vernalis* has been a repeated object of study. Both Hirsch et al. (2015) and Kropf et al. (2020) used amplified fragment length polymorphisms (AFLPs) to investigate hypotheses of peripherality utilizing *Adonis vernalis*. Kropf et al. (2020) investigated populations from Germany to Romania, while Hirsch et al. additionally sampled Spanish, Ukrainian and Siberian populations up to the Urals. The Spanish populations were genetically distinct to all other populations and may have been separated from the other populations since the early Holocene, as suggested by Hirsch et al. (2015). Within populations from Germany to Romania or Siberia, both studies found an east-west separation along their transects mediated by isolation by distance. Kropf et al. (2020) point out that the populations in the Romanian study area are large, stable and have existed for a long time. The colonization of Central Europe was assumed to be postglacial, with *A. vernalis* migrating to Germany in one wave from the Pannonian region. This was also confirmed by the almost complete absence of private loci in Hirsch et al. (2015). In Germany, *A. vernalis* probably faced severe habitat loss, possibly due to anthropogenic impacts. In Hirsch et al. (2015) the highest expected heterozygosity (H_E) was found in populations from Romania and Ukraine, but the fitted curve rather indicated Russia as the area with highest H_E. The same result was found for the proportion of polymorphic bands (Hirsch *et al.*, 2015; Kropf *et al.*, 2020).

1.4. Aim of the study

In recent years, steppe plants and their common history with the Eurasian steppe belt have been brought into the focus of research (Franzke *et al.*, 2004; Hurka *et al.*, 2012; Friesen *et al.*, 2015; Seregin, Anačkov and Friesen, 2015; Volkova, Herden and Friesen, 2017; Žerdoner Čalasan *et al.*, 2019; Friesen, Smirnov, *et al.*, 2020; Friesen, Zerdoner Calasan, *et al.*, 2020; Kirschner *et al.*, 2020). Steppe taxa with different habitat requirements, different species age, different origin and different distribution areas may have been affected by habitat shifting in various ways, which may reflect different aspects and times in steppe history. To get a picture of the entire steppe history, it is therefore important to study different steppe taxa.

As part of the project “Biogeographical dynamics of plant taxa and climate-landscape history of the Eurasian steppe belt: Genes documenting history”, I analysed *Kraschenninnikovia ceratoides* and *Adonis vernalis*. The subjects of interest were the genetic relationship within the species, ploidy level, place of origin and possible refugia during unfavourable conditions. With these results I want to explore the history of the Eurasian steppe belt. As the two species are of different ages, they may have undergone disparate evolutionary scenarios that could shed light on distinct aspects of the steppe evolution.

By analysing the DNA of our target species using genotyping-by-sequencing (GBS) and single gene sequencing, I want to answer the following questions and test the following hypotheses:

Since the steppe developed first in Central Asia and then in Europe, (old) steppe plants with a Eurasian-wide distribution pattern like *Kraschenninnikovia* should have originated in Central Asia as well, followed by an expansion of the distribution area to the west. Younger species like *Adonis vernalis* may have spread within the Eurasian steppe belt from west to east. Is this distribution range expansion reflected in our molecular data?

As the steppe area shifted repeatedly during the Pleistocene, the resident animal and plant species either had to endure or adapt to new conditions, persevere in refugia, or migrate with the steppe in order to survive. The response to these extreme abiotic factors may have affected the contact between populations and shaped the gene pool of future generations. Did Pleistocene macro cycles have a major influence on the genetic structure of the taxa?

The steppe formation may have occurred independently at different locations and time points resulting in the colonisation of habitats from different source populations. Can we use the results of our genetic analyses to identify regions that were colonized by different source populations?

2. Material and Methods

2.1. Material

Leaf material from individuals of *Krascheninnikovia ceratoides* and *Adonis vernalis* as well as from close relatives of the studied species was collected in the distribution area of the studied species in the Eurasian steppe belt during field trips of our project group and collaborators and dried on silica gel. For each population we aimed to collect one voucher and at least five leaf samples with a few meters distance between each other to avoid the collection of ramets. I completed our sampling with leaf samples of specimens from various herbaria (Figures 1 and 2).

The sampling P025 is composed of Kyrgyz individuals of *Krascheninnikovia*, sampled at two different locations about 80 km apart. Three North American populations determined as *K. ceratoides* subsp. *lanata* (P039, P040, P041) and two eastern Middle Asian populations of *K. ceratoides* subsp. *ceratoides* originally determined as *K. eversmanniana* (P069, P070) were included. Specimens of the genera *Axyris* (*A. hybrida*) and *Ceratocarpus* (*C. arenarius*) were collected as closest relatives of *Krascheninnikovia ceratoides* (Table 1). For *A. vernalis,* individuals of the taxa *A. volgensis* and *A. turkestanica* were collected as outgroups (Table 2).

If possible, one specimen per population was collected and included in the herbarium of the Institute of Botany of the University of Natural Resources and Life Sciences, Vienna (WHB). If collected by collaborators, the specimens were usually kept in the herbaria of the respective institutions and doublets were handed over to the WHB. The herbaria where the specimens can be found are given in Table 1 and Table 2.

For phylogenetic and dating analyses of individual gene data, as performed for *Krascheninnikovia*, I included additional sequences from the National Center for Biotechnology Information (NCBI) GenBank to cover a broader range of close relatives of the target species.

Table 1: Localities and codes of the populations of *Kraschenninnikovia ceratoides* and outgroups studied. The populations are grouped according to geographic-genetic groups as defined for single locus analyses. The DNA of some individuals was extracted from herbarium material; therefore, the ploidy could not be measured. The code of populations used for GBS are written in bold. FC, measured by flow cytometry; S, ploidy inferred by software nQuire and/or ploidyNGS; N, sample size for single locus analyses/**GBS**; D, diploid; T, tetraploid. Acronyms of Herbaria and Research Institutes that provided *K. ceratoides* samples: GUFEF (Gazi Üniversitesi Fen Edebiyat Fakültesi, Ankara, Turkey); HUJ (The Hebrew University of Jerusalem, Jerusalem, Israel); KBIH (Komarov Botanical Institute Herbarium, St. Petersburg, Russia); KW (M.G. Kholodny Institute of Botany, National Academy of Sciences of Ukraine, Kiev, Ukraine); NHML (Natural History Museum Herbaria, London, UK); NHMO (Natural History Museum Herbaria. Oslo, Norway); OSBU (Herbarium of the Botanical Institute, Osnabrück, Germany); RMRS (USDA-FS, Rocky Mountain Research Station, Provo, USA); SPARC (Semiarid Prairie Agricultural Research Centre, Ottawa, Canada); SU (Tomsk State University, Tomsk, Russia); UA (Universidad Autónoma de Madrid, Madrid, Spain); US (Universität Salzburg, Salzburg, Austria); UW (University of Wyoming College of Agriculture, Laramie, USA); UZ (Universidad de Zaragoza, Huesca, Spain); WHB (University of Natural Resources and Life Sciences, Vienna, Vienna, Austria).

Taxon	**Locality**	**Code**	**Ploidy FC (*N*)**	**Ploidy S (N)**	***N***	**Source**	**ITS**	**ETS**	***atpB-rbcL* spacer**	***rpl32-trnL* spacer**	***trnL-trnF* spacer**
Outgroups											
Axyris hybrida	Mongolia: Khövsgöl Province (48.601331° N, 99.181319° E)	**Ax**			1/**1**	WHB 68600 (Bernhardt)	LR537390	LR537117			
Ceratocarpus arenaria	Russia: Rostow Oblast (47.333690° N, 43.954000° E)	**P228_1**			3/**3**	WHB 73141 (Pfanzelt)	LR537383	LR537109			
		P228_2					LR537384	LR537110			
		P228_3					LR537385	LR537111			
Ceratocarpus arenaria	Ukraine	P231			3/**0**	KW 5854 (Schiian et al.)	LR537386	LR537112			
***Kraschenninnikovia ceratoides* subsp. *ceratoides*: Western Europe and Morocco**											
K. c. subsp. *ceratoides*	Morocco: Atlas: Wadi Abyad	KcMor			4/**0**	UA (Moreno Saiz)	LR537411				
K. c. subsp. *ceratoides*	Spain: Zaragoza: Osera	KcSp1			2/**0**	UZ (Pérez-Collazos)	LR537416			LR585005	LR585038
K. c. subsp. *ceratoides*	Spain: Zaragoza: Pina de Ebro	KcSp2			2/**0**	UZ (Pérez-Collazos)				Identical to LR585005	Identical to LR585038
K. c. subsp. *ceratoides*	Spain: Zaragoza: Fuentes	KcSp3			2/**0**	UZ (Pérez-Collazos)	LR537417 LR537418			Identical to LR585005	Identical to LR585038
K. c. subsp. *ceratoides*	Spain: Teruel: Alfambra	KcSp4			3/**0**	UZ (Pérez-Collazos)				Identical to LR585005	Identical to LR585038
K. c. subsp. *ceratoides*	Spain: Granada: Baza	KcSp6			4/**0**	UZ (Catalán)				Identical to LR585005	Identical to LR585038
K. c. subsp. *ceratoides*	Spain: Aragon	P142			1/**0**	(Pérez-Collazos)	LR537368	LR537088			
K. c. subsp. *ceratoides*	Austria	KcAus2			1/**0**	US (Peer)				LR585013	LR585046

Taxon	Locality	Code	Ploidy FC (*N*)	Ploidy S (N)	*N*	Source	ITS	ETS	*atpB-rbcL* spacer	*rpl32-trnL* spacer	*trnL-trnF* spacer
K. c. subsp. *ceratoides*	Austria	KcAus3			1/**0**	NHMO (Pimentel)				Identical to LR585013	Identical to LR585046
K. c. subsp. *ceratoides*	Austria: Lower Austria, Oberschoderlee (48.641944° N, 16.347722° E)	**P028**	T (2)	T (5)	1/**5**	WHB 65005 (Bernhardt et al.)	LR537373	LR537093	LR537431		
K. c. subsp. *ceratoides*	Austria: Lower Austria, Goggendorf (48.615000° N, 15.942139° E)	**P029**	T (1)	T (5)	1/**5**	WHB 65006 (Bernhardt et al.)	LR537349	LR537068	LR537425		
K. c. subsp. *ceratoides*	Romania: Cluj County (46.968139° N, 23.553611° E)	**P026**	T (4)	T (5)	1/**5**	WHB 64899 (Bernhardt et al.)	LR537341	LR537060	LR537420		
***Krascheninnikovia ceratoides* subsp. *ceratoides*: Eastern Europe and Caucasus**											
K. c. subsp. *ceratoides*	Ukraine: Luhansk	P230			1/**0**	KW 5853 (Pfanzelt)	LR537374	LR537095			
K. c. subsp. *ceratoides*	Ukraine: Luhansk	P232			1/**0**	KW 5857 (Pfanzelt)	LR537379	LR537103			
K. c. subsp. *ceratoides*	Ukraine: Luhansk	P233			1/**0**	KW 5858 (Pfanzelt)		LR537096			
K. c. subsp. *ceratoides*	Russia: Dagestan	P131	D (1)		1/**0**	- (Gadzhiataev et al.)	LR537367	LR537087			
K. c. subsp. *ceratoides*	Russia: Voronezh Oblast (49.927085° N, 40.772559° E)	**P160**	T (1)	T (5)	1/**5**	WHB 73014 (Seidl)	LR537369	LR537089			
K. c. subsp. *ceratoides*	Russia: Belgorod Oblast (50.759154° N, 37.945007° E)	**P161**	T (1)	T (5)	1/**5**	WHB 73013 (Seidl)	LR537370	LR537090			
K. c. subsp. *ceratoides*	Russia: Tatarstan (54.1° N, 53.3° E)	**P215**		T (1)	1/**1**	OSBU 7992 (Neuffer et al.)	LR537372	LR537092			
K. c. subsp. *ceratoides*	Russia: Orenburg Oblast (51.549028° N, 56.702278° E)	**P057**	D (1)	D (5)	1/**5**	WHB 71528 (Neuffer et al.)	LR537355	LR537074			
K. c. subsp. *ceratoides*	Russia: Samara: Sergievskiy	KcRus1			2/**0**	TSU (Olonova)				Identical to LR585005	Identical to LR585038
K. c. subsp. *ceratoides*	Russia: Astrachan: Nizchniy Baskunchak	KcRus3			1/**0**	TSU (Olonova)				LR585014	LR585047
K. c. subsp. *ceratoides*	Russia: Astrachan: Nizchniy Baskunchak	KcRus4			3/**0**	TSU (Olonova)				Identical to LR585005	Identical to LR585038
K. c. subsp. *ceratoides*	Russia: Siberia	KcRus6			1/**0**	KBIH (Catalán)	Identical to LR537416			LR585015	LR585048
K. c. subsp. *ceratoides*	Russia: Siberia	KcRus7			1/**0**	KBIH (Catalán)	Identical to LR537416			LR585016	LR585049
K. c. subsp. *ceratoides*	Russia: Siberia	KcRus8			1/**0**	KBIH (Catalán)	Identical to LR537415			LR585010	LR585043
K. c. subsp. *ceratoides*	Russia: Siberia	KcRus9			1/**0**	KBIH (Catalán)	Identical to LR537415				
K. c. subsp. *ceratoides*	Russia: Southern federal district: Sarepta	KcRus15			1/**0**	KBIH (Catalán)	Identical to LR537416			Identical to LR585005	Identical to LR585038
K. c. subsp. *ceratoides*	Russia: Southern federal district: Sarepta	KcRus16			1/**0**	NHMO (Pimentel)	Identical to LR537416			Identical to LR585005	Identical to LR585038
K. c. subsp. *ceratoides*	Kazakhstan: West Kazakhstan Region (50.861694° N, 53.178361° E)	**P062**	D (1)	D (1)	1/**1**	WHB 71523 (Neuffer et al.)	LR537356	LR537075			

Taxon	Locality	Code	Ploidy FC (*N*)	Ploidy S (N)	*N*	Source	ITS	ETS	*atpB-rbcL* spacer	*rpl32-trnL* spacer	*trnL-trnF* spacer
***Krascheninnikovia ceratoides* subsp. *ceratoides*: Western Asia, Pakistan and Nepal**											
K. c. subsp. *ceratoides*	Turkey: Central Anatolia: Göreme	KcTur1			1/**0**	Bermejo/Blanco	LR537397	LR537120	LR537438	LR585006	LR585039
K. c. subsp. *ceratoides*	Turkey: Central Anatolia: Zelve	KcTur2			2/**0**	GUFEF (Aytaç)	Identical to LR537416			LR585007	LR585040
K. c. subsp. *ceratoides*	Turkey: Central Anatolia: Evciler	KcTur3			1/**0**	GUFEF (Aytaç)	Identical to LR537416			LR585008	LR585041
K. c. subsp. *ceratoides*	Turkey: East Anatolia: Hosap	KcTur4			1/**0**	NHML (Carine)	LR537419			Identical to LR585014	Identical to LR585047
K. c. subsp. *ceratoides*	Turkey: Central Anatolia: Kayseri	KcTur5			1/**0**	NHML (Carine)	Identical to LR537416			Identical to LR585006	Identical to LR585039
K. c. subsp. *ceratoides*	Pakistan: Gojal: Chapursan valley	KcPak1			1/**0**	US (Peer)	LR537394	LR537113	LR537437	Identical to LR585005	Identical to LR585038
K. c. subsp. *ceratoides*	Pakistan: Gilgit-Baltistan: Ghizar valley	KcPak2			1/**0**	US (Peer)	LR537391	LR537058		Identical to LR585005	Identical to LR585038
K. c. subsp. *ceratoides*	Pakistan: Gilgit-Baltistan: Taspur valley	KcPak3			1/**0**	US (Peer)	Identical to LR537405			Identical to LR585006	Identical to LR585039
K. c. subsp. *ceratoides*	Pakistan: Gilgit-Baltistan: Gilgit valley	KcPak4			2/**0**	US (Peer)	LR537412			Identical to LR585013	Identical to LR585046
K. c. subsp. *ceratoides*	Nepal: Mahakali	KcNep1			1/**0**	NHML (Carine)	LR537395	LR537118		LR585012	LR585045
K. c. subsp. *ceratoides*	Nepal: Koshi	KcNep2			1/**0**	NHML (Carine)	LR537396	LR537119			
***Krascheninnikovia ceratoides* subsp. *ceratoides*: Middle Asia**											
K. c. subsp. *ceratoides*	Kazakhstan: Chagan	P031	D (1)		1/**0**	OSBU 24791 (Hurka et al.)	LR537343	LR537062	LR537422		
K. c. subsp. *ceratoides*	Kazakhstan: Qaraghandy Region (48.562028° N, 70.904444° E)	**P032**	T (5)	T (5)	1/**5**	OSBU 24791 (Hurka et al.)	LR537344	LR537063	LR537423		
K. c. subsp. *ceratoides*	Kazakhstan: Qaraghandy Region (48.101139° N, 67.567139° E)	**P033**	T(1)	T (5)	1/**5**	OSBU 24909 (Hurka et al.)	LR537345	LR537064	LR537424		
K. c. subsp. *ceratoides*	Kazakhstan: Qaraghandy Region (48.049750° N, 67.184417° E)	**P034**	D(1)	D (4), T (1)	1/**5**	OSBU 24893 (Hurka et al.)	LR537350	LR537069			
K. c. subsp. *ceratoides*	Kazakhstan: Almaty Region (43.927306° N, 78.503389° E)	**P069**	T (1)	T (5)	1/**5**	WHB 71443 (Friesen)	LR537358	LR537077			
K. c. subsp. *ceratoides*	Kazakhstan: Almaty Region (44.345417° N, 78.830694° E)	**P070**	D (1)	D(5)	1/**5**	WHB 71442 (Friesen)	LR537359	LR537078			
K. c. subsp. *ceratoides*	Kazakhstan: East Kazakhstan Region (47.157389° N, 80.692917° E)	**P072**	D (5)	D (5)	1/**5**	WHB 71444 (Friesen)	LR537357	LR537076			
K. c. subsp. *ceratoides*	Kazakhstan: Almaty Region (45.813278° N, 80.367972° E)	**P073**	T (5)	T (5)	1/**5**	- (Friesen)		LR537079			
K. c. subsp. *ceratoides*	Kazakhstan: Almaty Region (43.072083° N, 78.426278° E)	**P074**	T (5)	T (5)	1/**5**	WHB 71450 (Friesen)	LR537347	LR537066			
K. c. subsp. *ceratoides*	Kazakhstan: Almaty Region (44.226444° N, 78.811944° E)	**P076**	T (4)	T (5)	0/**5**	WHB 71452 (Friesen and Seidl)					

Taxon	Locality	Code	Ploidy FC (*N*)	Ploidy S (N)	*N*	Source	ITS	ETS	*atpB-rbcL* spacer	*rpl32-trnL* spacer	*trnL-trnF* spacer
K. c. subsp. *ceratoides*	Kazakhstan: Eastern Kazakhstan Region (47.968056° N, 83.268000° E)	**P077**	T (5)	T (5)	1/**5**	WHB 71453 (Friesen)	LR537348	LR537067			
K. c. subsp. *ceratoides*	Kazakhstan: Almaty Region (46.605472° N, 80.581139° E)	**P079**	T (1)	T (5)	0/**5**	WHB 71445 (Friesen and Seidl)					
K. c. subsp. *ceratoides*	Kazakhstan: East Kazakhstan Region (47.303694° N, 84.847444° E)	**P081**	T (5)	T (5)	1/**5**	WHB 71457 (Friesen)	LR537360	LR537080			
K. c. subsp. *ceratoides*	Kazakhstan: East Kazakhstan Region (48.732361° N, 84.630556° E)	**P269**	D (5)	D (5)	0/**5**	WHB 76587 (Bernhardt and Seidl)					
K. c. subsp. *ceratoides*	Kazakhstan: Aktobe Region (50.143139° N, 54.730833° E)	**P101**	T (3)	T (5)	1/**5**	OSBU 25690 (Neuffer et al.)	LR537365	LR537085			
K. c. subsp. *ceratoides*	Kazakhstan: Aktobe Region (48.857889° N, 59.208639° E)	**P102**	T (5)	T (5)	0/**5**	OSBU 25776 (Hurka et al.)					
K. c. subsp. *ceratoides*	Kazakhstan: Aktobinskaya Oblast	P103			1/**0**	OSBU 25792 (Neuffer et al.)	LR537366	LR537086			
K. c. subsp. *ceratoides*	Kyrgyzstan: Chong-Alay	P211			1/**0**	OSBU 15711 (Neuffer et al.)		LR537107			
K. c. subsp. *ceratoides*	Kyrgyzstan: Naryn (41.89831° N, 74.29642° E or 41.41817° N, 75.02267° E)	**P025_D**	D (1)	D (1)	1/**1**	WHB 64399 (Köttl)	LR537340	LR537059			
K. c. subsp. *ceratoides*	Kyrgyzstan: Naryn (41.89831° N, 74.29642° E or 41.41817° N, 75.02267° E)	**P025_T**		T (4)	0/**4**	WHB 64399 (Köttl)					
K. c. subsp. *ceratoides*	Tajikistan: Gorno-Badakhshan, Western Pamir (37.294167° N, 72.225833° E)	**P067**	T (4)	T (5)	1/**0**	WHB 71501 (Schönswetter)	LR537346	LR537065			
***Krascheninnikovia ceratoides* subsp. *ceratoides*: Mongolia, northern China and Russian Altai Mountains**											
K. c. subsp. *ceratoides*	Russia: Siberia	KcRus5			1/**0**	KBIH (Catalán)	LR537415			Identical to LR585005	Identical to LR585038
K. c. subsp. *ceratoides*	Russia: Siberia: Altai Mountains	KcRus10			1/**0**	KBIH (Catalán)	LR537413				
K. c. subsp. *ceratoides*	Russia: Siberia: Altai Mountains	KcRus11			1/**0**	KBIH (Catalán)	Identical to LR537415				
K. c. subsp. *ceratoides*	Russia: Siberia: Altai Mountains	KcRus12			1/**0**	KBIH (Catalán)	LR537414				
K. c. subsp. *ceratoides*	Russia: Siberia: Altai Mountains	KcRus13			1/**0**	KBIH (Catalán)				Identical to LR585005	Identical to LR585038
K. c. subsp. *ceratoides*	Russia: Siberia: Altai Mountains	KcRus14			1/**0**	NHMO (Pimentel)	Identical to LR537415			Identical to LR585013	Identical to LR585046
K. c. subsp. *ceratoides*	Russia: Altai Krai (51.141306° N, 81.197472° E)	**P030**	D (2)	D (5)	1/**5**	OSBU 24701 (Neuffer et al.)	LR537342	LR537061	LR537421		
K. c. subsp. *ceratoides*	Russia: Kalmykia	P240			1/**0**	WHB 73019 (Kropf)	LR537377	LR537100			
K. c. subsp. *ceratoides*	Russia: Altai Republic (50.072778° N, 88.374444° E)	**P241**	T (1)	T (5)	0/**5**	WHB 72629 (Neuffer and Friesen)					
K. c. subsp. *ceratoides*	Russia: Altai Republic (49.993450° N, 88.805546° E)	**P242**	T (1)	T (5)	1/**5**	WHB 72632 (Batlai)	LR537382	LR537108			

Taxon	Locality	Code	Ploidy FC (*N*)	Ploidy S (N)	*N*	Source	ITS	ETS	*atpB-rbcL* spacer	*rpl32-trnL* spacer	*trnL-trnF* spacer
K. c. subsp. *ceratoides*	Russia: Altai Republic (50.402260° N, 86.689237° E)	**P243**	T (1)	T (5)	1/**5**	WHB 72630 (Batlai)	LR537376	LR537099	LR537432		
K. c. subsp. *ceratoides*	Russia: Altai Republic (50.071611° N, 88.412167° E)	**P036**	T (2)	T (5)	1/**5**	WHB 68953 (Neuffer)	LR537381	LR537106			
K. c. subsp. *ceratoides*	Mongolia: Töv Province (47.638944° N, 104.897639° E)	**P093**	D (2)	D (2)	1/**2**	WHB 71181 (Bernhardt)	LR537361	LR537081	LR537428		
K. c. subsp. *ceratoides*	Mongolia: Khövsgöl Province (49.513056° N, 99.090250° E)	**P094**	D (5)	D (5)	1/**5**	WHB 71087 (Bernhardt)	LR537362	LR537082	LR537429		
K. c. subsp. *ceratoides*	Mongolia: Bayan-Ölgii Province (48.933333° N, 89.800000° E)	**P207**		T (1)	0/**1**	OSBU 10608 (Neuffer)					
K. c. subsp. *ceratoides*	Mongolia: Chowd	P208			1/**0**	OSBU 10243 (Neuffer et al.)	LR537387	LR537114	LR537434		
K. c. subsp. *ceratoides*	Mongolia: Bayan-Ölgii Province (49.050000° N, 89.733333° E)	**P209**		T (1)	1/**1**	OSBU 10359 (Neuffer et al.)	LR537389	LR537116			
K. c. subsp. *ceratoides*	Mongolia: South Gobi Province (43.848056° N, 103.170556° E)	**P210**		T (1)	1/**1**	OSBU 11936 (Neuffer et al.)	LR537363	LR537083			
K. c. subsp. *ceratoides*	Mongolia: Öwörchangai	P212			1/**0**	OSBU 12250 (Neuffer et al.)	LR537364	LR537084			
K. c. subsp. *ceratoides*	Mongolia: Chowd	P213			1/**0**	OSBU 22691 (Neuffer et al.)	LR537371	LR537091	LR537430		
K. c. subsp. *ceratoides*	Mongolia: Gobi-Altai	P214			1/**0**	OSBU 22566 (Neuffer et al.)	LR537380	LR537105	LR537433		
K. c. subsp. *ceratoides*	Mongolia: Gobi-Altai Province (45.874167° N, 98.102889° E)	**P218**		T (1)	1/**1**	OSBU 22540 (Neuffer et al.)	LR537388	LR537115			
K. c. subsp. *ceratoides*	Mongolia: Gobi-Altai Province (45.007130° N, 93.257260° E)	**P235**	T (3)	T (5)	1/**5**	WHB 72467 (Batlai)	LR537378	LR537101			
K. c. subsp. *ceratoides*	Mongolia: Gobi-Altai Province (45.587150° N, 93.440340° E)	**P237**	D (1)	D (5)	1/**5**	WHB 72472 (Batlai)	LR537375	LR537097			
K. c. subsp. *ceratoides*	Mongolia: Gobi-Altai Province (45.952933° N, 94.271800° E)	**P238**	D (1)	D (5)	1/**5**	WHB 72470 (Batlai)		LR537098			
K. c. subsp. *ceratoides*	Mongolia: Ömnögovi	KcMon1			1/**0**	KBIH (Catalán)	Identical to LR537405			LR585011 LR585019	LR585044 LR585052
K. c. subsp. *ceratoides*	Mongolia: Ömnögovi	KcMon2			1/**0**	KBIH (Catalán)	LR537393	LR537104	LR537436	LR585018 LR585020	LR585051 LR585053
K. c. subsp. *ceratoides*	Mongolia: Ömnögovi	KcMon3			1/**0**	KBIH (Catalán)	Identical to LR537405			LR585021	LR585054
K. c. subsp. *ceratoides*	China: Inner Mongolia: Cela	KcMon4			2/**0**	RMRS (Kitchen)	LR537409			LR585017	LR585050
K. c. subsp. *ceratoides*	China: Inner Mongolia: Cear	KcMon5			2/**0**	RMRS (Kitchen)	LR537410				
K. c. subsp. *ceratoides*	China: Xianyang: Xian	Carbor			1/**0**	NHML (Carine)	Identical to LR537405			LR585031	LR585064

Taxon	Locality	Code	Ploidy FC (*N*)	Ploidy S (N)	*N*	Source	ITS	ETS	*atpB-rbcL* spacer	*rpl32-trnL* spacer	*trnL-trnF* spacer
***Krascheninnikovia ceratoides* subsp. *ceratoides*: North America**											
K. c. subsp. *lanata*	Canada: Saskatchewan: Gull Lake	KL01			1/**0**	SPARC (Schellenberg)	LR537404		LR537440	LR585022	LR585055
K. c. subsp. *lanata*	USA: Colorado: Comanche national park	KL03			1/**0**	RMRS (Kitchen)				Identical to LR585022	Identical to LR585055
K. c. subsp. *lanata*	USA: Nevada: Edwards Valley	KL06			2/**0**	RMRS (Kitchen)	Identical to LR537404			LR585023	LR585056
K. c. subsp. *lanata*	USA: Arizona: Fredonia	KL07			1/**0**	RMRS (Kitchen)	Identical to LR537392			LR585024	LR585057
K. c. subsp. *lanata*	USA: California: Rosamond	KL08			1/**0**	RMRS (Kitchen)	Identical to LR537405				
K. c. subsp. *lanata*	USA: Idaho: Kuna	KL09			2/**0**	RMRS (Kitchen)	LR537405		LR537441	LR585025	LR585058
K. c. subsp. *lanata*	USA: Utah: Desert experiment ranch	KL11			1/**0**	RMRS (Kitchen)	Identical to LR537392			LR585026	LR585059
K. c. subsp. *lanata*	USA: Utah: Starvation	KL12			1/**0**	RMRS (Kitchen)	Identical to LR537392			LR585027	LR585060
K. c. subsp. *lanata*	USA: Utah: Hatch	KL13			1/**0**	RMRS (Kitchen)	Identical to LR537392			LR585028	LR585061
K. c. subsp. *lanata*	USA: Wyoming: Casper	KL14			1/**0**	RMRS (Kitchen)	Identical to LR537405			LR585029	LR585062
K. c. subsp. *lanata*	USA: Wyoming: Shell	KL15			1/**0**	RMRS (Kitchen)	Identical to LR537405			Identical to LR585022	Identical to LR585055
K. c. subsp. *lanata*	USA: Wyoming: Crystal Lake	KL16			1/**0**	UW (Hild)	Identical to LR537405			LR585030	LR585063
K. c. subsp. *lanata*	USA: Wyoming: South of Chey on 85, mi. 308	KL17			1/**0**	UW (Hild)	Identical to LR537392			Identical to LR585028	Identical to LR585061
K. c. subsp. *lanata*	USA: Wyoming: Briggsdale campground	KL18			2/**0**	UW (Hild)	Identical to LR537392			Identical to LR585022	Identical to LR585055
K. c. subsp. *lanata*	USA: Wyoming: Hwy 14 & Arapaho Refuge road	KL19			1/**0**	UW (Hild)	LR537406		LR537442	Identical to LR585022	Identical to LR585055
K. c. subsp. *lanata*	USA: Wyoming: Riverside	KL20			1/**0**	UW (Hild)	Identical to LR537392			Identical to LR585022	Identical to LR585055
K. c. subsp. *lanata*	USA: Wyoming: 8 mi. S of Laramie on 230	KL21			1/**0**	UW (Hild)	LR537392	LR537102		Identical to LR585027	Identical to LR585060
K. c. subsp. *lanata*	USA: Colorado: Foothills west of Berthoud	KL22			1/**0**	NHMO (Pimentel)	LR537407			Identical to LR585022	Identical to LR585055
K. c. subsp. *lanata*	USA: California (35.541667° N, 117.900000° W)	**P039**	D (1)	D (5)	1	- (Leitner)	LR537351	LR537070	LR537426		
K. c. subsp. *lanata*	USA: California (36.541667° N, 117.750000° W)	**P040**	D (5)	D (4)	1	- (Leitner)	LR537352	LR537071			
K. c. subsp. *lanata*	USA: Utah (40.781917° N, 112.785167° W)	**P041**	D (5)	D (5)	1	- (Leitner)	LR537353	LR537072	LR537427		

Taxon	Locality	Code	Ploidy FC (*N*)	Ploidy S (N)	*N*	Source	ITS	ETS	*atpB-rbcL* spacer	*rpl32-trnL* spacer	*trnL-trnF* spacer
K. c. subsp. *lanata*	USA: Utah	P042	D (1)		1/**0**	- (Leitner)	LR537354	LR537073			

Table 2: Localities and codes of the populations of *Adonis vernalis* and outgroups used for GBS. N, sample size; MD, missing data; D, diploid; T, tetraploid.

Taxon	Locality	Code	Ploidy FC (*N*)	Ploidy S (N)	*N*	Source
outgroups						
Adonis turkestanica (Korsh.) Adolf	Tajikistan (39.12361° N, 68.25306° E)	Aturk			1	WHB 71502 (B. Frajman & P. Schönswetter)
Adonis volgensis Steven ex DC.	Russia, Rostov Region, ca 2 km SW of Yagodinka (47.61557° N, 40.31656° E)	P223/Avol_4			1	- (S. Pfanzelt et al.)
Adonis volgensis Steven ex DC.	Russia, Orenburg Region, 40 km E of Orenburg (51.83006° N, 55.71411° E)	P063/Avol_5			1	OSBU 25528, WHB 71521 (B. Neuffer et al.)
Adonis volgensis Steven ex DC.	Kazakhstan, Kostanay Region, 220 km S of Kostanay (51.68892° N, 61.57342° E)	Avol_1			1	OSBU 25833, WHB 71517 (B. Neuffer et al.)
Adonis volgensis Steven ex DC.	Kazakhstan, North Kazakhstan Region, 30 km S of Novoishimskiy (52.94283° N, 66.62603° E)	Avol_2			1	OSBU 25849, WHB 71518 (B. Neuffer et al.)
Adonis volgensis Steven ex DC.	Kazakhstan, Akmola Region, 10 km E of Kokshetau (53.28764° N, 69.26183° E)	Avol_3			1	OSBU 25874, WHB 71514 (B. Neuffer et al.)
Adonis vernalis L.: Spain						
A. vernalis	Spain, Granada, Sierra de Huétor NE of Granada (37.30139° N, 3.44556° W)	P125		D (5)	5	- (G. Schneeweiss & P. Schönswetter)
Adonis vernalis L.: Germany						
A. vernalis	Germany, Saxony-Anhalt, Harslebener Berge S of Halberstadt (51.83046° N, 11.07173° E)	P011		D (5)	5	- (F. Blattner)
A. vernalis	Germany, Saxony-Anhalt, N of Friedrichsaue (51.85763° N, 11.33289° E)	P009		D (5)	5	- (F. Blattner)
A. vernalis	Germany, Saxony-Anhalt, Unstruthänge W of Zscheiplitz (51.21618° N, 11.72131° E)	P015		D (4)	4	- (F. Blattner)
A. vernalis	Germany, Brandenburg, Oderberge S of Lebus (52.40544° N, 14.53353° E)	P049		D (5)	5	WHB 69157 (K.-G. Bernhardt et al.)
A. vernalis	Germany, Bavaria, Garchinger Heide N of Munich (48.29032° N, 11.65305° E)	P143		D (5)	5	WHB 72504 (A. Seidl)
Adonis vernalis L.: Western Pannonian						
A. vernalis	Austria, Lower Austria, Steinberg-Spitzerberg N of Prellenkirchen (48.09514° N, 16.97203° E)	P001	D (1)	D (3)	5	WHB 63392 (K.-G. Bernhardt)
A. vernalis	Austria, Burgenland, between Winden am See and Jois (47.96169° N, 16.77300° E)	P006/P008		D (5+4)	10	WHB 65147, 68984, 68985 (K.-G. Bernhardt)
A. vernalis	Slovakia, Nitra Region, N of Nitra (48.34945° N, 18.09278° E)	P118		D (5)	5	- (K. Plenk)
A. vernalis	Slovakia, Košice Region, NE of Kečovo (48.49328° N, 20.48883° E)	P119		D (5)	5	- (K. Plenk)

Taxon	Locality	Code	Ploidy FC (*N*)	Ploidy S (N)	*N*	Source
A. vernalis	Hungary, Győr-Moson-Sopron, Fertőrákos (47.72539° N, 16.64203° E)	P095		D (5)	5	WHB 72564 (G. Király)
A. vernalis	Hungary, Borsod-Abaúj-Zemplén, S of Szomolya (47.86292° N, 20.51653° E)	P096		D (5)	5	WHB 72568 (G. Király)
A. vernalis	Hungary, Veszprém, Castle of Sümeg (46.98222° N, 17.28194° E)	P126		D (5)	5	- (K. Plenk)
Adonis vernalis L.: Eastern Pannonian						
A. vernalis	Serbia, Vojvodina, N of Krušedol (45.12503° N, 19.94517° E)	P117		D (3)	3	- (M. Kropf)
A. vernalis	Romania, Cluj, N of Cluj-Napoca, NNW of Vultureni (46.96814° N, 23.55361° E)	P003		D (5)	5	WHB 64548-64550 (K.-G. Bernhardt)
A. vernalis	Romania, Mureș, W of Târgu Mureș, SSE of Pănet (46.53903° N, 24.47525° E)	P005		D (5)	5	WHB 64553, 64554 (K.-G. Bernhardt)
A. vernalis	Romania, Brașov, NNE of Brașov, SE of Sânpetru (45.70478° N, 25.64053° E)	P004		D (5)	5	WHB 64556 (K.-G. Bernhardt)
Adonis vernalis L.: Western Pontic						
A. vernalis	Romania, Constanța, SW of Murfatlar (44.16008° N, 28.39094° E)	P002		D (5)	5	WHB 64559 (K.-G. Bernhardt)
A. vernalis	Crimea, SW of Chornomorske, 8 km NNE of Olenevka (45.44391° N, 32.58656° E)	P086		D (3)	3	WHB 71509 (P. A. Volkova & L. A. Abramova)
A. vernalis	Crimea, SE of Simferopol, 3 km ENE of Mount Karatau (44.85453° N, 34.51514° E)	P085		D (5)	5	WHB 71511 (P. A. Volkova & L. A. Abramova)
A. vernalis	Ukraine, Zaporizhzhia Region, W of Troitske (47.06439° N, 35.43555° E)	P222		D (5)	5	WHB 74133 (S. Pfanzelt et al.)
Adonis vernalis L.: Middle Pontic						
A. vernalis	Russia, Kursk Region, Peresyp' SE of Oboyan', SW of Pristen' (51.09167° N, 36.48000° E)	P168		D (5)	5	WHB 73164 (A. Seidl et al.)
A. vernalis	Russia, Kursk Region, Ekaterinovka NE of Manturovo (51.50194° N, 37.30194° E)	P170		D (5)	5	WHB 73167 (A. Seidl et al.)
A. vernalis	Russia, Voronezh Region, 5 km NW of Rossoshki (51.25785° N, 38.86136° E)	P114		D (2)	2	WHB 72670 (N. Tikhomirov)
A. vernalis	Russia, Voronezh Region, N of Sloboda (51.18139° N, 40.28472° E)	P167		D (5)	5	WHB 73172 (A. Seidl et al.)
Adonis vernalis L.: Eastern Pontic						
A. vernalis	Russia, Ulyanovsk Region, 1 km NE of Vyrypayevka (54.11792° N, 47.03575° E)	P115		D (5)	5	WHB 72674 (P. A. Volkova & M. Yu. Grigoryan)
A. vernalis	Russia, Ulyanovsk Region, 2 km N of Nizhnyaya Maza (52.94503° N, 47.92386° E)	P113		D (5)	5	WHB 72671 (N. Tikhomirov)
A. vernalis	Russia, Samara Region, 2 km NW of Klimovka (53.50139° N, 48.99197° E)	P116		D (5)	5	WHB 72675 (P. A. Volkova & M. Yu. Grigoryan)

Taxon	Locality	Code	Ploidy FC (*N*)	Ploidy S (N)	*N*	Source
Adonis vernalis L.: Southern Ural						
A. vernalis	Russia, Republic of Bashkortostan	P065		D (5)	5	OSBU 25539, WHB 71529 (S. V. Smirnov)
A. vernalis	Russia, Republic of Bashkortostan	P061		D (5)	5	OSBU 25541, WHB 71524 (S. V. Smirnov)
A. vernalis	Russia, Republic of Bashkortostan, N of Meteli (56.03577° N, 57.95074° E)	P138		D (1)	1	- (P. A. Volkova)
A. vernalis	Russia, Chelyabinsk Region, S of Miass (54.94453° N, 59.98342° E)	P058		D (5)	5	OSBU 25542 (S. V. Smirnov)
A. vernalis	Russia, Chelyabinsk Region, S of Chelyabinsk (54.97225° N, 61.24278° E)	P059		D (5)	5	OSBU 25543 (S. V. Smirnov)
A. vernalis	Russia, Novosibirsk Region	P064		D (4)	5	OSBU 25536, WHB 71522 (S. V. Smirnov)
Adonis vernalis L.: Western Siberia						
A. vernalis	Kazakhstan, Akmola Region, N of Marinovka (52.03467° N, 69.18492° E)	P060		D (5)	5	OSBU 25538 (S. V. Smirnov)
A. vernalis	Russia, Omsk Region, W of Omsk, ca 6 km NE of Moskalenki (54.98428° N, 72.05650° E)	P316	D (1)	D (1)	1	WHB 74893 (S. Pfanzelt et al.)
A. vernalis	Russia, Omsk Region	P056		D (5)	5	OSBU 25537, WHB 71520 (S. V. Smirnov)
Adonis vernalis L.: Eastern Siberia						
A. vernalis	Russia, Novosibirsk Region, between Verkh-Kargat and Starogornostalevo (54.69697° N, 79.19881° E)	P317	D (3)	D (3)	3	WHB 74897 (S. Pfanzelt et al.)
A. vernalis	Russia, Altai Region, Proslaukha ca 10 km NE of Baevo (53.34014° N, 80.95722° E)	P318	D (2)	D (2)	2	WHB 74901 (S. Pfanzelt et al.)
A. vernalis	Russia, Altai Region, ca 40 km S of Barnaul, N of Kalmanka (52.95975° N, 83.55089° E)	P007		D (5)	5	OSBU 24705 (B. Neuffer et al.)

2.2. Methods

2.2.1. Wet lab methods

Genome size. Genome size and ploidy level of *K. ceratoides* (N=99) and *A. vernalis* (N=3) specimens were measured by flow cytometry using the CyStain PI Absolute P kit (Sysmex, Görlitz, Germany) according to the manufacturer's manual using leaf tissue from the sample together with an internal standard: Pisum sativum L. 'Kleine Rheinländerin' (2C=8.8 pg; (Doležel and Greilhuber, 2010); as internal standard for measurements of *K. ceratoides*) or *Allium cepa* 'Alice' (2C = 34.89 pg (Doležel *et al.*, 1998); as internal standard for measurements of *A. vernalis*). In a CyFlow Space (532 nm diode laser; Sysmex) the nuclear DNA content was measured until at least 5000 measurements had been performed.

DNA Extraction. The genomic DNA was extracted from approximately 20 mg silica gel-dried leaf material by first disrupting it with plastic beads in the TissueLyser II (QIAGEN) and then extracting the DNA with the DNeasy Plant Mini Kit (Qiagen, Hilden, Germany), the NucleoSpin Plant II kit (Macherey&Nagel, Düren, Germany) or the innuPREP Plant DNA kit (Analytic Jena, Jena, Germany) following the standard protocol using CTAB containing lysis solution SLS (Analytic Jena) according to the manufacturers' instructions. If necessary, less leaf material was used, e.g., when leaves were taken from herbarium vouchers.

DNA quality was checked under UV light in a 1% agarose gel run at 90 V until the bands of the ladder were clearly separated. The concentration of the extracted DNA from each sample was quantified with a DS-11 FX Spectrophotometer Fluorometer (DeNovix, Wilmington, Delaware, USA), using the DeNovix dsDNA Broad Range kit (DeNovix) according to the manufacturer's manual.

Single target sequencing. Using *Krascheninnikovia* material, several nucleic and chloroplast loci were amplified via PCR. Amplification of the ITS region was performed using the primers ITS5 and ITS4 (White *et al.*, 1990). The external transcribed spacer (ETS) region was sequenced using the primers ETS-Atr and 18S-E (Baldwin and Markos, 1998; Zacharias and Baldwin, 2010). To amplify the atpB-rbcL spacer, we used the primers atpB-rbcL (f) and atpB-rbcL (r) (Xu *et al.*, 2000; Kadereit, Mucina and Freitag, 2006). For the rpl32-trnL region, the primers trnL(UAG) and rpL32-F were used (Shaw *et al.*, 2007). The primers c and f (Taberlet *et al.*, 1991) were used to amplify the trnL-trnF region. PCR amplification conditions for each genomic region are indicated in Appendix A. Amplification products were purified using Exonuclease I and FastAP Thermosensitive Alkaline Phosphatase (Thermo Fisher Scientific, Waltham, Massachusetts, USA). The DNA concentration was then measured by NanoDrop spectrophotometer (NanoDrop Technologies, Wilmington, Delaware, USA) or with a DS-11 FX Spectrophotometer Fluorometer (DeNovix). Both, forward and reverse, DNA strands were sequenced. Cycle sequencing reactions consisted of 1 µL BigDye Terminator v3.1 Ready Reaction Mix (Thermo Fisher Scientific), 1.5 µL 5× sequencing buffer, 1 µL of 1 µM or 3.5 µM primer and 6.5 µL of PCR product. Cycling conditions after an initial temperature of 96 °C for 5 min were 25 cycles at 96 °C for 10 s, 50 °C for 5 s and 60 °C for 4 min. Excess dye-labelled nucleotides from the sequence reaction were cleaned up using Sephadex columns followed by a run on a 3500 Genetic Analyzer (Applied Biosystems).

GBS library preparation. Genotyping-by-sequencing library preparation was conducted following Poland *et al.*, 2012, using the restriction enzymes *MspI* and *PstI*. Samples were sequenced in two runs on separate lanes in two consecutive runs on a HiSeq 2500 System (Illumina, California, USA) for good genome coverage. Illumina HiSeq allowed the sequencing of fragments of about 100 bp length (single-end reads).

Since diploid and tetraploid individuals were found in the samples of *K. ceratoides*, twice the amount of DNA was used for tetraploids to achieve the same genome coverage as for diploids. Two individuals per study species were sequenced twice to assess the reproducibility of the method.

2.2.2. In silico methods

Geographical regions. The populations were assigned to geographical regions using the framework of Brummitt (Brummitt, 2001). I did not use the framework of Takhtajan (Takhtajan, 1986) as it covers rather large floristic regions in the Northern Hemisphere, which would result in a rough clustering with most populations in the Circumboreal and the Irano-Turanian regions.

For the reconstruction of the ancestral regions of *Krascheninnikovia* based on single gene data, I defined six areas: (A) Western Europe [corresponding to Southwestern, Southeastern and Middle Europe of Brummitt (2001)] and Morocco, (B) Eastern Europe and Caucasus, (C) Western Asia including Pakistan and Nepal, (D) Middle Asia including adjacent populations from southern Siberia, (E) Mongolia and northern China including also adjacent populations from southern Siberia (Russian Altai Mountains), and (F) North America. For the same analysis using GBS data, I defined different regions as only samples from the Eurasian steppe belt were used: Central Europe (CEur), eastern Europe (EEur), western Middle Asia (WMAs), central Middle Asia (CMAs), eastern Middle Asia (EMAs), southern Middle Asia (SMAs), the Russian Altai Mountains (RusAlt), western Central Asia (WCAs), southern Central Asia (SCAs), eastern Central Asia (ECAs), and North America (NAm) (Figure 1).

The populations of *A. vernalis* were assigned to the regions of Spain, Germany, western Pannonian, eastern Pannonian, western Pontic, middle Pontic, eastern Pontic, southern Ural, western Siberia, and eastern Siberia (Figure 2).

Paleoclimate modelling. The modelling of possible habitats under paleoclimate was constructed based on an R script by Bob Muscarella using the packages dismo (Hijmans *et al.*, 2011), rJava (Urbanek, 2020), rgeos (Bivand and Rundel, 2020), ggplot2 (Wickham, 2016), ENMeval (Muscarella *et al.*, 2014), rgdal (Bivand, Keitt and Rowlingson, 2021), HH (Heiberger and Robbins, 2014), rworldmap (South, 2011) and red (Cardoso, 2020) and paleoclimate data of http://www.paleoclim.org/ (Otto-Bliesner *et al.*, 2006; Dolan *et al.*, 2015; Hill, 2015; Fordham *et al.*, 2017; Karger *et al.*, 2017, no date). The coordinates of the study species used are composited of own collection data and data gained at http://www.plantarium.ru/. Bioclimatic parameters with low collinearity were selected by minimizing the variance inflation factor: Only parameters which showed in combination a variance inflation factor of five or less were chosen. For *Krascheninnikovia*, the parameters bio1, 4, 8, 9, 16, 17, 18 and 19 were chosen. For *A. vernalis*, the parameters bio1, 2, 8, 10, 14, 16, and 19 were selected. The parameters one to eleven reflect temperature variance (bio1: annual mean temperature, bio2: mean diurnal range of temperature, bio4: temperature seasonality, bio8: mean temperature of wettest quarter, bio9: mean temperature of driest quarter, bio10: mean temperature of warmest quarter), while parameters twelve to nineteen reflect differences in precipitation (bio14: precipitation of driest month, bio16: precipitation of wettest quarter, bio17: precipitation of driest quarter, bio18: precipitation of warmest quarter, bio19: precipitation of coldest quarter).

GBS raw data analysis. The raw data is available at the European Nucleotide Archive (accessions ERS5794424 to ERS5794612 and ERS10698927 to ERS10699120). After assigning all reads to the corresponding individual, the barcodes were cut off the sequences. To process the raw data, I used ipyrad (Eaton and Overcast, 2020) and STACKS (Catchen *et al.*, 2013). For ipyrad, the data type was set to “ddrad”. The quality of the reads was checked strictly with the program cutadapt, allowing up to five bases of low quality (Q < 20) per read. The reads were sorted and filtered, where a threshold of at least 85% of sequence similarity of reads was used to consider reads to be at the same locus. I allowed a depth range from six to 10,000. Loci where less than 10% of the individuals had data were dropped. Additionally, reads with less than 35 bases, more than 5% uncalled bases (“N”), with more than 5%

heterozygotes in consensus, with more than 20% single nucleotide polymorphisms (SNPs), or more than nine indels were excluded from the analysis. Based on the highest ploidy level found in the samples, I allowed up to four alleles for *Krascheninnikovia* and two for the *Adonis* data set.

For comparison and because of the multiple ploidy levels of *Krascheninnikovia*, I used STACKS v.2.55 (Catchen *et al.*, 2013) for the sorting, filtering and *de novo* assembly of raw read data on the *Krascheninnikovia* data set as well. To find the optimal parameter settings, I ran STACKS 'denovo_map' on a reduced data set: 16 populations (P026, P034, P040, P057, P062, P067, P073, P094, P160, P207, P209, P210, P215, P218, P237, P242) distributed over the entire sampling area were chosen, comprising 56 samples in total. I varied one of the three following parameters while keeping the others at their default value: the minimal number of identical reads required per stack, m, was tested in a range from three to six; the differences between loci within an individual, M, was tested for one to four base pair differences; the differences allowed between catalog loci, n, was tested for one to eight base pair differences. The ranges for the parameters were 3 to 6 for m, 1 to 4 for M and 1 to 8 for n. The parameter value that maximized the number of variant loci present in at least 80% of all individuals were used for the complete data set: m=3, M=3 and n=8. I set the number of stacks per locus to five to account for possibly present allelic variation in tetraploids. Diploid and tetraploid samples were treated identically. The STACKS 'population' program using the 'write random SNPs' flag was used to produce unlinked SNP data sets, with and without the *Axyris* and *Ceratocarpus* outgroups.

The analysis in ipyrad was conducted twice, with and without outgroups. In STACKS, outputs containing all samples and only samples of *Krascheninnikovia*, respectively, were produced.

Phylogenetic analysis – single locus data sets (*Krascheninnikovia*). After single locus sequencing forward and reverse sequences were assembled and edited using Geneious ver. 11.1.5 (Biomatters, Auckland, New Zealand). Alignments of the consensus sequences were calculated per species and closely related outgroups using PASTA (Mirarab *et al.*, 2015) or MAFFT using the Q-INS-i strategy for ITS (Katoh, Rozewicki and Yamada, 2019). Since sequences of all loci were not available for all samples, I tested for data combinability by conducting a partition homogeneity test in PAUP* ver.4.0beta10 (Swofford, 2002) on the following sets of data of *Krascheninnikovia*: (1) rpl32-trnL and trnL-trnF; (2) ITS1, ITS2 and ETS; and (3) atpB-rbcL, ITS and ETS. Partitioned and combined maximum likelihood (ML) analyses were performed using the software IQ-TREE (Minh *et al.*, 2020). Based on the BIC value calculated using jModelTest ver. 2.1.10 (Darriba *et al.*, 2012), the model of nucleotide substitution was selected for each dataset. The best fit model was SYM + G for ETS, ITS1 and ITS2, SYM + G+I for atpB-rbcL (but SYM + G was selected for simplicity) and GTR + G for the other chloroplast regions. Out of 100 random Maximum Parsimony (MP) trees, the best-scoring ML trees were chosen and branch support for the best tree estimated from 1,000 bootstrap replicates using the ultrafast bootstrap option. The distance matrix produced by the IQ-TREE analysis was visualized using SplitsTree (Huson and Bryant, 2005).

Divergence time estimation – single locus data sets (*Krascheninnikovia*). To estimate the divergence time of *Krascheninnikovia* and its close relatives I used the ITS1, ITS2 and ETS regions, which returned a similar age estimate when used alone or combined. I excluded the 5.8S rDNA and the atpB-rbcL intergenic spacer from the dating analysis due to the low variability which would lead to high variance in age estimates at lower taxonomic levels. Molecular dating analyses of the ITS1-ITS2-ETS matrix were performed using BEAST ver. 2.5.2 (Bouckaert *et al.*, 2014). I included DNA sequences from the GenBank of 113 additionally taxa of the Chenopodioideae clade, where the genus is nested in (Kadereit *et al.*, 2005). The Palaeocene pollen fossil *Chenopodipollis multiplex* dated at 65–56 Mya was used for calibrating the crown group of the Chenopodioideae (Kadereit *et al.*, 2003, 2005, 2010). I used a uniform prior to constrain the age of the root node to the age of this fossil. The interface BEAUti was used to create the BEAST input file using the following parameters: (1) symmetric models with unequal rates but equal base frequencies (SYM; (Zharkikh, 1994)) with gamma distributed rate variation among sites with four categories of rates defined for each of the three partitions separately, (2) a relaxed molecular clock model with uncorrelated rates drawn from a log-normal distribution that was unlinked

across partitions, and (3) a birth-death model of lineage diversification with random start to infer the tree topologies. The MCMC chain was run for 50 million generations, saving data every 1000 generations, producing 50,000 estimates of dates and trees. This analysis was repeated five times. Convergence statistics were analysed in Tracer ver. 1.7.1. The trees were combined using LogCombiner ver. 2.5.2 with a burn-in of 10%. I used TreeAnnotator to produce the maximum clade credibility tree from the post-burn-in trees using median node heights and to determine the 95% probability density of ages for all nodes in the trees. The tree was visualised in FigTree ver. 1.4.3.

Ploidy guessing from GBS data set (*Krascheninnikovia* and *Adonis vernalis*). To estimate the ploidy of the individuals from GBS data, nQuire (Weiß *et al.*, 2018) and ploidyNGS (Augusto Corrêa dos Santos, Goldman and Riaño-Pachón, 2017) were used, which take bam files as input. These were built using the Burrows-Wheeler Alignment tool (BWA) (Li and Durbin, 2009), with the concatenated consensus sequence of the respective individual serving as reference. I used the following BWA settings: maximum gap length of twelve, maximum of one gap per read and a mismatch parameter of 0.01 (Li, 2011). The bam-files were then taken as input for nQuire using denoising and for ploidyNGS selecting the "guess ploidy" option.

Genetic cluster analysis – GBS data set (*Krascheninnikovia* and *Adonis vernalis*). To infer population genetic structure, I performed a STRUCTURE-like analysis using the R (R Core Team, 2013) package LEA (Frichot and François, 2015), using only ingroup samples. All considered hypothetical ancestral populations were tested with 100 repetitions each. Per population the affiliation to each hypothetical ancestral population was calculated as mean over its individuals and shown as pie charts on a map. A Discriminant Analysis of Principal Components (DAPC) was performed using the function dapc of the package adegenet in R (Jombart, 2008), with data in Variant Call Format (vcf) obtained from ipyrad as input. A Principle Coordinate Analysis (PCoA) was performed using the R package dartR (Gruber et al., 2018), again using the vcf file of ingroups.

Phylogenetic analysis – GBS data set (*Krascheninnikovia* and *Adonis vernalis*). Phylogenetic analyses were carried out by exercising the maximum likelihood criterion using RAxML ver. 8.2.12 (Stamatakis, 2014) with the GTRCAT model. To receive bootstrap support (BS) for the nodes, I performed standard bootstrapping with the option autoMRE. Coalescence-based analyses were performed using SVDQuartets (Chifman and Kubatko, 2014), executed in the software PAUP* ver. 5.0 (Swofford, 2002) on the concatenated consensus sequences of the filtered loci gathered in a NEXUS-file. One million random quartets were evaluated, and 1,000 bootstrap replicates were performed.

Unlinked SNPs of 6,029 loci were retained in the PHYLIP file of the *Krascheninnikovia* data set as consensus sequences per population, after removing all uninformative sites (Bradley, 2018). Phylogenetic analyses were conducted by applying the maximum likelihood criterion (Stamatakis, 2014) using IQ-TREE v.2.0.3 (Minh *et al.*, 2020) with the GTR+G model and correction for ascertainment bias (Lewis, 2001). SH-like approximate likelihood ratio test (aLRT) (Guindon *et al.*, 2010) and ultrafast bootstrapping (UFBoot) (Minh, Nguyen and von Haeseler, 2013) were performed with 1,000 repetitions each to obtain bootstrap support (aLRT/UFBoot BS) for nodes. The outgroups *Axyris* and *Ceratocarpus* are genetically too distant to assess the correct rooting, so midpoint rooting was used, which resulted in a tree with basal positions for populations of the Russian Altai. The splits data was visualised in SplitsTree v4.14.8 (Huson and Bryant, 2005) and the consensus tree in FigTree v1.4.3 (Rambaut, 2010).

Divergence time estimation – GBS data set (*Krascheninnikovia* and *Adonis vernalis*). To estimate the divergence time of the GBS data, an ultrametric dated tree was built using PATHd8 (Britton *et al.*, 2007) based on the ML tree. I calibrated the tree using the age of diversification within the respective species of the single gene analysis.

SNAPP, a BEAST2 package, was used to calculate a dated tree using a subset of the populations including samples of *A. vernalis*, *A. volgensis* and *A. turkestanica*. Secondary dating was used based on

the node ages calculated using *matK* sequences of *A. vernalis* and close relatives (Lindhuber, 2020). A lognormal distribution was used, reflecting the node age of the most recent common ancestor of *A. vernalis* and *A. volgensis* (offset 0, mean 2.66, standard deviation 0.2) and of *A. vernalis* and *A. turkestanica* (offset 0, mean 4.4, standard deviation 0.2). As input tree a phylogenetic tree was generated using SVDQuartets on a reduced dataset. The resulting trees were then visualised using DensiTree ver. 2.2.7 (Bouckaert and Heled, 2014).

Ancestral range reconstruction – single locus data sets (*Kraschenninnikovia*) and GBS (*Kraschenninnikovia* and *Adonis vernalis*). For the ancestral range reconstruction, the area definition as described above was used. The presence or absence of populations in the defined areas was indicated in binary. When individuals of different areas had an identical sequence, they were combined into one entry, which was treated as present in more than one area. As input tree I used a ML phylogenetic tree, which I transformed into an ultrametric tree with help of the program PATHd8 (Britton *et al.*, 2007).

I used the BioGeoBEARS package ver. 1.1.1 (Matzke, 2013, 2014, 2018) for R ver. 3.4.3 (R Core Team, 2013) to calculate the likelihoods of three commonly used models for biogeographical inference: DEC, a dispersal-extinction cladogenesis model (Ree and Smith, 2008), DIVALIKE, a likelihood version of the dispersal-vicariance analysis (Ronquist, 1997) and BAYAREALIKE, the Bayesian inference of historical biogeography for discrete areas (Landis *et al.*, 2013). All three models were calculated with and without the "jumping" parameter 'J' that allows founder-event speciation in the reconstruction and compared using AICc to determine the best fitting model for the dataset. I used the maximum clade credibility tree with median node heights obtained from BEAST, which I pruned so that it only included samples of the target species. The maximum number of ancestral areas was set to two.

Given the young age of our species and the recent diversification (*Kraschenninnikovia*, inferred from the divergence time analysis: ~2.2 Mya; clade comprising *Adonis vernalis* and *A. volgensis*: less than 2.66 Mya (Lindhuber, 2020)), respectively, no temporal scenario was included in the analysis.

I tested two alternative dispersal hypotheses: with equal dispersal rates among areas (M0) and with differential dispersal rates reflecting the geographic connectivity among the operational areas (M1). In this model, dispersal rates were set to 0.8 when two areas were contiguous and to 0.2 when two areas were separated by another area.

Private allelic richness – GBS data set (*Kraschenninnikovia* and *Adonis vernalis*). To calculate private allelic richness per region, a rarefaction analysis was performed in HP-Rare (Kalinowski, 2005). Populations were assigned to biogeographic regions as described above. Only loci with called bases present in all populations were used. Rarefaction sample sizes for each 'SNP locus' were two populations from each region, and two alleles ('genes' in HP-Rare) from each population. Mean rarefaction and standard deviation were then calculated per region.

Isolation by distance – GBS data set (*Kraschenninnikovia* and *Adonis vernalis*). To test if the study species diversified by isolation by distance, pairwise F_{ST}-values were calculated in R using the function "pairwise_Gst_Nei" of the package adegenet v1.3.2 and correlated with the geographical distance [km] between populations. A 95% confidence interval was calculated in R using the function "predict" of the package stats v4.1.0. The significance was tested via Mantel test (function "mantel.correlog" of the package vegan v2.4.2 using 9999 permutations).

Expected heterozygosity – GBS data set (*Kraschenninnikovia* and *Adonis vernalis*). Expected heterozygosity (H_E) was calculated according to the equation:

Equation 1: Expected Heterozygosity

$$1 - \frac{1}{m}\sum_{l=1}^{m}\sum_{i=1}^{k} p_i^2$$

Where p_i is the frequency of the i^{th} of k alleles. H_E was calculated as 1 minus the summed squared frequencies of all of k alleles, that are summed up and averaged across all m loci. To do so, a file was created where every individual allele was coded as a distinct number using the alleles output file of ipyrad as a template. H_E was then calculated in R.

3. Results

3.1. Krascheninnikovia

The raw data analysis of the *Krascheninnikovia* GBS dataset was carried out using ipyrad and STACKS respectively. In the following, I will discuss the results of the downstream analyses of the STACKS dataset only, as both variants produced comparable results. The results of the downstream analyses of the ipyrad dataset can be found in Appendix B.

Ploidy. I measured the genome content of 99 individuals of *Krascheninnikovia*, which had a mean 2C genome size (± standard deviation) of 2.8 ± 0.3 pg (diploids; N=38), or 5.8 ± 0.2 pg (tetraploids; N=61), respectively. The genome size measurement of 85 samples could not be conducted, because of the low quality of the leaf material due to the age or its storage (e.g., populations of Eastern Europe: P215; Central Middle Asia: P034; Western Central Asia: P207, P209, P218; Eastern Central Asia: P210; Table 1) or because all material was used for DNA extraction. In P034 only one diploid was recognized physically. Within the combined Kyrgyz samples P025 the genome size of one individual (P025-I0223) could be measured and was found to be diploid. The measured populations were uniformly di- or tetraploid. In most regions, like South Central Asia and Central, South and East Middle Asia, diploid and tetraploid populations could be found, while the populations of Central Europe, Western Middle Asia and the Russian Altai Mountains were all tetraploid (Figure 1C; Table 1). The three measured populations of North America were diploid.

For the samples with GBS data, I additionally used software to guess the ploidy level of the samples utilising their GBS data. Most of the measurements by flow cytometry were confirmed by the ploidy level estimation based on GBS data using nQuire and ploidyNGS (Table 1). The only contradiction was found in the North American sample P041-I0372, which was inferred to be tetraploid, but diploid when measured by flow cytometry. Because of the clear results when measured by flow cytometry, this sample was considered diploid. Of those samples not measured using flow cytometry, the populations of Eastern Europe (P215), Western Central Asia (P207, P209, P218) and Eastern Central Asia (P210) were identified as tetraploids; in P025, all individuals were found to be tetraploid except P025-I0223, which was diploid in both analyses, by flow cytometry and by the software. Hence, I hypothesized that P025-I0223 originated from one of the two Kyrgyz localities, while the other four P025 individuals originated from the other locality, which are about 80 km apart. Consequently, P025-I0223 (hereinafter P025_D) and the other four individuals (hereinafter P025_T) were treated as two different populations in all analyses. In population P034, one individual (P034-I0317) was found to be tetraploid, while the others were diploid. In all populations apart from P025 and P034, the estimated ploidy of unmeasured samples corresponded to the ploidy of measured individuals of the same population (Figure 1C , Table 1).

Data sets. The matrices of nuclear and plastid sequence alignments contained accessions of *Krascheninnikovia,* and the close genera used as outgroups, *Axyris* and *Ceratocarpus*. The accessions used are specified in Table 1. Identical haplotypes were represented by a single accession in the phylogenetic analyses. For the dating analysis, the ITS1, ITS2 and ETS data matrices of 191 accessions with unique sequences were used, including 57 accessions of *Krascheninnikovia*, four of *Axyris*, five of *Ceratocarpus* and 125 of other Chenopodioideae genera. Of the 686 characters, 539 were variable.

Of 24,249 loci, composed of 2,625,739 sites, 21,254 variant and unlinked sites of the raw GBS data remained in the STACKS VCF file of *Krascheninnikovia*. Of those loci, 6029 were kept after removing all uninformative sites. In the PHYLIP file including the outgroups, only 500 SNPs of *Axyris* and 525 SNPs of *Ceratocarpus* were retained, while the populations of *Krascheninnikovia* comprised on average 3731 (± 883) SNPs. Due to this huge difference in the amount of recovered data, the analyses including the outgroups may not be meaningful and were dismissed.

Trees and networks. Since the partition homogeneity tests of single loci were not significant ($p > 0.05$), the tested data matrices (rpl32-trnL and trnL-trnF; ITS1, ITS2 and ETS; atpB-rbcL, ITS and ETS) were combined. I calculated a split network of the combined matrix of ITS, ETS and atpB-rbcL using IQ-TREE (Figure 3). According to the resulting network, the samples were divided into four strongly supported clades.

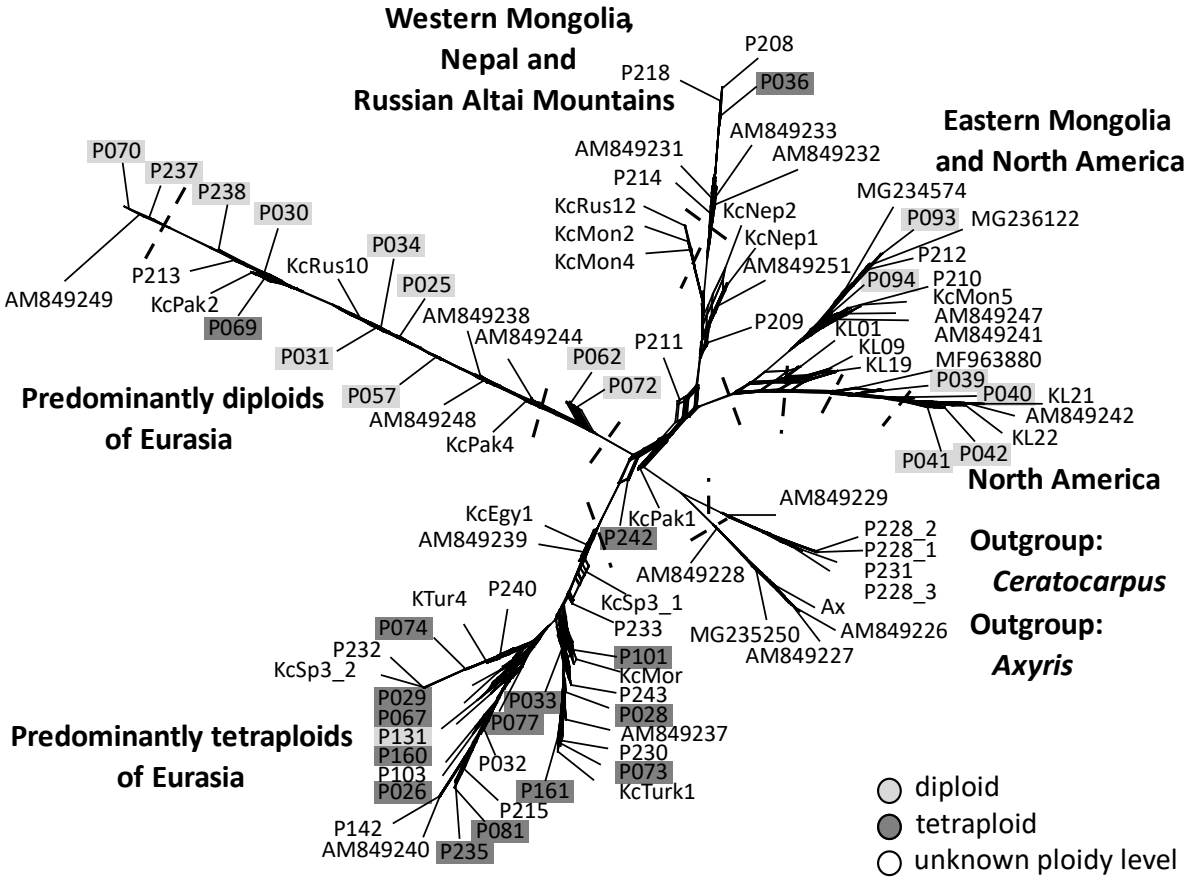

Figure 3: Phylogenetic SplitsTree (splits output of IQ-TREE) based on analyses of ITS1, 5.8S rDNA, ITS2, ETS and atpB-rbcL sequences of *K. ceratoides*. Ploidies are indicated by shade in the chart. AM849239 represents identical sequences of KcSp1, KcSp2, KcSp4, KcSp5, KcSp6, KcAus1, KcAus3, KcRus1, KcRus2, KcRus3, KcRus4, KcRus6, KcRus7, KcRus13, KcRus15, KcRus16, KcEgy2, KcTur2, KcTur3, KcTur5.

The largest clade (BS 92%) consists of predominantly tetraploids from Eurasia (populations west of the Altai Mountains). Diploid individuals from a largely overlapping area (but extending further to the east and less far west) were grouped in another clade (BS 91%), together with one tetraploid population (P069; 'Predominantly diploids of Eurasia' in Figure 3). In the third clade (BS 75%), individuals from western Mongolia, Nepal and the Russian Altai Mountains region are grouped together. The fourth clade (BS 80%) contains individuals from eastern Mongolia, Canada and the USA (CAs and NAm). This is the only clade that combines accessions of both subspecies (subsp. ceratoides and subsp. lanata). Some of the American individuals are grouped together in a highly supported clade (BS 92%), while others are mixed with Mongolian samples. Therefore, the monophyly of the subspecies is not supported. Some Asian samples [P211 (Kyrgyzstan); P209, KcMon2, KcMon4 and AM849251 (Mongolia/CAs); P242 and KcRus12 (Russian Altai Mountains/RusAlt); and the samples from Nepal] are not resolved in any of the well-supported clades described. The split network showed KcPak1 as the earliest diverging lineage, splitting after the outgroups *Axyris* and *Ceratocarpus* (Figure 3). In the ML tree, KcPak1 was sister to all other accessions of *Krascheninnikovia* (Figure 4). Relationships within and between groups were often poorly resolved and supported.

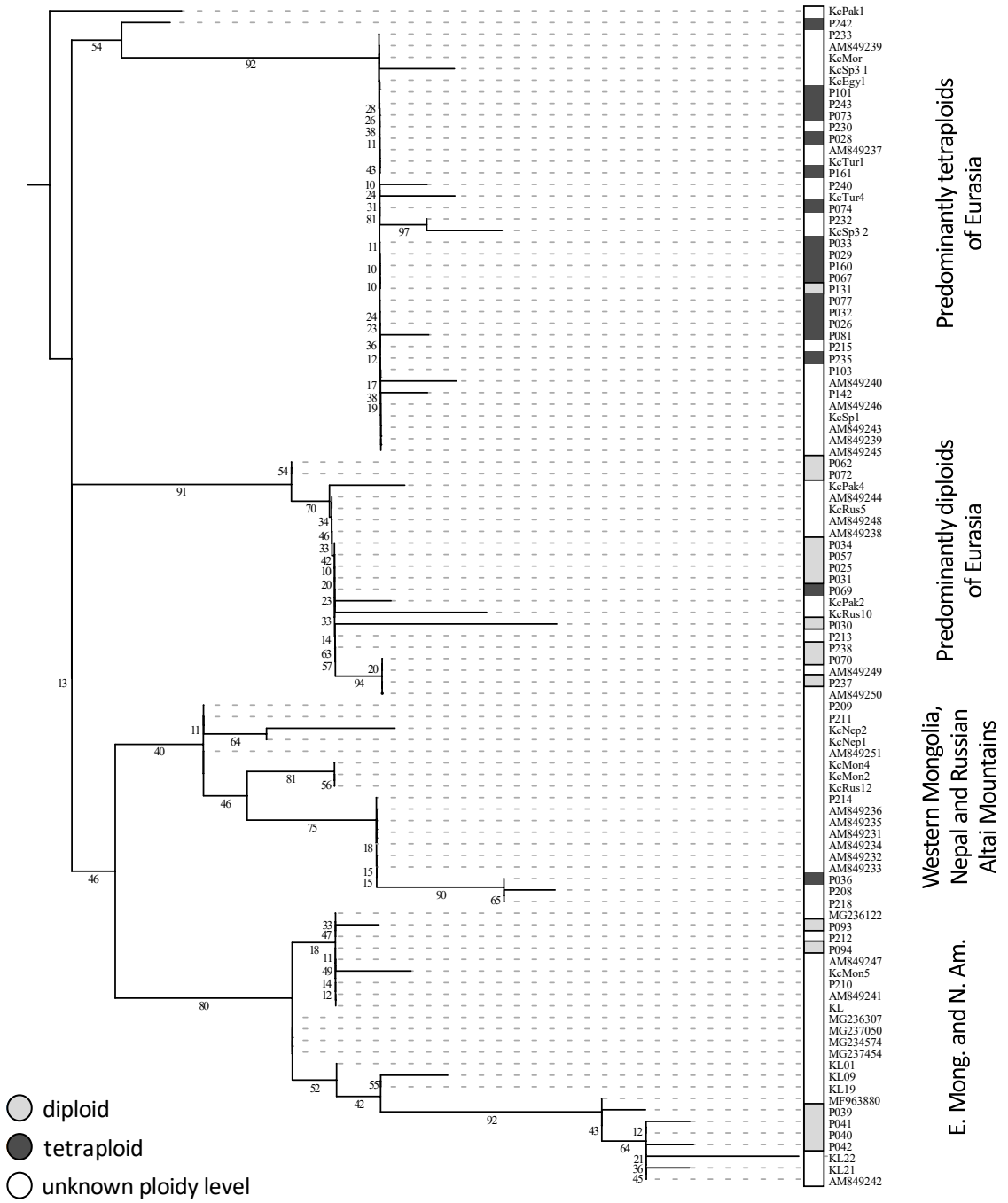

Figure 4: Phylogenetic IQ-TREE maximum likelihood tree based on ITS1, 5.8S rDNA, ITS2, ETS and atpB-rbcL sequences of *K. ceratoides*. Numbers indicate the bootstrap support. Ploidies are indicated by shade in the chart. KL represents identical sequences of KcMon1, KcMon3, KcPak3, Carbor, KL08, KL09, KL14, KL15, KL16, KL18. KcSp1 represents identical sequences of KcSp1, KcSp2, KcSp4, KcSp5, KcSp6, KcAus1, KcAus3, KcRus1, KcRus2, KcRus3, KcRus4, KcRus6, KcRus7, KcRus13, KcRus15, KcRus16, KcEgy2, KcTur2, KcTur3, KcTur5.

Dating. The topology that was recovered in the BEAST analysis was mostly congruent with other Chenopodioideae analyses (Kadereit and Yaprak, 2008; Kadereit et al., 2003, 2005, 2010; Di Vincenzo et al., 2018) (Figure 5). All samples of *Kraschenninnikovia* were resolved in a monophyletic clade, which was sister to *Ceratocarpus*. *Kraschenninnikovia*, *Ceratocarpus* and *Axyris* formed a monophyletic clade, referred to as Axyrideae.

The divergence of the Axyrideae from its sister group was estimated at ~36 ± 8 Mya. *Axyris* diverged from the *Ceratocarpus*/*Kraschenninnikovia* clade ~22 ± 6 Mya and *Kraschenninnikovia* and *Ceratocarpus* diverged ~17 ± 5 Mya. According to our analyses, the diversification within *Kraschenninnikovia* started ~2.2 ± 0.9 Mya, when the Eurasian clade with mostly tetraploid individuals split from the clade comprising the other lineages (posterior probability (PP) = 99%; divergence ~0.7 Mya). The clade with mostly diploid Eurasian individuals split from the other accessions ~2.0 Mya (PP = 98%; divergence ~0.7 Mya). The samples from North America split over two subgroups (PP = 100% for both clades; splits ~1.8 and ~1.4 Mya, with divergence ~0.5 and ~0.7 Mya, respectively). The fourth, recently diverged clade, consists of individuals from Western Mongolia, adjacent regions of the Russian Altai Mountains and Nepal (PP = 79%, Figure 5).

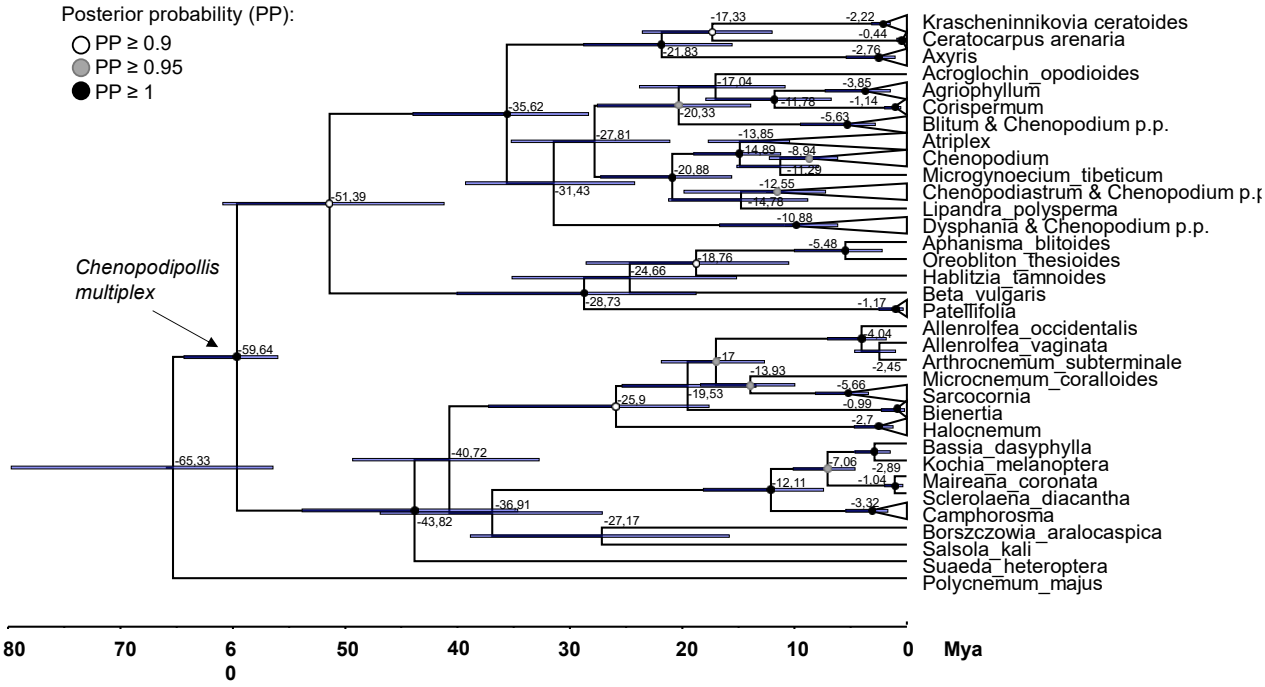

Figure 5: Divergence time estimation of single gene loci. BEAST maximum clade credibility dated tree of *Kraschenninnikovia ceratoides* and outgroup Chenopodiaceae species based on analysis of ITS1-ITS2-ETS data. Fossil-based calibration imposed to the Chenopodiaceae Palaeocene pollen fossil of *Chenopodipollis multiplex* was used to calibrate the root node at 65–56 Mya, following Kadereit et al. (2003, 2005, 2010) and Di Vincenzo et al. (2018). The chronogram shows the divergence time estimates and 95% confidence intervals for each node. Numbers are expressed in million years.

Ancestral range. The reconstructions of divergence times and ancestral range within *Kraschenninnikovia* are condensed in Figure 6. Based on the AICc values I selected the DEC + J model using different dispersal rates among areas. According to the analysis, the ancestral area of *Kraschenninnikovia* was most likely in Mongolia and northern China as well as adjacent populations from southern Siberia combined with Middle Asia (DE in Figure 6) (0.18). An initial vicariance event within *K. ceratoides* took place shortly after ~2.2 Mya, when the ancestor of the predominantly tetraploid Eurasian clade (in Middle Asia) separated from the ancestor of the other clades (in Mongolia and northern China). The predominantly tetraploid Eurasian lineage dispersed shortly after ~0.7 Mya from Middle Asia to Eastern Europe and later to Western Europe, Turkey and Morocco as well as to Mongolia. The ancestor of the predominantly diploid Eurasian lineage separated from the other lineages that originated east of the Altai Mountains ~2.0 Mya. This clade diverged within the area of Mongolia and northern China from ~0.7 Mya onwards and its descendant lineages dispersed from this area to Middle Asia, Pakistan and later Eastern Europe. Two lineages are resolved in the group comprising samples from areas east of the Altai Mountains that both migrated to North America more

recently. The first lineage dispersed to North America between ~1.8 and ~0.5 Mya. The second lineage expanded its range from the area of eastern Mongolia to North American between ~1.4 and ~0.7 Mya. Thereafter, populations in North America and in eastern Mongolia became isolated from each other. From the Mongolian and northern Chinese ancestral range of the most recently evolved group, new dispersals to Middle Asia, Pakistan and Nepal were also inferred.

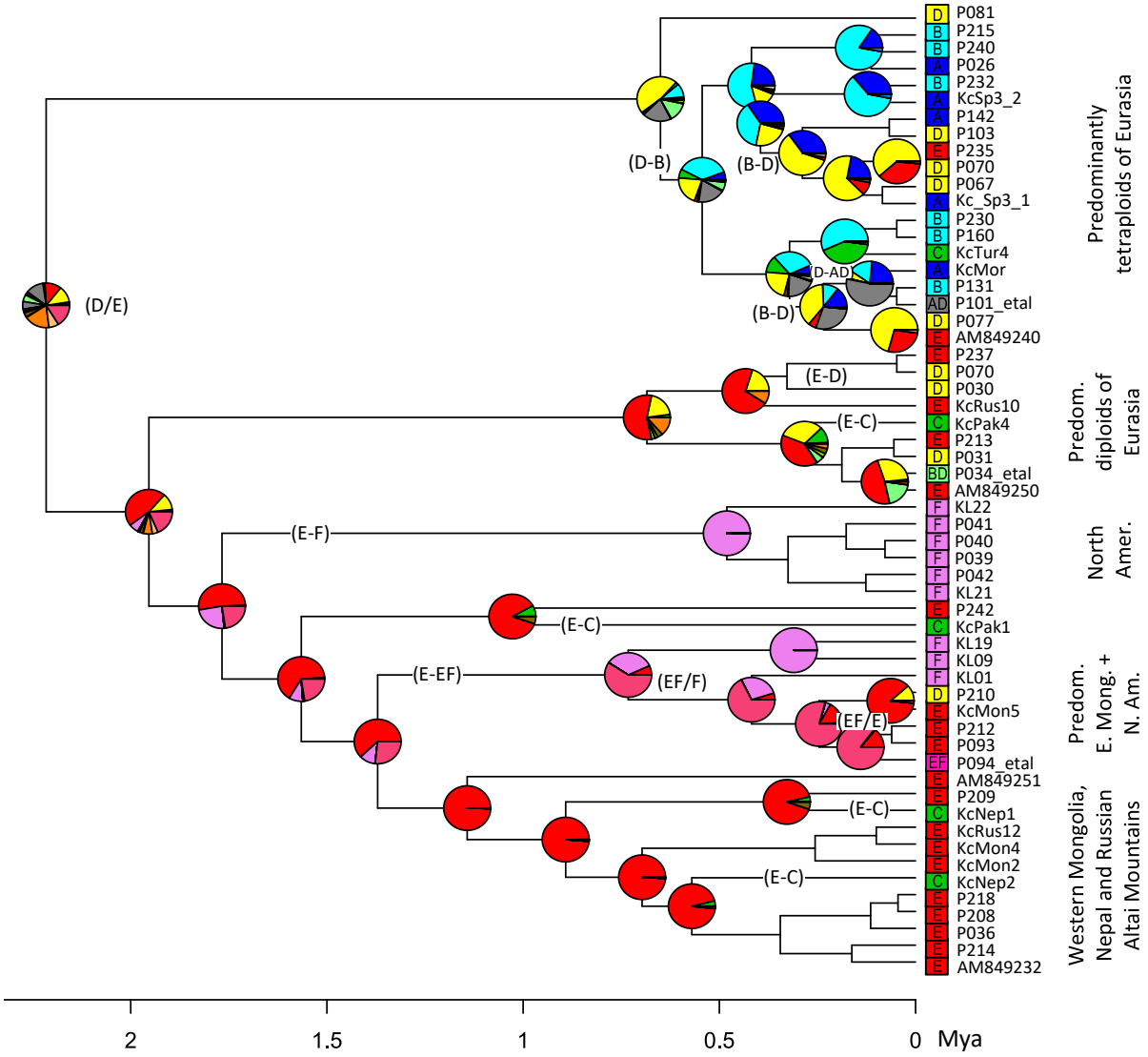

Abbr.	Description
A	Western Europe and Morocco
B	Eastern Europe and Caucasus
C	Western Asia, Pakistan and Nepal
D	Middle Asia
E	Mongolia, northern China and Russian Altai Mountains
F	North America
AD	BD	DE	EF

M1	A	B	C	D	E	F
A	1	0.8	0.8	0.2	0.2	0.2
B	0.8	1	0.8	0.8	0.2	0.2
C	0.8	0.8	1	0.8	0.2	0.2
D	0.2	0.8	0.8	1	0.8	0.2
E	0.2	0.2	0.2	0.8	1	0.2
F	0.2	0.2	0.2	0.2	0.2	1

Figure 6: Ancestral range reconstruction of *Krascheninnikovia* using the single gene dataset. Biogeographic reconstruction of *Krascheninnikovia ceratoides*, based on the Lagrange DEC + J model. Pie charts at nodes indicate the relative probabilities for alternative ancestral ranges (codes for operational areas correspond to those indicated in Appendix D) and are marked with the node age. Inferred dispersal (x-y), vicariance (x/y), range expansion (x-xy) and peripheral isolation (xy/y) events with the highest marginal probability are shown on the tree. The maximum clade credibility tree obtained from BEAST was pruned to only contain samples of

Krascheninnikovia. The matrix M1 shows the dispersal rates between the areas. The table with the area description also indicates the colour coding. P101_etal represents identical sequences of P028, P029, P032, P033, P073, P101, P161, P243, KcEgy1, KcEgy2, KcSp1, KcSp2, KcSp4, KcSp5, KcSp6, KcTur1, KcTur2, KcTur3, KcTur5, KcAus1, KcAus3, KcRus1, KcRus2, KcRus3, KcRus4, KcRus6, KcRus7, KcRus13, KcRus15, KcRus16; P034 represents identical sequences of P025, P034, P057, P062, P069, P072, Kc_Pak2, KcRus5, KcRus8, KcRus9, KcRus11, KcRus14, KcAfg3; P094_etal represents identical sequences of P094, KcMon1, KcMon3, KcPak3, Carbor, KL08, KL09, KL14, KL15, KL16, KL18.

Genetic clusters. LEA assigned all individuals to hypothetical ancestral populations based on their genetic composition. After 100 repetitions, eight hypothetical ancestral populations (K) were chosen based on the cross-entropy criterion (Figure 7). The red cluster (Figure 8) is mainly represented by populations from Central Europe, eastern Europe, and western Middle Asia (all west of the Ural Mountains, mostly tetraploids except for populations P057 and P062 from eastern Europe). The dark green cluster mainly contains tetraploid populations from western, central, eastern, and southern Middle Asia, and southern Central Asia. The light green cluster is mainly represented by diploid populations from eastern and southern Middle Asia and from southern Central Asia and is present in the diploids of eastern Europe and central Middle Asia. The black cluster is represented by three individuals of P081 of eastern Middle Asia, the light blue cluster by P238 of southern Central Asia. The dark blue cluster is mainly comprised of populations from the Russian Altai Mountains and western Central Asia. Populations from eastern Central Asia form the orange cluster. The populations from North America belong to the lilac cluster. Some admixture is observed, especially between the light green, dark green, and red clusters (Figure 8).

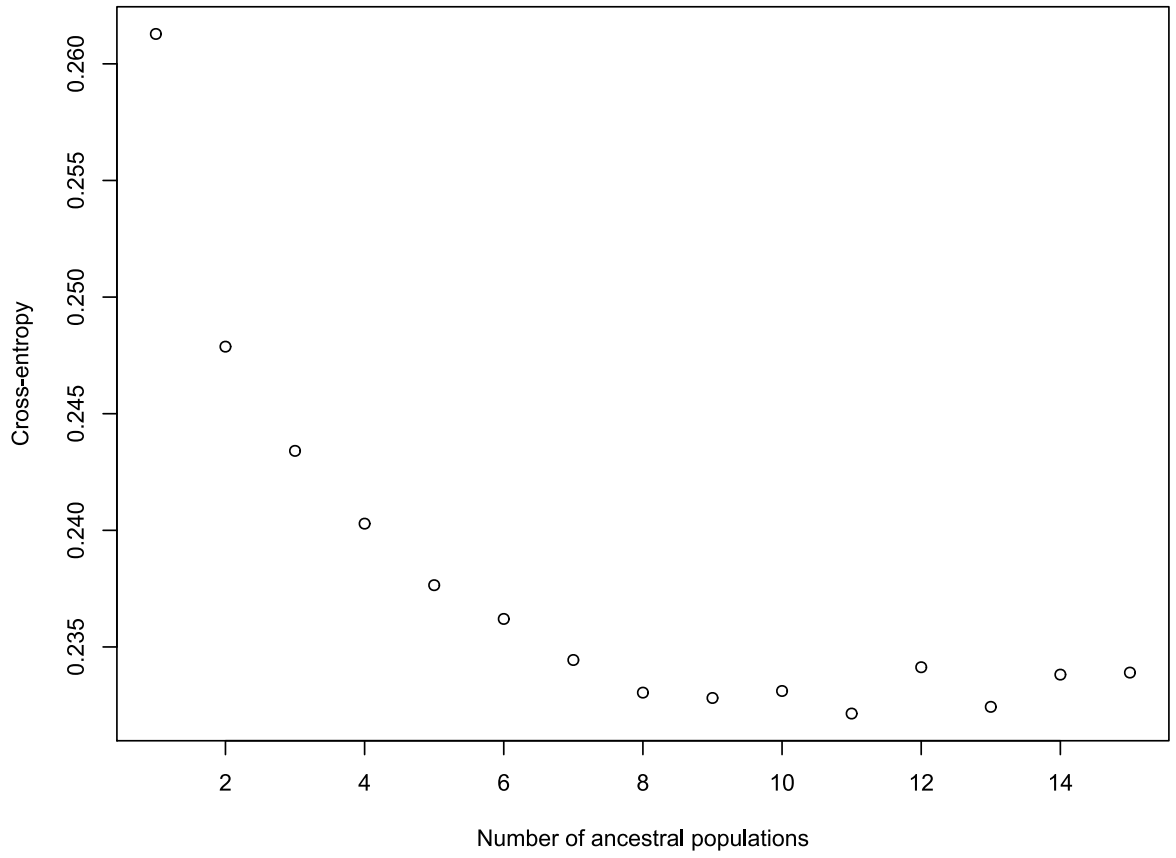

Figure 7: Cross-entropy for one to fifteen hypothetical ancestral populations. In LEA, 15 hypothetical ancestral populations (*K*) were tested with 100 repetitions each. According to the cross-entropy criterion implemented in

LEA to determine the optimal number of clusters, data fit best to eleven distinguishable genetic lineages. However, it was decided to consider only eight clusters, since the cross-entropy values differ only little for K=8 to K=11.

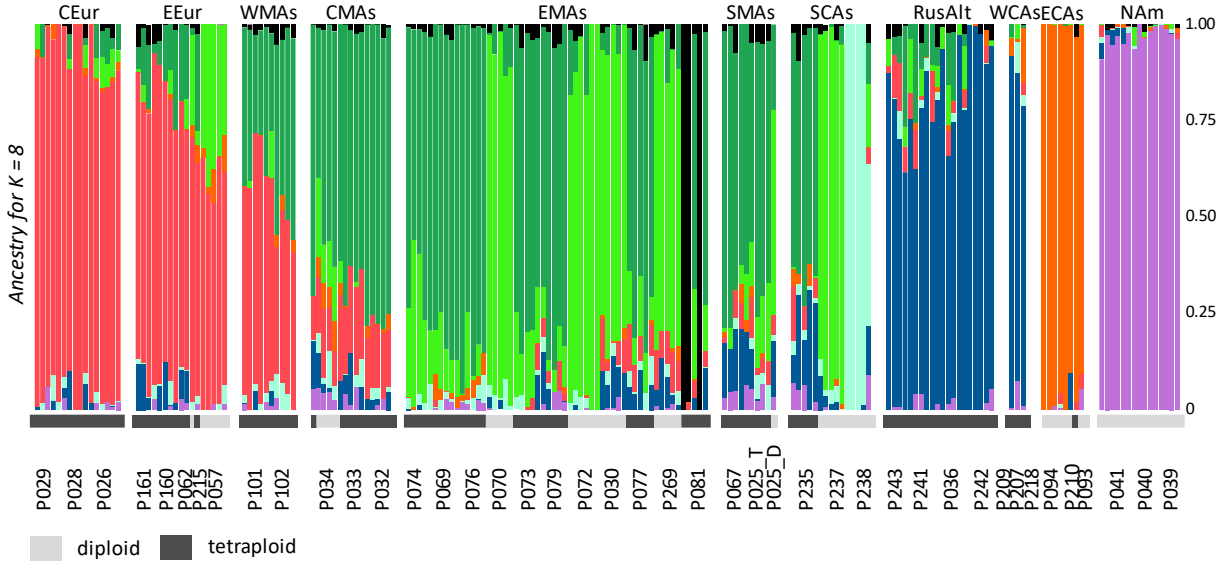

Figure 8: Genetic cluster membership of *Krascheninnikovia* (GBS) as inferred using LEA is shown as a barplot. Vertical bars denote individuals. Eight clusters were retained, which are indicated by different colours. The samples are ordered by their assigned geographical region from west to east. Ploidy is indicated by grey (diploid) and black (tetraploid) bars.

To illustrate the consecutive splits between the hypothetical ancestral populations, the cluster membership was depicted as pie charts on a map for all *K* values from two to eight (Figure 9). The deepest split, with two hypothetical ancestral populations (*K* = 2), was inferred between the populations east of the Khangai Mountains in Central Mongolia (North America and eastern Mongolia), and the populations west of the Khangai Mountains. The second deepest split (*K* = 3) is in the area of the Ural Mountains, dividing the populations west of the Khangai Mountains. With *K* = 4, the Mongolian populations east of the Khangai Mountains and the North American populations each form a group of their own. The populations between the Ural and Khangai Mountains split in two groups according to their ploidy with *K* = 5: diploid populations are assigned to the light green cluster, while tetraploid populations are assigned to the dark green cluster. With *K* = 6, the populations of the Russian Altai and western Central Asia form their own group (dark blue). With *K* = 7, population P238 from southern Central Asia forms its own cluster (light blue), as does P081 with *K* = 8 (black).

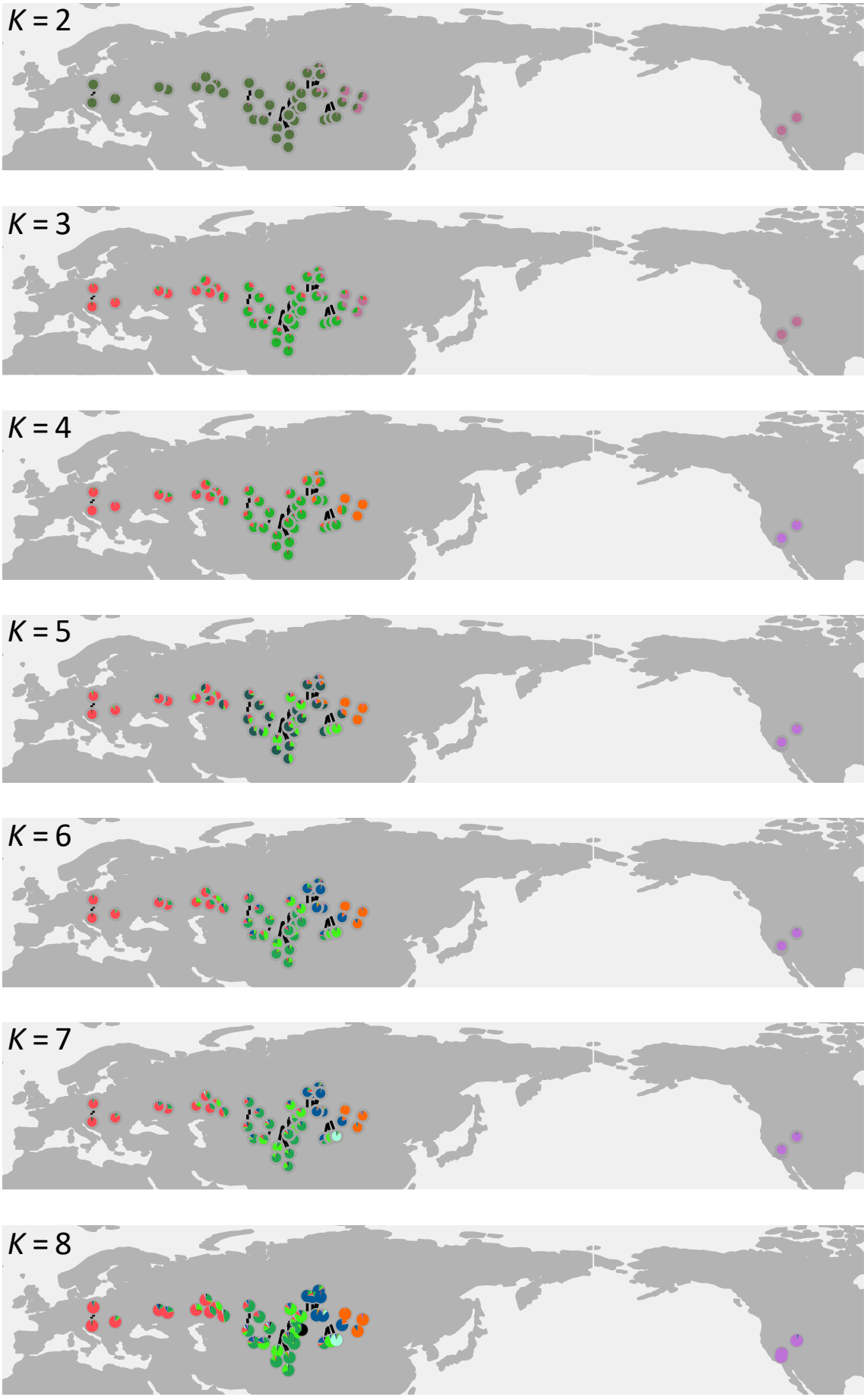
K = 2
K = 3
K = 4
K = 5
K = 6
K = 7
K = 8

← Figure 9: Genetic clustering of samples of *Kraschenninnikovia* (GBS) as inferred from LEA is shown as pie charts for *K* = 2 to *K* = 8 clusters. The first split occurred in Central Asia, dividing the populations west and east of the Khangai Mountains (*K* = 2), followed by a split in the area of the Ural Mountains (*K* = 3). At *K* = 4, the American populations separate; at *K* = 5, the diploids and tetraploids of Middle Asia and adjacent areas each form their own group. At *K* = 6, the populations of the Altai Mountains form their own cluster. At *K* = 7 and *K* = 8, P238 and P081 form their own cluster.

DAPC. Similarly to LEA, DAPC analysis clusters individuals according to their genetic composition (Figure 10). Four clusters were retrieved: (1) populations from Europe (Ural Mountains to Central Europe, including western Middle Asia), (2) the populations from Middle Asia and southern Central Asia, (3) the populations of the Russian Altai and western Central Asia, and (4) the populations of eastern Central Asia and North America, mirroring the first splits of the analysis performed using the LEA package.

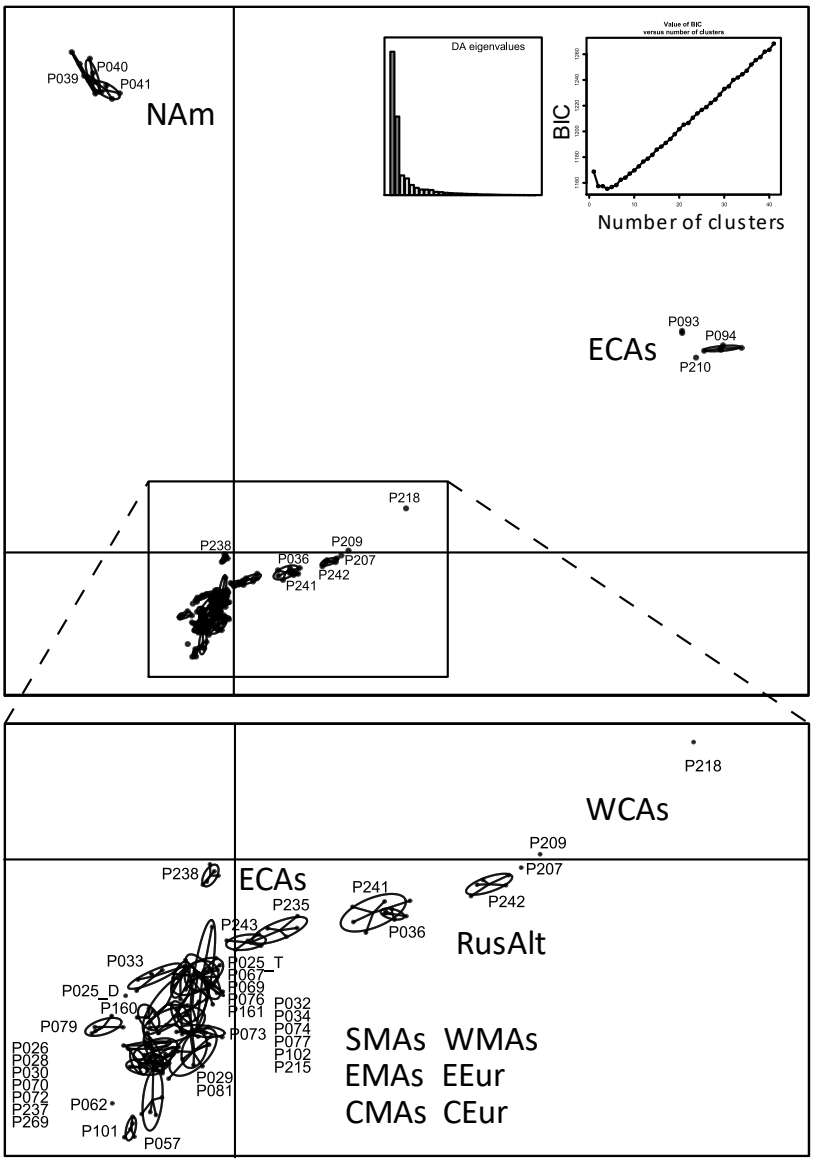

Figure 10: Genetic clustering of samples of *Kraschenninnikovia* (GBS) as calculated by dapc package of R. Four clusters were retained. One cluster comprises the European populations, one the Middle Asian and southern Central Asian populations, one the populations of western Central Asia and the Russian Altai, and another the eastern Central Asian and North American populations. The lower part of the graph shows an enlarged section of the upper part.

PCoA. Samples from Europe, Middle Asia, southern Central Asia, the Russian Altai and western Central Asia clustered together in the Principal Coordinate Analysis (Figure 11). Apart from this group, two other clusters were found: samples from eastern Central Asia and samples from North America. The populations of western Central Asia and the Russian Altai are genetically different to other populations of the majority group. Among the samples from Europe, Middle Asia and southern Central Asia, diploids and tetraploids segregated along the second PCoA axis.

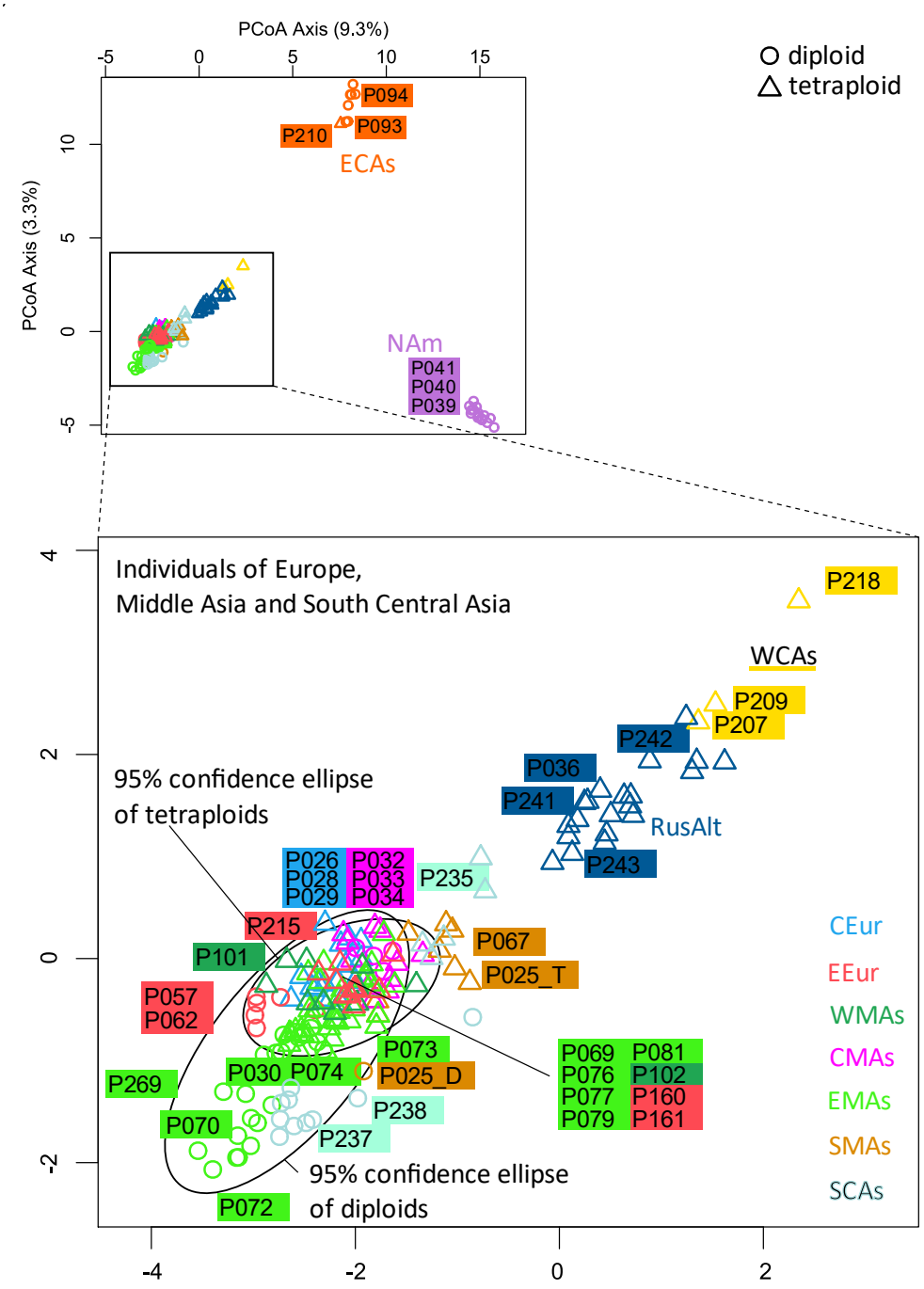

Figure 11: PCoA scatterplot. Symbols representing samples of the same geographical area were coloured according to Figure 2. Circles indicate diploids, triangles tetraploids. The lower part of the graph shows an enlarged section of the upper part. Distinct from most of the samples, the populations of eastern Central Asia and North America each form their own cluster. Within the remaining populations, those from western Central Asia and from the Russian Altai are genetically distinct. Within the densely scattered other populations, there is a visible trend, which separates diploids and tetraploids from each other.

Phylogenetic analysis. According to the ML tree, *K. ceratoides* comprises two fully supported major genetic groups: populations from the Russian Altai, eastern Central Asia, and North America form one clade, which is sister to a clade comprising the remaining accessions from the Russian Altai and from southern Central Asia to Central Europe (Figure 12A and B). Within the first group, two well-supported clades of populations from eastern Central Asia and North America, respectively, derive from populations of western Central Asia and one population of the Russian Altai (99.9 aLRT/100 UFBoot BS). In the second group, populations from the Russian Altai Mountains constitute the basally branching lineages, forming a grade from which the southern Central Asian, Middle Asian and European populations are derived (Figure 12B). The populations of central Middle Asia form a well-supported clade (98.8/99), as do the populations west of the Ural Mountains (63.2/94, excluding P102: 93.6/98). In this clade, populations P101 and P102 from western Middle Asia are paraphyletic sister groups to the European clade. The replicates of the two individuals, for which GBS analysis was performed twice (P029-I0272, P072-I0637), occur next to each other in the IQ-TREE analysis (100/100) when using data per individual, confirming the reproducibility of the method (data not shown).

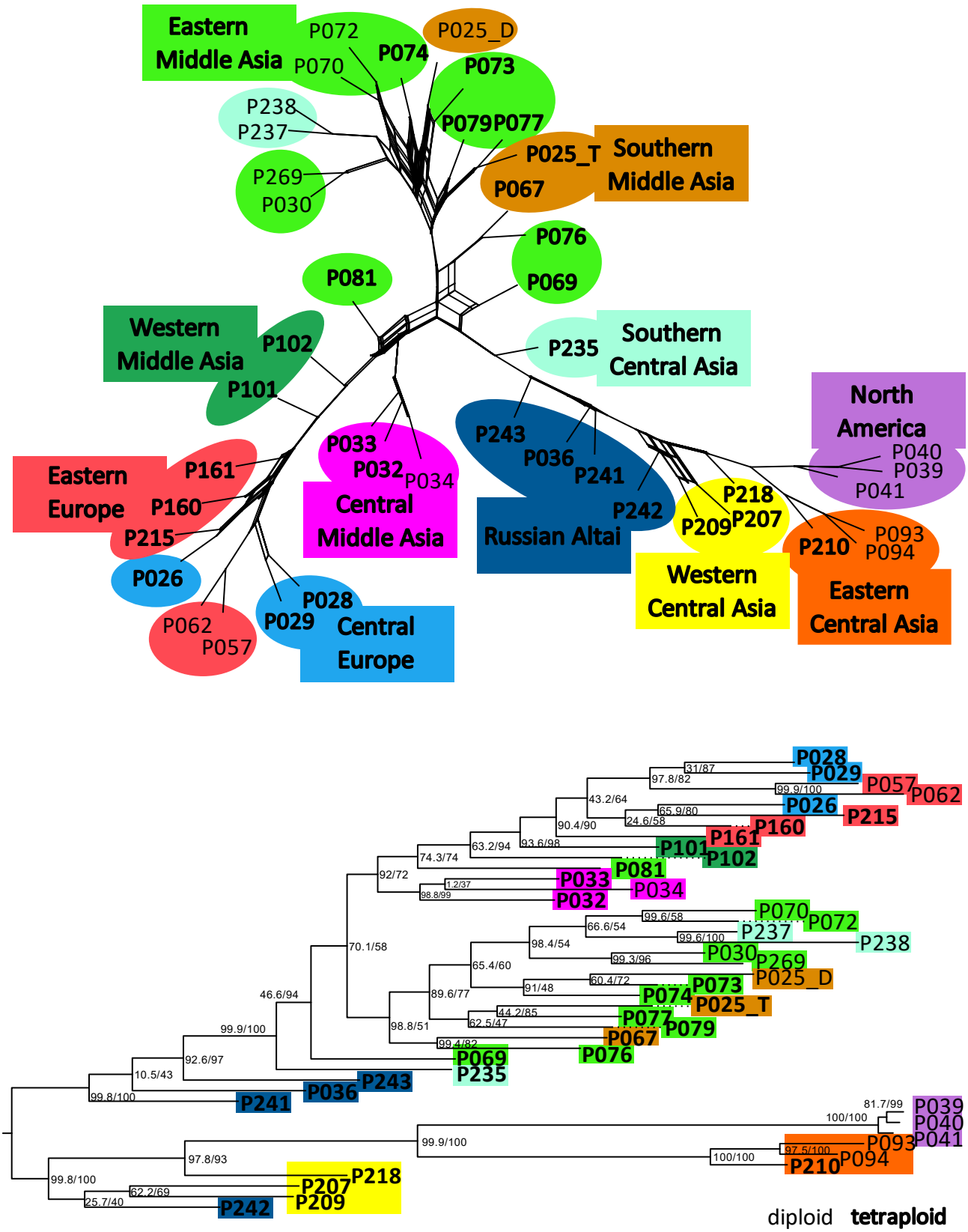

Figure 12: Phylogenetic IQ-TREE maximum likelihood tree based on *Krascheninnikovia* GBS data with GTR+G model and ascertainment bias correction. A thousand repetitions of ultrafast bootstrapping (UFBoot) and of approximate likelihood-ratio test (aLRT) were performed. The origins of the populations are indicated by colour. Top: Phylogenetic network. Tetraploids are shown in bold. Bottom: Phylogenetic tree. The support values are indicated at the nodes (SH-aLRT/bootstrap support value). Midpoint rooting was used.

Biogeographic analysis with BioGeoBEARS. In the analysis of the GBS data of *K. ceratoides,* DIVALIKE+J was chosen as the most likely model based on the AICc values. Based on our BioGeoBEARS analysis, the ancestral range of *K. ceratoides* lies within the area of the Altai Mountains: western Central Asia (yellow) and the Russian Altai Mountains (dark blue) (Figure 13). From western Central Asia, *K. ceratoides* migrated east to eastern Central Asia (orange) and from there to North America (lilac). From the Russian Altai Mountains, it migrated to southern Central Asia and to eastern Middle Asia (light green). From eastern Middle Asia, it then migrated again to southern Central Asia (light blue) and to southern Middle Asia (brown). It migrated further west to central Middle Asia (pink) and to western Middle Asia (dark green), and on to eastern Europe (red) and Central Europe (blue).

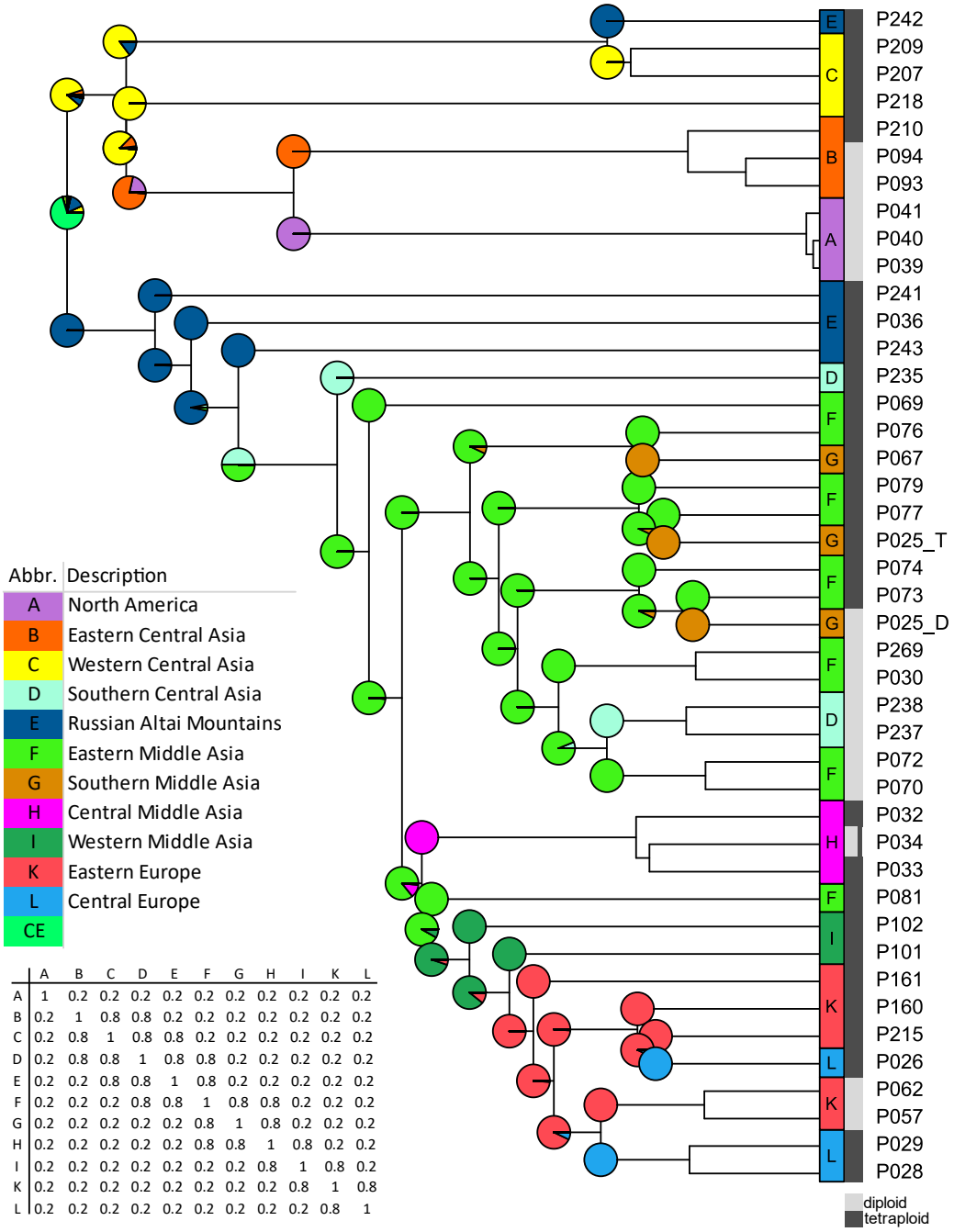

	A	B	C	D	E	F	G	H	I	K	L
A	1	0.2	0.2	0.2	0.2	0.2	0.2	0.2	0.2	0.2	0.2
B	0.2	1	0.8	0.8	0.2	0.2	0.2	0.2	0.2	0.2	0.2
C	0.2	0.8	1	0.8	0.8	0.2	0.2	0.2	0.2	0.2	0.2
D	0.2	0.8	0.8	1	0.8	0.8	0.2	0.2	0.2	0.2	0.2
E	0.2	0.2	0.8	0.8	1	0.8	0.2	0.2	0.2	0.2	0.2
F	0.2	0.2	0.2	0.8	0.8	1	0.8	0.8	0.2	0.2	0.2
G	0.2	0.2	0.2	0.2	0.2	0.8	1	0.8	0.2	0.2	0.2
H	0.2	0.2	0.2	0.2	0.2	0.8	0.8	1	0.8	0.2	0.2
I	0.2	0.2	0.2	0.2	0.2	0.2	0.2	0.8	1	0.8	0.2
K	0.2	0.2	0.2	0.2	0.2	0.2	0.2	0.2	0.8	1	0.8
L	0.2	0.2	0.2	0.2	0.2	0.2	0.2	0.2	0.2	0.8	1

Figure 13: Ancestral range reconstruction of *Krascheninnikovia* (GBS). Phylogeographic analysis using the DIVALIKE model of the R package BioGeoBEARS. Colours indicate the origin of the samples. *Krascheninnikovia* spread from the Altai Mountains to the East, reaching eastern Central Asia and North America, and to the West, reaching Middle Asia and Europe.

Private allelic richness. The highest private allelic richness was found in western Central Asia (0.014±0.002), followed by eastern Central Asia (0.013±0.004) and the Russian Altai Mountains (0.011±0.001; Figure 14). The lowest private allelic richness was found in North America (0.007±0.003).

Geographical region	Private allelic richness in geographic-genetic groups (average of population values)	SE
CEur	0.0090	0.0007
EEur	0.0090	0.0022
WMAs	0.0100	0.0020
CMAs	0.0105	0.0011
EMAs	0.0093	0.0021
SMAs	0.0092	0.0046
SCAs	0.0106	0.0022
RusAlt	0.0113	0.0009
WCAs	0.0144	0.0019
ECAs	0.0130	0.0038
NAm	0.0068	0.0029

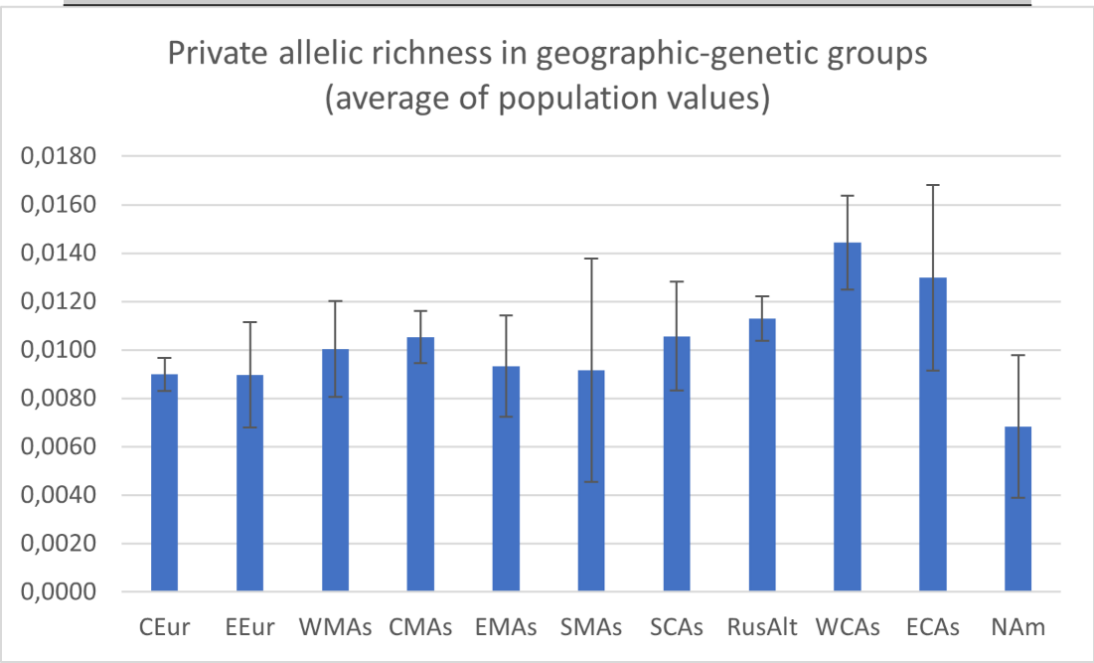

Figure 14: Private allelic richness of *Kraschenninnikovia* (GBS). Private allelic richness was computed for 1725 SNPs using HP-Rare. The highest private allelic richness was found in Central Asia.

Isolation by distance. No significant correlation was detected between geographic and genetic distance (Figure 15). The test was conducted twice, excluding (A and B) and including (C and D) the North American populations.

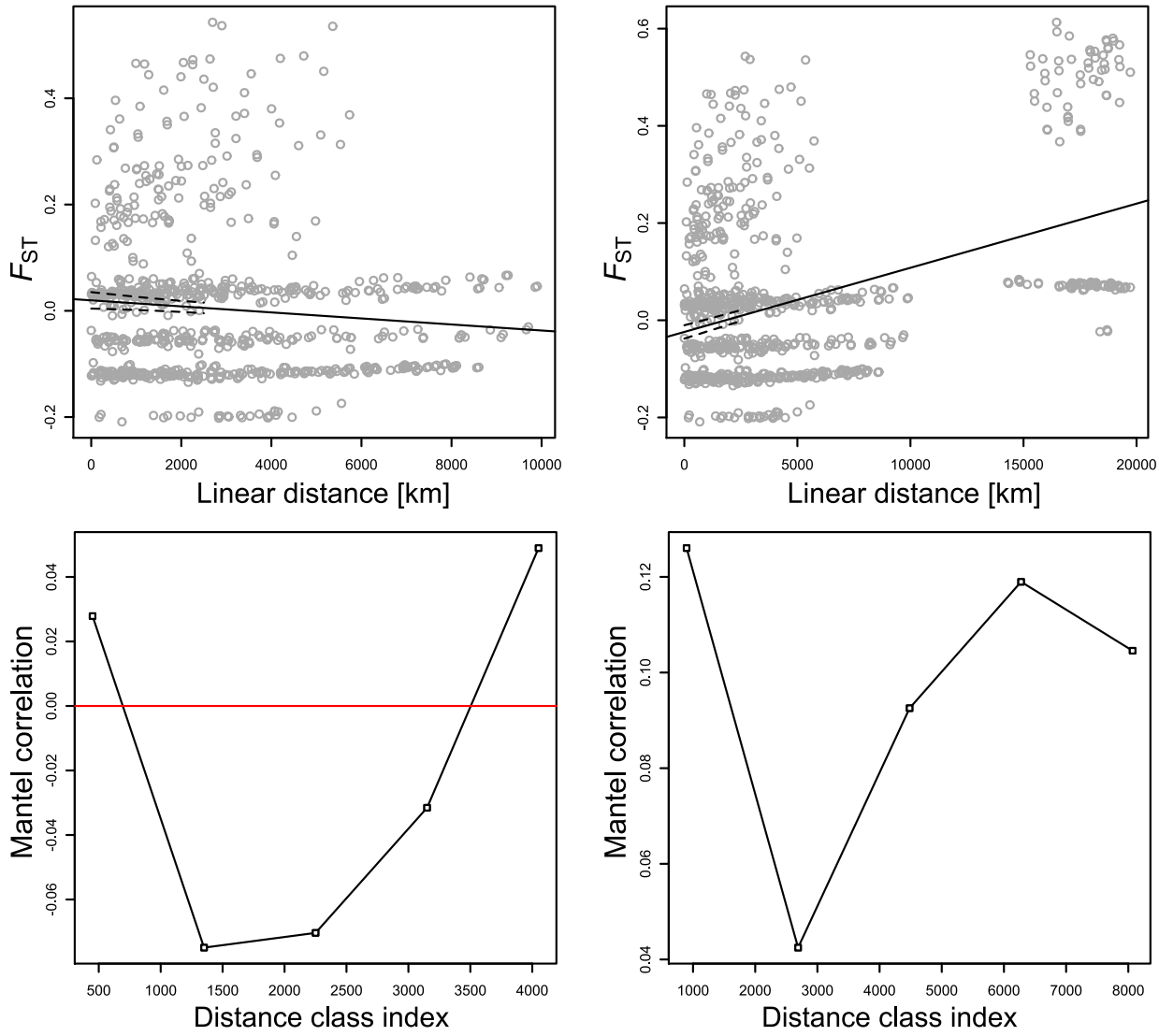

Figure 15: Isolation by distance of *Krascheninnikovia* (GBS). No significant isolation by distance could be found. First row: correlation between linear distance and F_{ST}. A: Eurasian populations; C: complete dataset. Second row: Mantel correlation. Significant tests would be marked as filled quadrats. B: Eurasian populations; D: complete dataset.

Paleoclimate modelling. The maps of modelled paleoclimate (Last Interglacial: LIG, Last glacial maximum: LGM, Heinrich Stadial 1: HS 1 and current climate: current) show suitable habitat in the southern range of the Eurasian steppe belt in current times and during glacial periods, while less suitable habitat was present during interglacial stadiums (Figure 16). Possible refugia were present near the Black Sea and in the high mountains of North China. In North America, a constant area with suitable habitat seems to have persisted even during interglacial phases. Suitable habitat in the Beringia land bridge was present especially during the Heinrich Stadial 1.

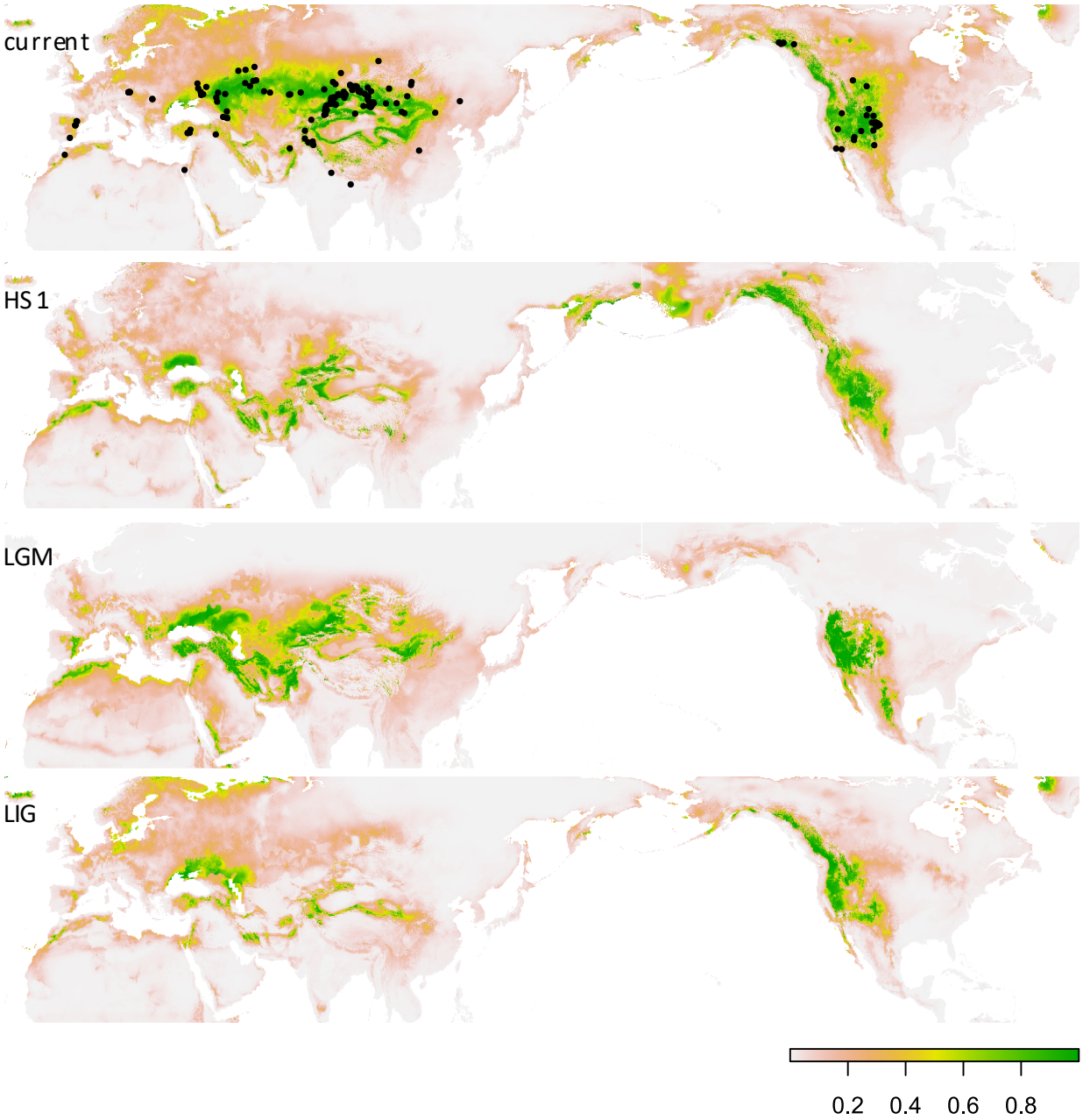

Figure 16: Paleoclimate reconstruction for *Krascheninnikovia* (GBS). Reconstruction of the habitat suitability of *Krascheninnikovia* at different times. Most suitable habitats are indicated in green. Used data points are indicated in first panel ("current").

3.2. Adonis

Ploidy. Because only diploid samples were expected in *Adonis vernalis*, the genome content of only three samples was measured. It had a mean genome size (± standard deviation) of 2C=19.1 ± 0.4 pg.

Ploidy level estimations based on GBS data using nQuire and ploidyNGS indicates a diploid genome for all individuals but one: P064_I0559 was guessed to be most likely triploid according to nQuire, while when using ploidyNGS, the ploidy of P064_I0559 remained unclear.

Data set. 4,384,129 SNPs in 43, 916 loci were retained by the ipyrad analysis of *Adonis vernalis*, *A. volgensis* and *A. turkestanica*. In the alignment, the samples of *A. vernalis* covered 23,562 SNPs on average (ranging from 11,879 to 31,121 SNPs), while the samples of the outgroup had on average 18,613 SNPs (ranging from 15,011 to 21,102 SNPs). In the alignment without the outgroup, 4,399,929 SNPs in 44,123 loci were recovered. The samples covered 23,903 SNPs on average, ranging from 12,032 to 31,518 SNPs.

Trees and networks. In the ML tree, *Adonis turkestanica* was chosen as outgroup (Figure 17). Samples of *A. volgensis* formed a sister clade to *A. vernalis*. Within *A. vernalis*, the Spanish population was sister to all other populations. The Romanian population P004 is sister clade to the other populations. The remaining populations split in two well supported groups: On the one hand populations of western Pannonian paraphyletic to German populations, on the other hand eastern Pannonian populations and the western Pannonian population P096 as a sister clade to eastern populations. The western Pontic populations are sister clades of the populations to the east, which do not show geographically related grouping. The Crimean populations forms a monophyletic clade (Figure 17). The branch support values within the populations are usually high. (Black dot: > 95%, grey dot: > 90%)

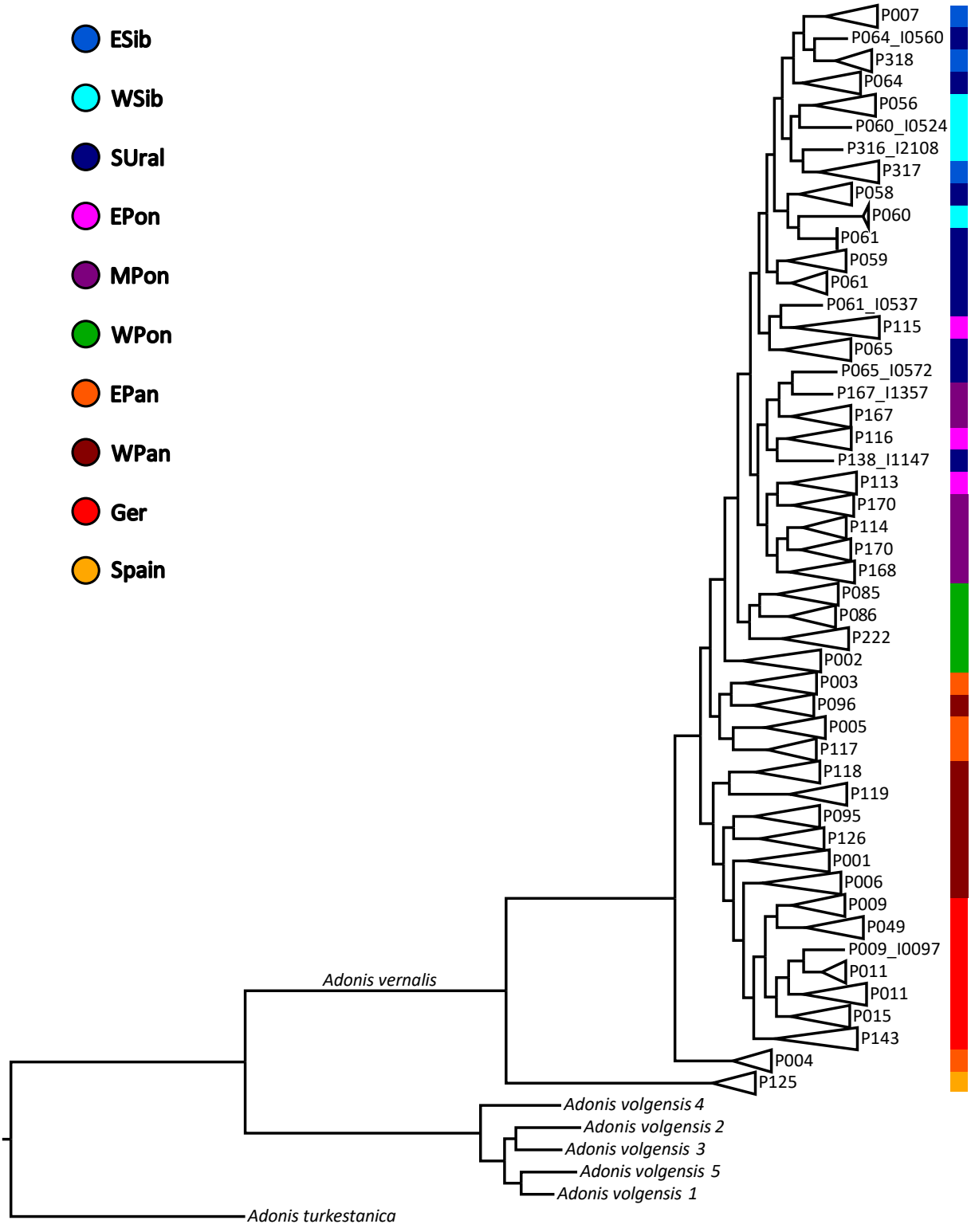

Figure 17: Phylogenetic IQ-TREE maximum likelihood tree based on *Adonis* GBS data with GTR model and ascertainment bias correction. A thousand repetitions of ultrafast bootstrapping (UFBoot) and of approximate likelihood-ratio test (aLRT) were performed. Branches of individuals of the same populations, which clustered together, were collapsed. Branch support is indicated by dots: black ≥ 95%, grey ≥ 90 %. The origins of the populations are indicated by colour.

Biogeographic analysis with BioGeoBEARS. The model BAYAREALIKE+J was chosen based on the AICc values. Based on our BioGeoBEARS analysis, there are two ancestral areas of *A. vernalis*, Spain and eastern Pannonia (Figure 18). While from Spain no range expansion was observed, from eastern Pannonia *A. vernalis* migrated to the West reaching western Pannonia twice, from where a northwest migration to Northern Germany was observed. Furthermore, a migration starting in eastern Pannonia to the east was visible, reaching the western Pontic region and from there Siberia and Kazakhstan.

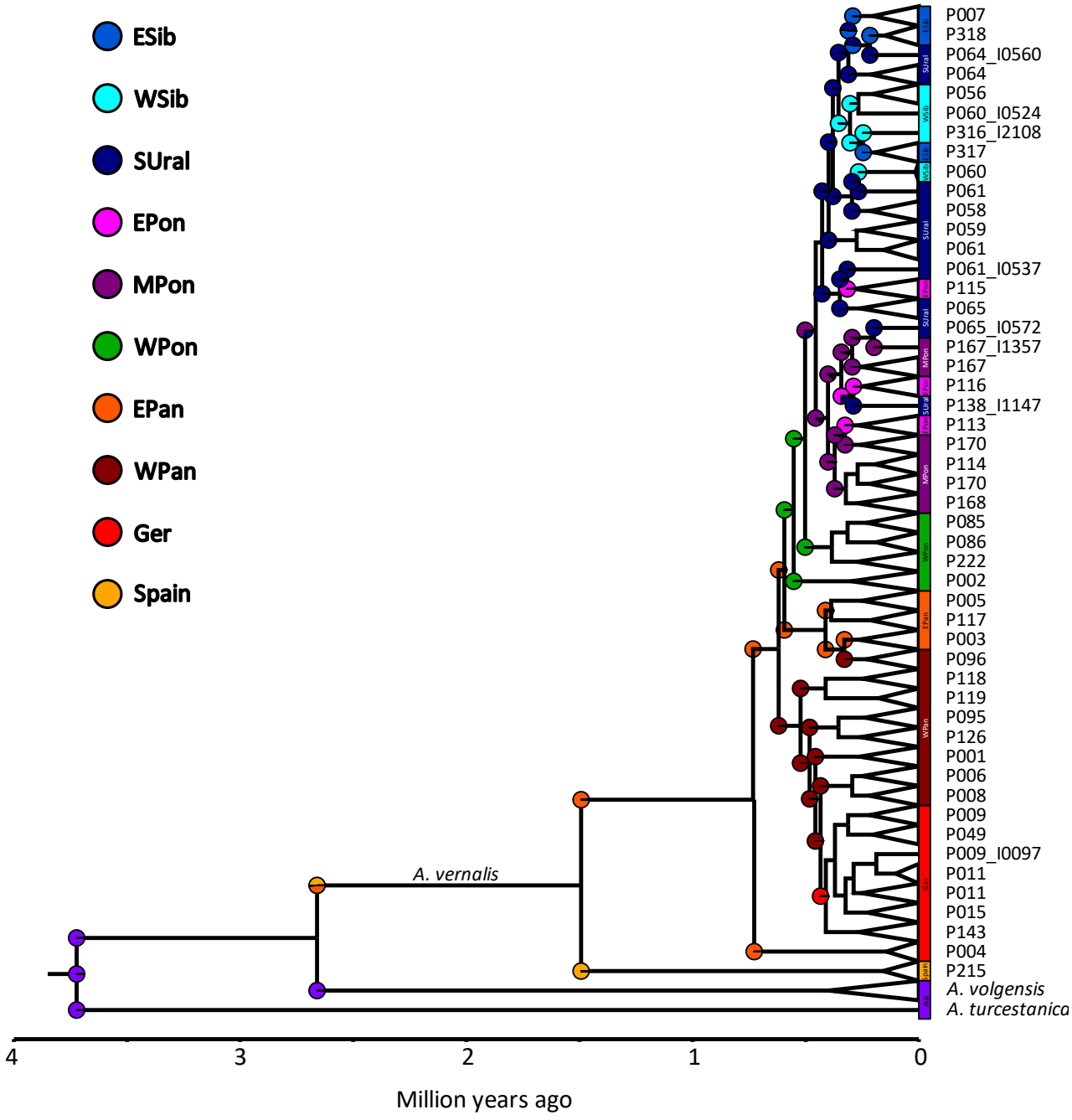

Figure 18: Ancestral range reconstruction of *Adonis vernalis* (GBS). Phylogeographic analysis using the BAYAREALIKE+J model of the R package BioGeoBEARS. Colours indicate the origin of the samples. The two source populations are from Spain and Romania. From Romania the species migrated east (reaching Siberia) and west (reaching Germany).

Dating. In the SNAPP analysis, the nodes of the most recent common ancestor (MRCA) between *A. turkestanica* and *A. vernalis* and of the MRCA between *A. volgensis* and *A. vernalis* were used for

secondary dating. The diversification within *A. vernalis* started according to this analysis with the separation of the Spanish population about 1.1 Mya (Figure 19). Within the remaining populations of *A. vernalis*, diversification started about 0.2 Mya.

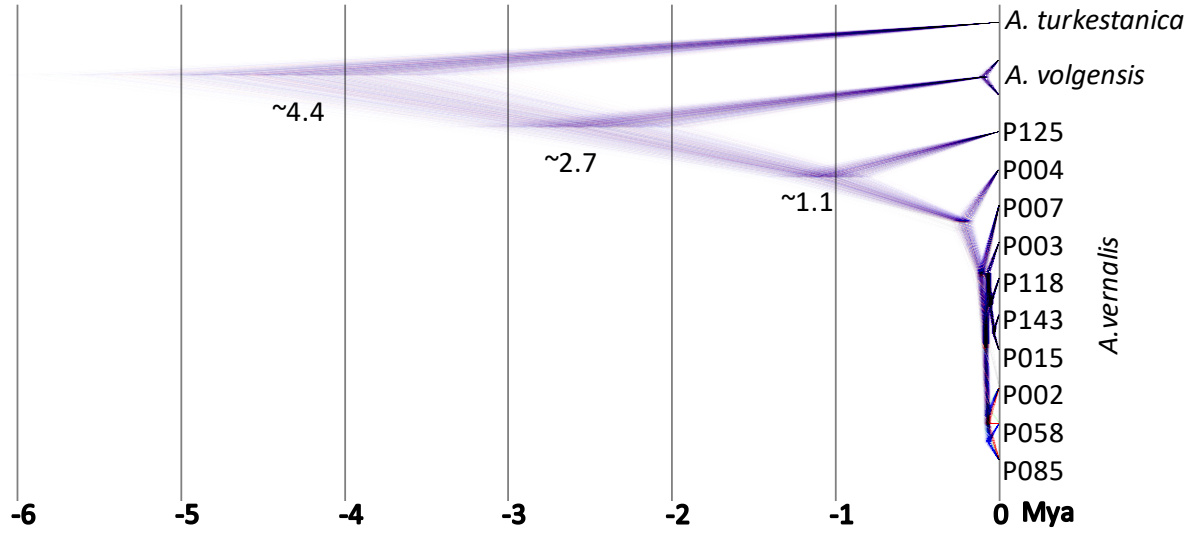

Figure 19: Molecular dating of *Adonis vernalis* (GBS) using SNAPP, visualised in DensiTree. Outgroup nodes were used for secondary dating. Diversification of *A. vernalis* started about 1.1 Mya.

Genetic cluster. In LEA, the most likely number of hypothetical ancestral populations according to the cross-entropy value was seven (Figure 20). To see the depth of splits between hypothetical ancestral populations, all numbers of hypothetical ancestral populations between two and seven were analysed.

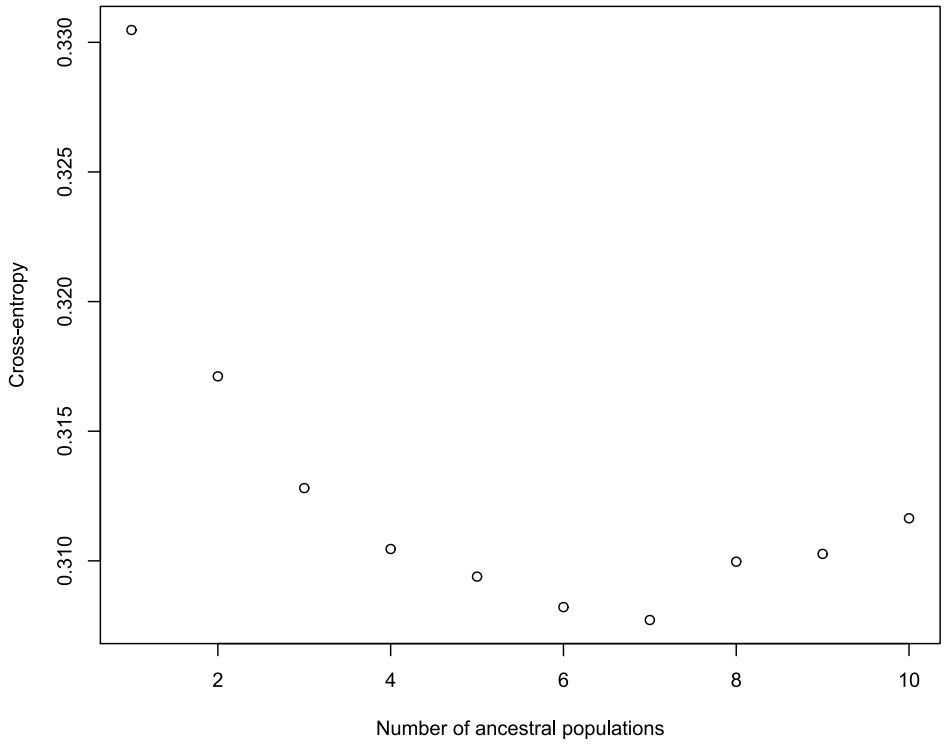

Figure 20: Cross-entropy for one to ten hypothetical ancestral populations. In LEA, ten hypothetical ancestral populations (K) were tested with 100 repetitions each. According to the cross-entropy criterion implemented in LEA to determine the optimal number of clusters, data fit best to seven distinguishable genetic lineages.

In the barplot, all individuals are sorted according to their area of origin, sorted from west to east (Figure 21). The Spanish population forms the yellow cluster. In Germany, western and eastern Pannonia, the red cluster is dominant. From the western Pontic region to the most eastern populations most individuals are assigned to the dark blue cluster. Admixture of the red and dark blue clusters is visible in eastern Pannonia and the western Pontic area. Individual clusters are present in western Pannonia (brown), western Pannonia (orange), western Siberia (light blue) and eastern Siberia (blue).

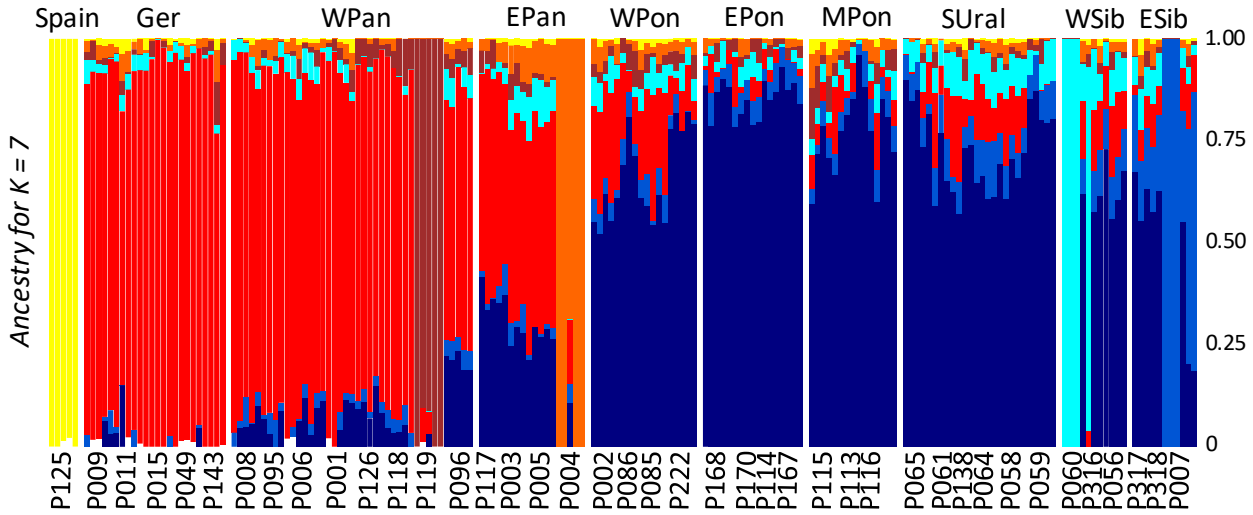

Figure 21: Genetic cluster membership of *Adonis vernalis* (GBS) as inferred using LEA is shown as a barplot. Vertical bars denote individuals. Seven clusters were retained, which are indicated by different colours. The samples are ordered by their assigned geographical region from west to east.

As visible in the pie charts (Figure 22), the first and deepest split divides the Spanish population from the others. With *K* = 3 the populations of Germany and western Pannonia split from the populations to the east of them. The fourth cluster is represented by one Romanian population (orange). With *K* = 5 and 6, two populations in the east form a cluster of their own (WSib: light blue, ESib: blue). With *K* = 7, a western Pannonian population forms its own cluster (brown).

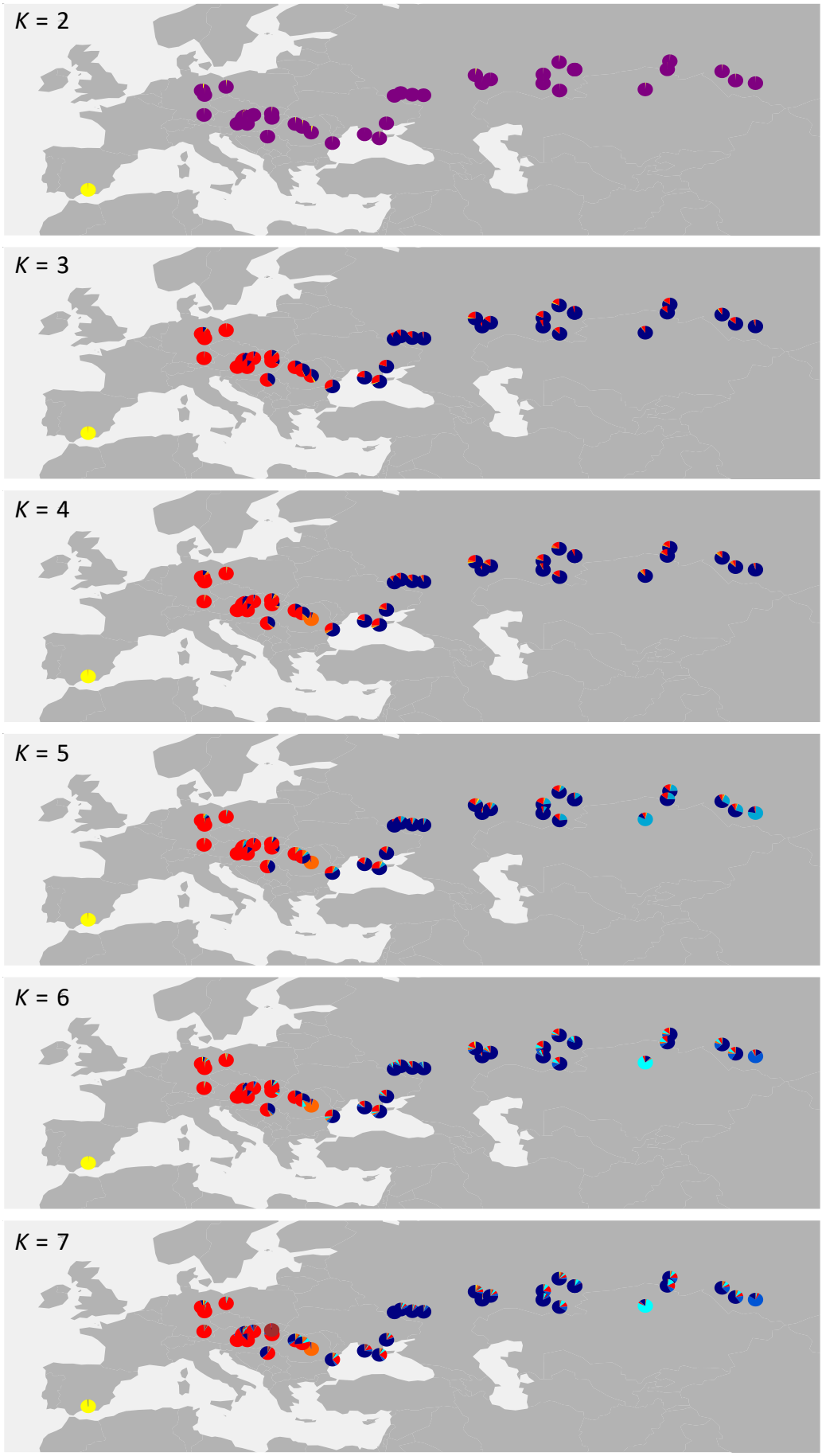
K = 2
K = 3
K = 4
K = 5
K = 6
K = 7

← Figure 22: Genetic clustering of samples of *Adonis vernalis* (GBS) as inferred by LEA is shown as pie charts for *K* = 2 to *K* = 7 clusters. The first split separates the Spanish population from the others (*K* = 2), followed by a split in Romania (*K* = 3). At *K* = 4 to 7, single or few populations form their own cluster in Western and Eastern Pannonian and in Siberia.

In the **Principal Component Analysis** (Figure 23, DAPC and Figure 24, PCOA), the Spanish population (yellow) forms its own cluster, which is clearly separated from the other populations. Within the remaining populations there is clustering visible from west to east: The range of the German populations (red) overlaps with populations of western Pannonia (brown). The eastern Pannonian populations are placed between populations west and east of them. The range of the western Pontic populations (green) overlaps with the populations of Siberia (blue and lilac shades).

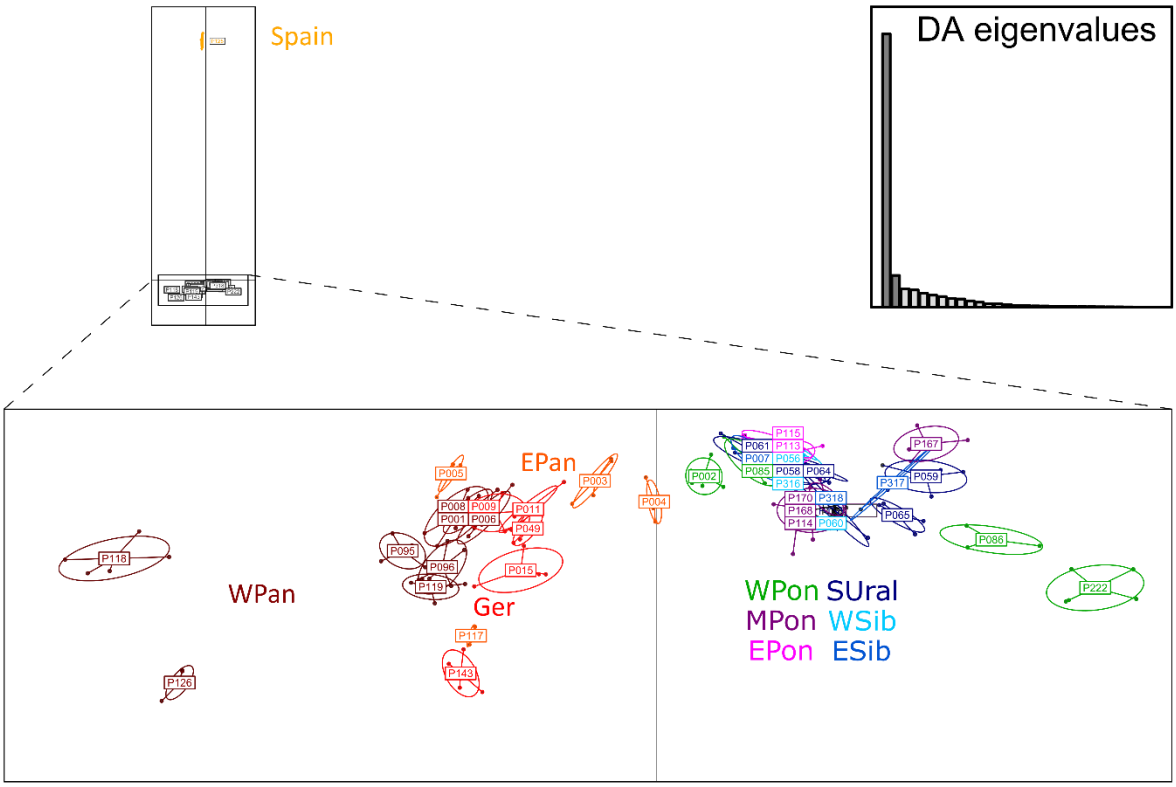

Figure 23: Genetic clustering of samples of *Adonis vernalis* (GBS) as calculated by dapc package of R. The lower part of the graph shows an enlarged section of the upper part. One cluster comprises the Spanish population. Within the second cluster, the populations are roughly separated according to their geographical degree of longitude.

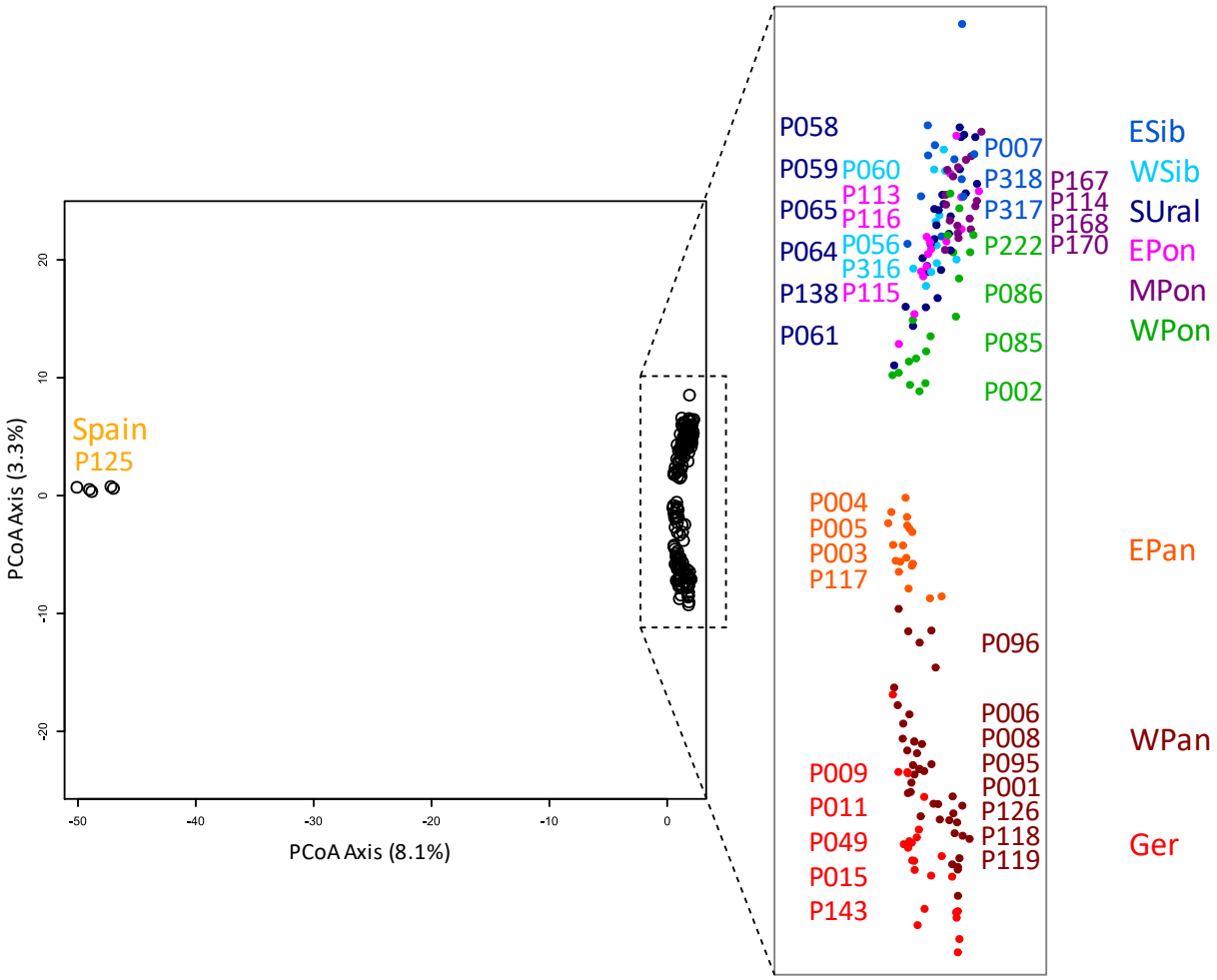

Figure 24: PCoA scatterplot of *Adonis vernalis* (GBS). Symbols representing samples of the same geographical area were coloured according to Figure 2. The right part of the graph shows an enlarged section of the left part. The Spanish population is clearly separated from the others. The remaining populations are divided according to their origin, from west to east.

Private allelic richness. Highest private allelic richness was found in Spain (0.144±0.001) (Figure 19). The second and third highest values were found in the Pontic region (MPon 0.019±0.002; EPon 0.018±0.004), while the lowest was found in Siberia (0.011±0.001; when WSib and ESib are calculated separately, the private allelic richness is 0.011±0.001 for both regions).

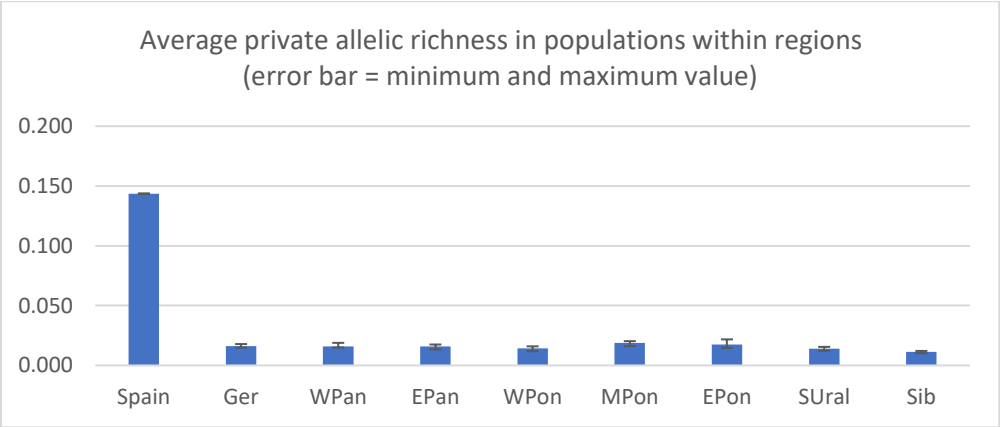

Figure 25: Private allelic richness of *Adonis vernalis* (GBS). Private allelic richness was computed for 35662 SNPs using HP-Rare. The highest private allelic richness was found in Spain.

Isolation by distance. With increasing geographical distance within all populations but the Spanish, the F_{ST} value increased significantly, affirming an isolation by distance (Figure 26).

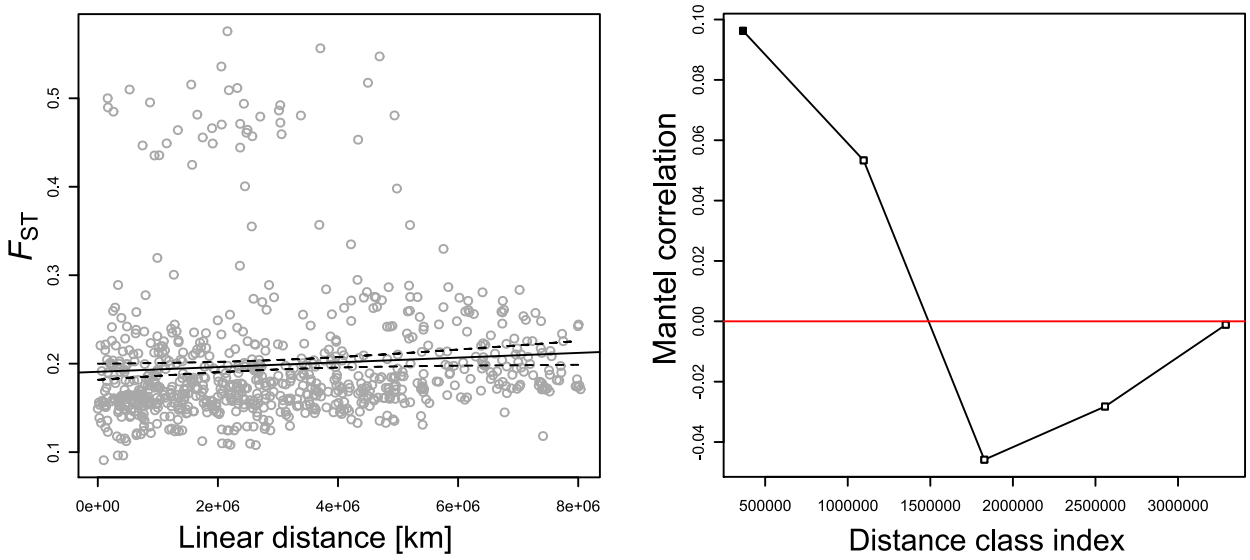

Figure 26: Isolation by distance of *Adonis vernalis* without the Spanish population (GBS). A significant isolation by distance was found.

The **expected heterozygosity** H_E was highest in populations from Germany (0.51), followed by western Pannonian (0.47) and western Siberia (0.46), and low in Spain (0.30) (Figure 27).

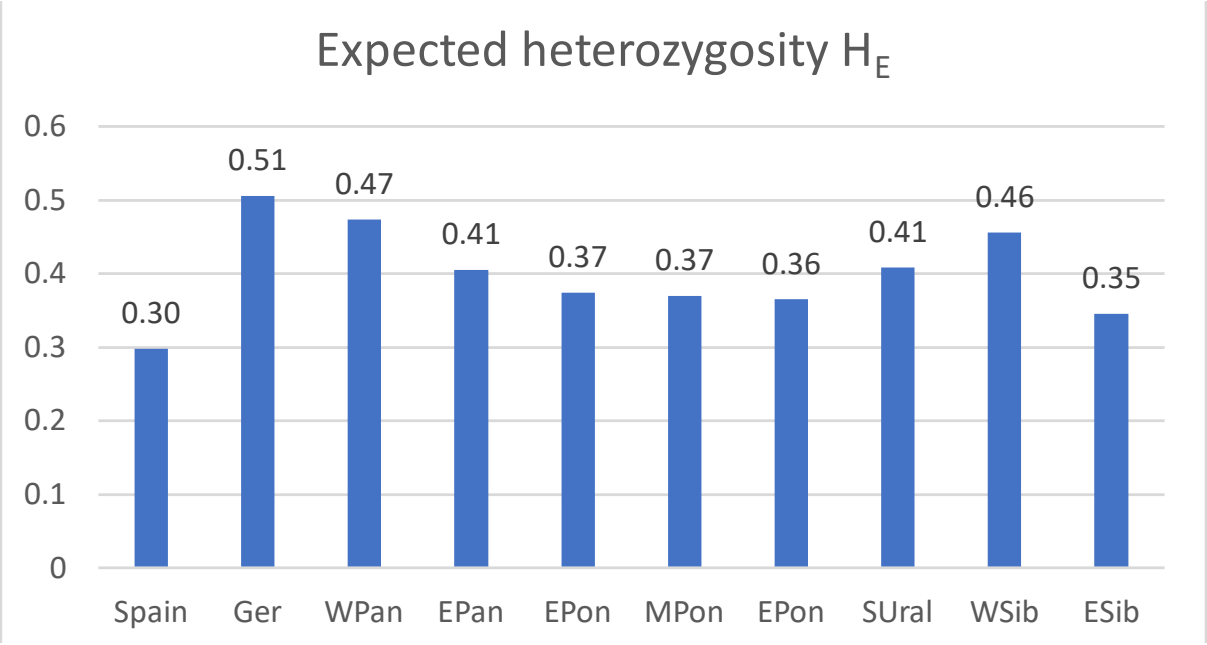

Figure 27: Expected heterozygosity of *Adonis vernalis* (GBS).

Paleoclimate modelling. The maps of modelled paleoclimate (Last Interglacial: LIG, Last glacial maximum: LGM, Heinrich Stadial 1: HS 1 and current climate: current) show suitable habitat in the Euro-Siberian part of the Eurasian steppe belt in current times (Figure 28). During the Last Interglacial, a more northern range of possible habitat was found. During the Last Glacial Maximum, only few possible refugia were present, mainly near the Black Sea and at the Mediterranean coastline. During the Heinrich Stadial 1, the suitable habitat slightly stretched from the Black Sea to the North.

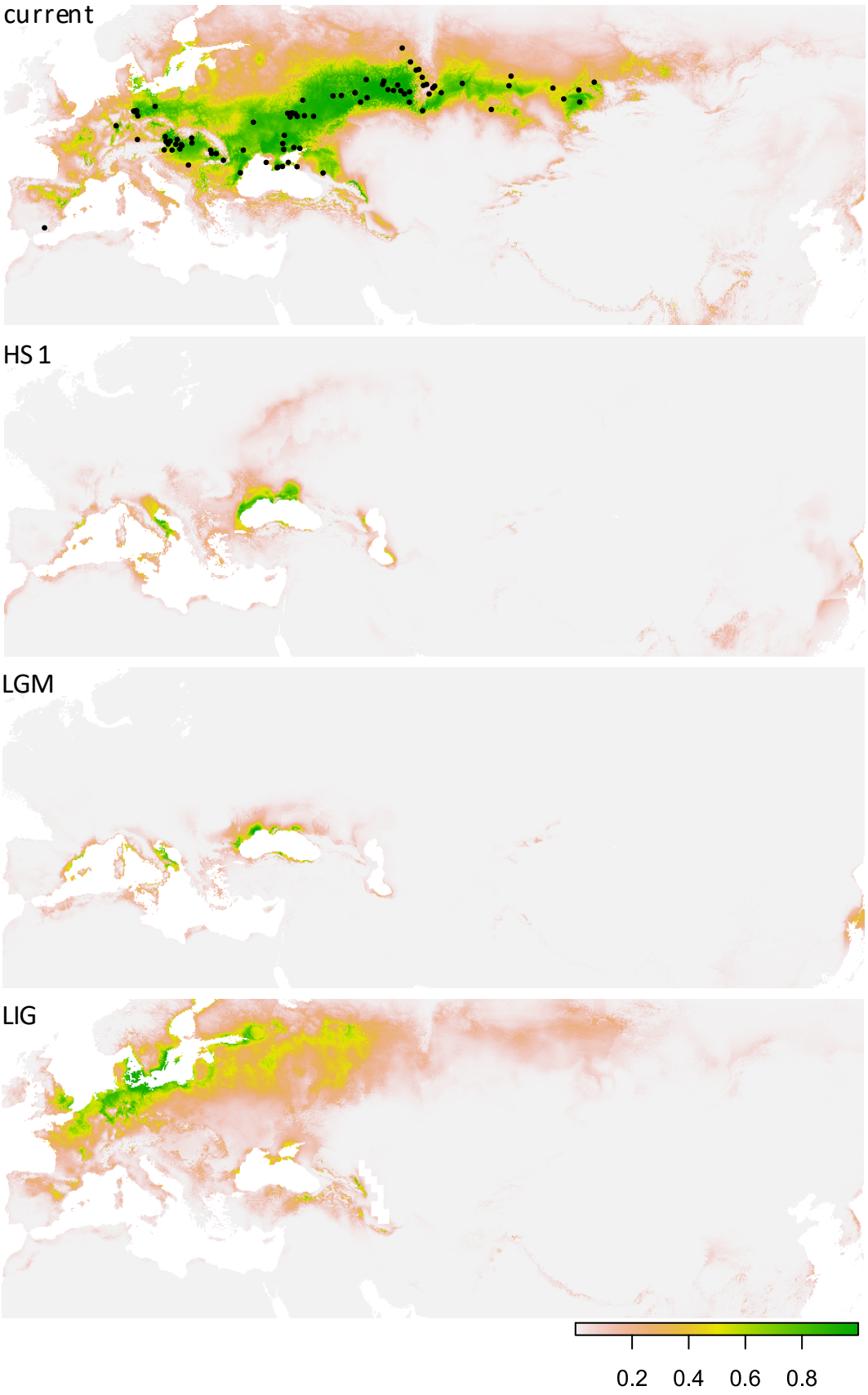

Figure 28: Paleoclimate reconstruction for *Adonis vernalis* (GBS). Reconstruction of the habitat suitability of *Adonis vernalis* at different times. Most suitable habitats are indicated in green. Used data points are indicated in the first panel ("current").

4. Discussion

I reconstructed the phylogeographic history of *Krascheninnikovia ceratoides* and *Adonis vernalis* as widespread and typical representatives of dry and forest steppes, respectively, to gain insights into the general evolutionary history of the Eurasian steppe belt. While *K. ceratoides* was able to benefit from the climatic cycles during the Pleistocene, the range of *A. vernalis* likely suffered great losses during glacial periods.

The precursors of the steppe emerged in Central Asia during the Miocene at the latest (Strömberg, 2011; Linder *et al.*, 2017; Hurka *et al.*, 2019). From there, the steppe began to spread, with numerous shifts in latitudinal range due to changing climatic conditions (Devyatkin, 1993; Arkhipov and Volkova, 1994; Tarasov *et al.*, 2000; Akhmetyev *et al.*, 2005; Arkhipov *et al.*, 2005). A continuous Eurasian steppe belt was first present in the late Miocene/early Pliocene (Hurka *et al.*, 2019). By the end of the Pliocene, true steppes were present in Central Asia, while forest-steppe assemblies were present in south-eastern Europe and on the West Siberian Plain (Frenzel, 1968). Cold steppe vegetation spread during the Pleistocene ice ages (Hurka *et al.*, 2019). Eurythermal species may have survived the last glacial maximum *in situ* (Hurka *et al.*, 2019).

4.1. Krascheninnikovia

To date, there is only one study that addresses the phylogenetic relationships, morphological variation and taxonomy within *Krascheninnikovia*, but no attempt has been made to estimate the time of origin of the genus was performed (Heklau and Röser, 2008). I reconstructed the phylogeny and biogeography of *Krascheninnikovia* and placed it in a temporal context through molecular dating. I analysed populations throughout most of its range using single loci, while focusing on populations in the Northern Hemisphere using GBS. With GBS, many more characters, loci and SNPs were found than with single locus analysis. The genetically similar groups resulting from both approaches were comparable for samples or populations of North America (P039, P040, P041) and eastern Central Asia (P093, P094, P210), each forming a clearly defined group. The GBS analysis shows a geographical trend from east to west, spanning all of western Eurasia from eastern Middle Asia to Europe; this trend is not visible in the single gene dataset.

4.1.1. Ploidy

Although the literature mentions five different ploidy levels, namely diploid, triploid, tetraploid, pentaploid and hexaploid, and the existence of populations with different ploidy levels, we only found pure diploid or tetraploid populations. However, it should be noted that the mixed population reported in the literature was found in Kyrgyzstan (Rubtsov et al., 1989) and our samples from this area could not be measured due to their age.

In most regions diploid and tetraploid populations coexist (Ghaffari et al., 2014). In Eurasia, both ploidies were present in Eastern Europe, Middle Asia, Southern Central Asia and Eastern Central Asia (Table 1, Figure 1) (Zakharjeva and Soskov, 1981; Takhtajan, 1990). Most diploid samples of eastern Middle Asia (P030, P070, P072, P269) and southern Central Asia (P237, P238) belong to the light green cluster of the LEA analysis (Figure 8), suggesting common ancestry and thus a possible second migration of diploids into these regions. The same cluster membership was also shared by the diploid individuals from central Middle Asia (P034) and Eastern Europe (P057, P062), which are admixed. Although the diploids and the tetraploids did not form well-supported clusters in the DAPC, IQ-TREE and SVDQuartets analyses (Figures 10 and 12, Appendix B), only the diploid populations of eastern

Middle Asia and southern Central Asia were well supported; the division into a predominantly diploid and a predominantly tetraploid clade in Middle Asia and adjacent regions was also found in the single gene dataset. The westward migration of *K. ceratoides* may have been accomplished by diploid individuals, followed by (auto-)polyploidization in the newly colonised areas, a process that occurred independently several times in response to climatic fluctuations in the Pleistocene (Tremetsberger *et al.*, 2009).

4.1.2. Dating

The divergence times estimated in this study are consistent with other studies. The ITS1-ITS2-ETS phylogenetic tree (Figure 5) showed a similar topology to that in Kadereit et al. 2003; 2005), and BEAST analysis dated the split between *Kraschenninnikovia*/*Ceratocarpus* and *Axyris* at 21.8 ± 6.2 Mya. A Chenopodioideae phylogeny using a relaxed molecular clock implemented in BEAST based on atpB-rbcL sequences revealed a split node age of 21.2 Mya between *K. ceratoides* and *Axyris prostrata* (Kadereit *et al.*, 2010). A BEAST analysis based on ITS sequences by Di Vincenzo et al. (2018) dated the split of *Axyris* from *Kraschenninnikovia* and *Ceratocarpus* to 25.7 Mya (14.5–36.0 Mya) and the split of *Kraschenninnikovia* from *Ceratocarpus* to 12.8 Mya (5.3–23.1 Mya; values are for birth-death tree prior and lognormal calibration prior), which is also broadly consistent with my results (15.6–28.8 Mya and 12.0–23.5 Mya).

The data support the monophyly of Axyrideae (*Kraschenninnikovia*, *Ceratocarpus* and *Axyris*) as proposed by other authors (Heklau and Röser, 2008; Kadereit *et al.*, 2010, Figure 5), as well as the sister group relationship of *Kraschenninnikovia* and *Ceratocarpus*. Kadereit et al. (2010) supported this relationship based on flower and fruit morphology, as the female flowers of *Kraschenninnikovia* and *Ceratocarpus* lack a perianth and are enclosed by two bracts that are persistent in fruit, producing only one type of fruit/seed, while *Axyris* presents a three-parted simple perianth and shows heterocarpy and heterospermy (production of seeds with different testa thickness). This contradicts the conclusions of Heklau and Röser (2008), who suggested a closer relationship of *Kraschenninnikovia* and *Axyris* based on detailed morphological, morphometric and molecular analysis.

4.1.3. Origin

Central Asia is thought to have been the cradle of Eurasian temperate grassland vegetation at the beginning of the Pleistocene (~2 Mya; Janis, 1993; Willis and McElwain, 2014), a period corresponding to the Gelasian (Gibbard *et al.*, 2010).

Due to the abundance of populations and individuals (Braun-Blanquet and Bolòs, 1957), the high and variable ploidy levels (Rubtsov *et al.*, 1989) and the high morphological variation (Rechinger, 1963; Komarov, 1964; Täckholm, 1974; Welsh *et al.*, 1987; Davis, 1988; Castroviejo and Soriano, 1990; Tutin *et al.*, 1993; Heklau, 2006; eFloras, 2008) of Central Asian populations of *Kraschenninnikovia*, it was thought to have originated there.

According to the analyses, *Kraschenninnikovia ceratoides* is an autochthonous steppe element, which originated in the steppe belt (Figures 6 and 13) similarly to some species of the genus *Allium* (Li *et al.*, 2010). Ancestral range analysis of single gene data revealed Mongolia and northern China in combination with Middle Asia to be the ancestral range of the genus (Figure 6). The ancestral area with the second highest support was Mongolia and northern China in combination with North America. Since the closest relatives of *Kraschenninnikovia*, *Ceratocarpus* and *Axyris* are distributed in Asia, it seems plausible that *Kraschenninnikovia* originated from the area of Mongolia, North China and Middle Asia, which is consistent with my result. The results of the reconstruction of the ancestral range using the GBS dataset confirmed western Central Asia with the adjacent Altai Mountains as the area of

origin (Figure 13), from where dispersal to the Northern Hemisphere began. The populations in eastern and western Central Asia harbour a diverse gene pool, as indicated by the high private allelic richness (Figure 14). Therefore, they may have served as a good source of dry steppe plants to recolonise surrounding areas after times of unsuitable, more humid conditions during interglacial periods (Crawford and Whitney, 2010). If we assume an origin in Central Asia, paleoclimate reconstruction suggests a more southern origin of the species.

Interestingly, however, one sample from Pakistan (KcPak1) is resolved as the first branching lineage within the genus in the maximum likelihood tree and network (Figures 3 and 4), but not in the Bayesian time-tree (Figure 5). This sample, together with the other samples that are resolved in the ML analysis as early branching within *K. ceratoides* (P209, KcMon2, KcMon4 and AM849251: Mongolia; P211: Kyrgyzstan; P242 and KcRus12: Russian Altai Mountains; KcNep1 and KcNep2: Nepal) suggests that the origin of *K. ceratoides* could also lie further south, for example in the Tian Shan or Pamir Mountain region, as is also suspected for other Central Asian plant groups (e.g., *Lagochilus*; M. L. Zhang *et al.*, 2017; *Ammopiptanthus*; Shi *et al.*, 2017). Due to the low quality of the extracted DNA, these samples could not be used for the GBS analysis, which focused on Northern hemisphere populations.

Barbolini et al. (2020) found that herbs, including Chenopodioideae, were first prominent in Central Asia around ~15 Mya, coinciding with diversification within the Axyrideae. According to Barbolini et al. (2020), in western Central Asia, Chenopodioideae and Artemisia have been the prominent xerophytic herbs since the late Miocene, indicating an arid habitat. Under these suitable conditions, *Kraschenninnikovia* could have diversified during the Pleistocene. These findings confirm our dated analysis, but also confirm a possible more southern origin of *Kraschenninnikovia*, such as the Pamir Mountains.

If the area of origin is not south of the Altai, colonisation of the southern parts of the range in Nepal, Pakistan and Iran probably occurred from the Mongolian and northern Chinese ancestral area in several colonisation events (Figure 6). Hexaploid individuals (2n = 54) are mainly found in the southern parts of the range of *K. ceratoides*, namely in the Pamir Mountains of Tajikistan (Zakharjeva and Soskov, 1981), in Kyrgyzstan and China (together with diploids and tetraploids; Rubtsov et al., 1989; Yang *et al.*, 1996) and in Iran (together with tetraploids; Ghaffari *et al.*, 2014). Maybe a higher (namely hexaploid) ploidy level is favourable in the dry mountain regions south of the Eurasian steppe. Possible explanations include a higher drought tolerance of polyploids (e.g., Zhou *et al.*, 2019) or, more generally, a higher tolerance of polyploids to a wider range of environmental conditions (Barron *et al.*, 1995; Van de Peer, Maere and Meyer, 2009). A similar hypothesis could be formulated for the tetraploid European populations. This recent origin is consistent with other studies showing the repeated Pleistocene differentiation opportunities that led to several events of colonisation of new areas (dispersal) and fragmentation of ancestral areas (vicariance) due to the expansion and contraction of populations during glacial-interglacial periods (*Senecio* sect. *Senecio*, Coleman *et al.*, 2003; Rana, Veith *et al.*, 2003; *Dysosma vesipellis* Cheng, Qiu *et al.*, 2009; *Ligularia hodgsonii* Hook., Wang *et al.*, 2013; *Praomys delectorum* Thomas, Bryja *et al.*, 2014).

4.1.4. Refugia

The paleoclimate models show a constant suitable habitat for *Kraschenninnikovia* in North America, the Black Sea and Caspian Sea area and mountain ranges south of the Eurasian steppe belt since the last interglacial maximum.

In western Central Asia, the Altai Mountains are known as a refuge e.g. for cold-adapted species in warm and humid phases (Fedeneva and Dergacheva, 2003; Hais *et al.*, 2015) and may have acted as refuge for steppe and desert plants such as *K. ceratoides* during the interglacial phases in the Quaternary and as source for recolonization of the expanding steppe area during glacial periods.

The ancestral populations may have survived in different refugia in the Altai Mountains during the interglacial phases. During the ice ages, there were probably several habitats in the Altai Mountains that were ideal for steppe plants (Hais *et al.*, 2015), and it is possible that some of these spots (such as intermountain depressions) were also suitable for *K. ceratoides* during the interglacial periods (Fedeneva and Dergacheva, 2003).

4.1.5. Phylogeny

Five clades were mainly found in the single gene analyses: Eurasian samples (Spain to Russia, excluding Altai Mountains, including Gobi (south Central Asia), which split into two groups (predominantly diploids and predominantly tetraploids of Eurasia)); samples of western Mongolia (western Central Asia), Nepal and Russian Altai Mountains; samples of eastern Mongolia (eastern Central Asia) and North America; samples of North America. In GBS analyses, six main clades were found: western samples (western Middle Asia, eastern Europe and Central Europe); samples of central Middle Asia; samples of eastern and southern Middle Asia and southern Central Asia (Gobi); samples of the Russian Altai Mountains and western Central Asia; samples of eastern Central Asia; samples of North America.

Comparing both approaches, the samples from the Russian Altai Mountains, Central Asia and North America especially are similarly clustered. Differences can be seen in the Eurasian region, including Gobi (southern Central Asia). While a separation by ploidy was found in the single gene approach, a geographical separation is evident in the GBS approach: the Middle Asian samples did not split according to their ploidy in the IQ-TREE analysis but showed a trend in this direction within their clade. In the LEA analysis, on the other hand, there was a trend towards separation into two clusters depending on ploidy. In GBS, the European samples clearly differ from other Eurasian samples.

4.1.6. Migration barriers

Populations of *K. ceratoides* that are geographically close to each other are usually genetically similar (Figures 3, 4, 8, 10, 11 and 12). An exception are the populations of Central Asia, which belong to two distinct genetic lineages. While geographically close to the populations of western Central Asia, separated only by the Khangai Mountains, the eastern populations are genetically more similar to the populations of North America. The Khangai Mountains (with alpine vegetation, taiga, mountain steppe and forest-steppe) separate the populations east and west of the mountains and have long prevented gene flow until today. The split occurred in the early stages of diversification (~2.1 Mya), after *Krascheninnikovia* had migrated from western Central Asia to eastern Central Asia.

Even the populations of southern Central Asia (Gobi Desert), which are located south of the Mongolian Altai Mountains, are genetically more similar to the populations of eastern Middle Asia than to other Mongolian populations. For example, the tetraploid population P235 from southern Central Asia is assigned to the dark green cluster (mainly tetraploids of Middle Asia) and the yellow cluster (populations of Altai Mountains) in the LEA analysis. This suggests that the Altai Mountains are also an effective migration barrier.

During the Middle Pleistocene, glaciers dammed the Siberian Ob-Irtysh-Tobol river system, causing backwaters that reached the foothills of the Kazakh highlands and the Altai mountains. The resulting landscape of lakes and swampy areas was not suitable for steppe plants (Arkhipov and Volkova, 1994; Arkhipov *et al.*, 2005; Hurka *et al.*, 2019). According to the dated biogeographic analyses (Figure 13), this would also have affected *K. ceratoides*, which was present in the Kazakh plain and even further west at this time, by causing a range splitting and contraction followed by isolation and subsequent expansion. Repeated secondary contact could be the explanation for the lack of monophyly of individuals of eastern Middle Asia in the RAxML tree. It has been shown that the history of other steppe

plants has also been influenced by the backwaters, as in *Clausia aprica* (Stephan) Korn.-Trotzky (Hejcman *et al.*, 2013), *Goniolimon speciosum* (L.) Boiss. (Friesen, Zerdoner Calasan, *et al.*, 2020), *Capsella* Medik. (Franzke *et al.*, 2004) and *Allium cretaceum* N.Friesen & Seregin and *A. montanostepposum* N.Friesen & Seregin (Hurka *et al.*, 2012).

South of the Ural Mountains, the repeated transgressions of the Caspian Sea, which occurred several times during the Pleistocene (Dolukhanov *et al.*, 2009; Tudryn *et al.*, 2013; Yanina *et al.*, 2018), temporarily inhibited the east-west or vice versa migration of steppe plants ((Hurka *et al.*, 2019), their Table 6). Populations in this area are located west (P215) or south (P057, P062, P101, P102) of the South Urals. These populations are genetically an admixture of both gene pools, east and west of the Urals (Figure 8). The proportion of admixture gradually decreases in both directions, possibly due to secondary contact. According to the paleoclimatic model, the area north of the Caspian Sea was not suitable for *Krascheninnikovia* during the Heinrich Stadial 1, which may also have deepened the genetic differences.

4.1.7. Migration events

During the Pleistocene ice ages, plants adapted to cold and arid climate were able to migrate in the expanding steppe area. Consequently, the hypothesis of radiation and diversification of *K. ceratoides* suggests that during the Pleistocene, when the steppe area expanded during glacial periods, populations in the contact zone between western Mongolia, China and Middle Asia migrated (1) westwards, reaching Middle Asia, Europe, Anatolia and northern Africa and (2) eastwards, reaching eastern Mongolia and North America (Figures 6 and 13).

In the single gene dataset, the samples west of the Altai Mountains split into two lineages (Figures 3 and 6). The first lineage consists of predominantly tetraploid Eurasian samples (PP = 0.99) that colonised Eastern and Western Europe, Anatolia and northern Africa from Middle Asia about 650,000 years ago. The second lineage showed a basal separation into a group of predominantly diploid Eurasian samples (PP = 0.98) and another group that originated east of the Altai Mountains (with North America; PP = 0.18). The group of predominantly diploid Eurasian samples colonised Siberia and Eastern Europe from Mongolia and northern China about 680,000 years ago. Interestingly, both Eurasian groups seem to have spread but did not mix in Eurasia during the same ice ages. This could be due to the different levels of ploidy or because the two lineages evolved independently in different habitats during the interglacial period.

The relationship within the European populations is not so clear, as the bootstrap support is low (Figure 12). While in the RAxML analysis both Austrian populations are separated, suggesting two migration events from Eastern Europe to Central Europe, the SVDQ analysis hints to a single migration event. In LEA, one Austrian population (P029) forms its own cluster, while the other population (P028) is clustered with the other tetraploids of Europe (dark green cluster). Therefore, no final conclusion can be drawn about the number of migration events and the relationships within Europe.

Regarding the question of how and when Central Europe was colonized by *Krascheninnikovia*, the data argues for a stepping-stone like migration over a long-distance dispersal scenario, as in the ancestral range reconstruction a stepwise colonization from the Altai Mountains to Central Europe was found. In the ancestral range reconstruction of the single locus dataset (Figure 6), a migration from Central Asia via Middle Asia to Europe was also detected, but not as clear as in the analysis of the GBS dataset (Figure 13), as the European samples did not form a monophyletic group. A stepping-stone like migration to Central Europe would indicate that during glacial periods, possibly existing trees grew in patches - as opposed to dense tree cover (Willis and Vanandel, 2004), so that the steppe and semi-desert plant *Krascheninnikovia* could migrate step by step.

The colonisation of the western Mediterranean by *K. ceratoides* has long occupied researchers (Willkomm and Lange, 1870; de Bolòs, 1951; Braun-Blanquet and Bolòs, 1957; Costa Tenorio, Morla-Juaristi and Sáinz-Ollero, 2000) and two hypotheses for natural colonisation have been proposed (stepping-stone migration from Central Asia to the western Mediterranean in the Miocene or Pliocene versus migration or long-distance dispersal from Central Asia in the Quaternary; Braun-Blanquet and Bolós, 1957; Costa Tenorio et al., 2000; Pérez-Collazos and Catalán, 2007; Pérez-Collazos et al., 2009). The results suggest a relatively recent colonisation of the Mediterranean Basin in the Late Pleistocene (Hurka et al., 2019). The poor branch support does not allow us to specify with certainty the number of events and the source area(s) for the colonisation of the Mediterranean. Therefore, we cannot unambiguously determine the nature of the migration. However, since suitable (loess-rich) habitats existed between the Altai Mountains and western Europe during the glacial periods (Lang, 1994) and are still suitable today, as shown by the isolated populations between Asia and the Mediterranean (Austria and Romania), a stepping-stone scenario seems to be the simplest explanation. According to this hypothesis, the species extended its distribution area westwards during the glacial periods and survived in suitable, arid habitats during the interglacial periods. The genetic differences between the Mediterranean populations could be the result of their divergence during the interglacial periods or alternative migration routes separated in time or space. The stepping-stone scenario has been proposed for other steppe plants with disjunct Mediterranean distribution areas (Kadereit and Emre Yaprak, 2008). However, as some Mediterranean plants have a shared identical sequence with plants from Egypt, this study could not exclude the hypothesis of the eighth century introduction of *K. ceratoides* to the western Mediterranean as a fuel and forage plant by the Arabs (Willkomm, 1896; Costa Tenorio, Morla-Juaristi and Sáinz-Ollero, 2000).

The results of the GBS dataset indicates that *Kraschenninnikovia* migrated step by step from the Altai Mountain to Middle Asia and to Europe (~1.2 Mya). Then the European populations became separated from the populations east of the Urals ~1 Mya (Figure 13). The early split between the European populations and the populations east of it in the LEA and DAPC analyses also supports this hypothesis. The genetic split could be traced back to a migration barrier ~1 Mya that coincided with the Apsheron transgression of the Caspian Sea (Hurka *et al.*, 2019), suggesting that the separated populations each found refugia to survive the interglacial phases in the Ural mountains (Friesen, Smirnov, *et al.*, 2020; Friesen, Zerdoner Calasan, *et al.*, 2020) and west of the Caspian Sea (Varga, 2009; Stewart *et al.*, 2010; Friesen, Zerdoner Calasan, *et al.*, 2020) with a recent secondary contact in the zone south of the Urals. The same separation pattern was observed for the steppe plant *Camelina microcarpa* Andrz. Ex DC. in the same time frame (~1.2 ± 1 Mya) (Volkova, Herden and Friesen, 2017).

The hypothesis of a migration from Eastern Central Asia to North America put forward by Heklau and Röser (2008) was confirmed. The dispersal to North America may have occurred across the Beringia Strait, which connected the Asian and American continents during several arid glacial phases in the Pleistocene (Briggs, 1995; Yurtsev, 2001).

According to single gene analysis, two migration events from Asia to America seem to have taken place, starting from Mongolian and northern Chinese ancestral populations. Biogeographic analysis indicates a dispersal (E-F in Figure 6) and separate range expansion (E-EF; each with a posterior probability of 1.00 on the time-calibrated tree; Figure 5) from the ancestral Mongolian range across the Pacific Ocean during the Pleistocene between ∼1.8 and ∼0.5 Mya. At this time, steppe biomes existed in North America (Webb, 1977; Willis and McElwain, 2014) and the region could be reached via the Bering Strait. During the arid Pleistocene glaciation phases, a Beringian land bridge was established between Siberia and North America, which probably facilitated the passage of steppe plants (Briggs, 1995; Yurtsev, 2001). The ML analysis (Figure 4), however, does not support two separated North American groups. This is also consistent with the haplotype network analysis of chloroplast sequences, which only showed one group of related haplotypes for the New World, where the most common haplotype is represented by samples assigned to either of the two independent North American groups in the dated analysis (KL22 versus KL01 and KL19)(Seidl *et al.*, 2020). The answer to the question of single (Heklau

and Röser, 2008) or double colonisation of North America must therefore await analysis of more variable genetic markers. The existence of diploids and tetraploids in both Asia and America has been interpreted as independent polyploidisation processes (Heklau and Röser, 2008).

In the analyses of the GBS dataset, the populations of North America (USA) and eastern Central Asia (eastern Mongolia) form sister groups in the phylogenetic inferences (Figure 12), are genetically close (Figures 8 and 9) and form strongly supported clades or clusters (Figures 8, 10, 11, 12 and 13), which could be an indication of low or absent gene flow between the North American and other populations. Continuous gene flow or multiple migration events could not be detected due to insufficient coverage of the North American populations of *Krascheninnikovia*. Diversification within the studied populations of America occurred about 0.2 Mya. Comparison of the samples used in both datasets shows that the American samples (P039, P040, P041) and the populations of East Central Asia (P093, P094, P210) form a monophyletic clade in both data sets, but in contrast to the results of single gene analysis with the GBS dataset both clades are sisters and are closer to the root. In both datasets *K. ceratoides* subsp. *lanata* was nested within *K. ceratoides* subsp. *ceratoides* (Figures 4 and 12).

4.1.8. Subspecies

There is an ongoing debate about possible subspecies and species in the genus *Krascheninnikovia*. While some argue that *Krascheninnikovia* is monospecific with only two subspecies, *K. ceratoides* subsp. *ceratoides* and subsp. *lanata* ((Heklau and von Wehrden, 2011), I follow this view), others distinguish several entities at the specific level, like *K. arborescens*, *K. eversmanniana* and *K. compacta* from Middle and Central Asia (Braun-Blanquet and Bolòs, 1957; Tutin *et al.*, 1993; Fedeneva and Dergacheva, 2003; Ghaffari *et al.*, 2014; Hais *et al.*, 2015). As we did not include samples of all these potential taxa, apart from two populations identified as *K. eversmanniana* (P069 and P070), this study cannot be conclusive on this topic. However, the results of our analyses support the recognition of the subspecies *lanata* as defined by Heklau and Röser (2008), as the North American individuals form a clearly distinguishable genetic lineage. The data do not support the affiliation of the specimens identified as *K. eversmanniana* to a clade of their own, as they are embedded at different positions between morphologically typical specimens of subsp. *ceratoides* from eastern Middle Asia. A potential further subspecies could be represented by the samples from eastern Central Asia, which were clearly monophyletically arranged in all analyses. However, thorough morphological studies are needed to confirm this hypothesis. Therefore, we agree with the conclusions of Heklau and Röser (2008), who (currently) recognise two subspecific entities, i.e. subsp. *ceratoides* and subsp. *lanata* within the monotypic *Krascheninnikovia*.

4.2. Adonis vernalis

As *Adonis vernalis* is a suitable species for intraspecific studies due to its limited dispersal distance, the phylogeny and genetic differentiation of *A. vernalis* were investigated in at least two studies using AFLPs. I analysed populations of the entire range of *A. vernalis* using genotyping-by-sequencing methods to learn more about the biogeographical history of the species.

The optimal habitat of *A. vernalis* is dry, warm and with no or only light tree cover. According to the paleoclimate models, suitable habitats for *A. vernalis* existed in Europe during the interglacial stages of the Pleistocene. During glacial phases, these conditions could only be found on Black Sea coast and on the European Mediterranean coasts. During the Holocene, suitable habitat extended to Europe and to Siberia (Figure 28).

4.2.1. Phylogeny

The analyses show a large genetic distance between the Spanish and all other populations (Figures 17, 19, 21, 23 and 24). The Spanish population is the sister group to all other populations (Figures 17 and 18). No gene flow involving this population was detected within the data set. Moreover, the high value of private allelic richness in the Spanish population (Figure 25) indicates a long in situ history (Médail & Diadema, 2009). The clear separation of the Spanish populations, also observed by Hirsch (2015), occurred around 1.5 Mya (Figure 18) or around 1.1 Mya (Figure 19) during the Calabrian. Within the other populations, two main groups are visible: western (Germany to Pannonia) and eastern (Pontic to Siberia) populations (Figures 17, 18, 19, 21, 22, 23 and 24), with the Romanian population P002 belonging to the eastern group.

4.2.2. Origin

Since the most recent common ancestor of *A. vernalis* and the closely related species *A. volgensis* originates from Asia (with a differentiation of about 2.66 My) (Lindhuber, 2020), one could assume an Asian origin. However, the common Spanish and Romanian origin raises questions. It suggests a European origin but does not allow any further conclusions. Whether *A. vernalis* first appeared in the west (Spain) or east (Romania) of Europe or elsewhere remains unknown. It is also unclear whether *A. vernalis* was continuously distributed between Romania and Spain before the partition. It is possible that, at a certain point in time, only the source populations of Spain and Romania survived in refugia from an assumed wider distribution, while all other assumed populations died out. Further contact between the populations was no longer possible, resulting in the genetic differences visible in today's populations (Figures 17, 19, 22, 23 and 24).

Consequently, *A. vernalis* migrated from its area of origin once through western and central Europe (direction unclear) before almost all populations died out. Then a second migration started from Romania. The broad extinction may be a consequence of inhospitable conditions during the ice age, or the increased precipitation and higher humidity caused by the melting glaciers in the transition from the glacial to the interglacial states.

The same pattern was found in other European species whose populations survived the ice age in different refugia. The populations of the lepidoptera *Maniola jurtina*, for example, were separated during the ice age, which led to a differentiation between populations of the Iberian Peninsula and of Adriatic- and Pontic-Mediterranean origin. Central Europe was then colonised post glacial (Schmitt, 2007). The same biogeographical history could also be shown for the Lepidoptera *Polyommatus coridon* (Kühne *et al.*, 2017) and the conifer *Pinus sylvestris* (Cheddadi *et al.*, 2006).

4.2.3. Migration

If one assumes mainly barochory and myrmecochory as mode of dispersal for *Adonis vernalis*, the range of the species is very limited and the colonisation of the current distribution range would require a long time, even assuming continuous habitat. Perhaps greater distances were overcome through zoochory, whereas epizoochory is more likely than endozoochory due to the toxicity of the plant. Conceivable here, but not yet proven, is transport via the hoofs of grazing ungulates (Schulze, Buchwald and Heinken, 2014), or by mammals, in whose fur the seeds could get caught on their small hooks (Albert *et al.*, 2015), or by birds, which could have transported the seeds under their feet.

From Spain, no migration to other countries took place according to my analyses, but there are stable populations of *A. vernalis* until today, resulting in a high genetic differentiation and low expected heterozygosity (Figure 27). Starting from eastern Pannonia about 210 kya (Figure 19) (Chibanian,

Middle Pleistocene, Riss ice age), *A. vernalis* spread westwards and eastwards, resulting in genetically distinct clusters (Figure 13). A similar relationship was found in Hirsch et al. (2015), where Romanian populations were placed in the network between populations west and east of Romania. As Kropf et al. (2020) conclude, the population history in Romania might be characterized by large and stable population sizes, which would fit our hypothesis that populations in eastern Pannonia served as a source of colonization since the late Pleistocene. Hirsch et al. (2015) found highest values of expected heterozygosity in Romania and Ukraine, which also suggests the eastern Pannonian region as the source area. However, the calculated values of expected heterozygosity of the data in this study were about the same in western Pannonia and the Middle Pontic region, the eastern Pontic area and eastern Siberia. The lowest values were found in Spain, as in Hirsch et al. (2015) (Figure 27). Hirsch et al. (2015) divided the populations into central (Russian), intermediate (Ukraine and Romania) and peripheral (Central Europe and Spain) populations. Based on my results - and supported by their own H_E and PPB values - I would define the Ukrainian and Romanian populations as central, while all other populations are peripheral.

Starting from eastern Pannonia, *A. vernalis* colonised the Eurasian steppe belt. Moving westwards, it reached Germany about 86 kya during the Würm ice age (late Pleistocene) and probably expanded its range up to northern Germany after the retreat of the glaciers in the north (Figure 13). The relationships within European populations found in this study correspond to those of Kropf et al. (2020).

In southern Germany, *A. vernalis* is found in isolated habitats such as the Garchinger Heide near Munich, which was formed from gravel transported by the Alpine glaciers. During the last glacial maximum, the glaciers reached almost as far as Munich. The gravel provided a nutrient-poor, dry habitat and enabled the area to persist to this day as a habitat for endangered and rare plans from the Mediterranean and Pontic-Pannonian region as well as for alpine species, as it was not easy to cultivate and too dry for trees to grow, thus providing a habitat that lasted for centuries. *Adonis vernalis* may have reached the Garchinger Heide during the Würm glaciation about 86 kya.

A migration wave from eastern Pannonia towards the east took place around 119 kya during the Upper/Late Pleistocene, reaching the Pontic region and Siberia (Figure 18). In contrast to the western populations, the eastern populations did not show a clear separation due to geographic distance (Figures 23 and 24). This could be a consequence of a more contiguous habitat and consequently a constant gene flow in the east.

Genetic differentiation in the species studied correlates with the geographic distance of the populations, as shown by the Mantel test, confirming a mechanism of isolation by distance (Figure 26).

Probably at some point in the Mid Pleistocene there was a continuous steppe habitat suitable for thermophilic steppe plants from Eastern Europe or even Asia to Spain, where *A. vernalis* could migrate from east to west and reach Spain. Perhaps due to the increased humidity after the melting of the glaciers, *A. vernalis* lost a large part of its supposed habitat and remained only in refuges in Spain and eastern Pannonian. From Romania, the expansion of the present distribution area took place, starting during the last ice age (Figure 18). Today, the central European habitats are fragmented and their relationship to each other clearly depends on their geographically distance, while the populations in the east are not as clearly structured, perhaps due to the more continuous habitat.

5. Conclusio

Since the steppe developed first in Central Asia and only after that in Europe, old steppe plants are expected to share this part of steppe history: An origin in Central Asia, followed by a spread to the west in the Eurasian steppe belt, as seen in some species of the genus *Allium* (Li *et al.*, 2010). This could be shown for the autochthonous and old steppe species *Kraschenninnikovia*.

In contrast, younger steppe species may also have originated in Europe and migrated from Europe eastward to Asia. We could observe this in *A. vernalis*, which probably originated in Europe and migrated from eastern Pannonia to the east and thus to Asia. However, we could also detect a western migration to Germany in this species, which suggests that *A. vernalis* spread in the already existing steppe area and did not spread with the expanding steppe like possibly *Kraschenninnikovia*.

The Altai Mountains could be an important refuge for *Kraschenninnikovia*. It may have survived the millions of years between diversification and dispersal, retreating to possibly more southern mountains until climatic conditions were ideal for dispersal to the plains. However, the range of *A. vernalis* does not extend that far east, so the Altai Mountains did not play a role in the evolutionary history of the species. For *A. vernalis*, the Black Sea coast and areas in Romania and Spain seem to be important refuges.

The repeated transgressions of the Caspian Sea have left traces in the genetic structure of the populations of *Kraschenninnikovia*: A separation of the populations in this area over a longer period of time can be assumed due to the split in LEA. Some populations of *Kraschenninnikovia* may have survived the transgressions in Europe, while others may have found refuge in the southern Ural Mountains, for example. We cannot see this pattern in *A. vernalis*. Perhaps the species was not so widespread at that time, or the eastern populations died out during transgression.

While *Kraschenninnikovia* apparently benefitted from the changing climate in the Pleistocene, *Adonis vernalis* faced major habitat losses during glacial phases. The paleoclimatic models showed a broad range of suitable habitat for *Kraschenninnikovia*, while *Adonis vernalis* would have been restricted to Mediterranean and Black Sea coast lines during glacial phases.

While the origin of the Austrian *Kraschenninnikovia* populations is not completely clear and anthropogenic influence cannot be excluded, *A. vernalis* seems to have colonised Europe naturally. However, it could only survive in steppe-like areas and therefore had to retreat to such areas due to the changing climate. This may have led to today's fragmented distribution of populations, whose genetic information suggests a natural, gradual migration to the northwest. The limited dispersal possibilities of *A. vernalis* (a few metres per year) speak for a once continuous (meadow) steppe area in Europe, which was then scattered, separating *Adonis* populations from each other. The fact that *Kraschenninnikovia* also has old occurrences in today's comparatively humid Europe could indicate that the steppe in Europe used to be very dry and changed over time into a wetter steppe, in which *A. vernalis* was then able to expand.

References

Akhmetyev, M. A. *et al.* (2005) 'Chapter 8: Kazakhstan and Central Asia (plains and foothills)', in *Cenozoic Climatic and Environmental Changes in Russia*. Geological Society of America. doi: 10.1130/0-8137-2382-5.139.

Aktaeva, M. K. (1973) 'Kariologija i morfologicheskij analiz roda Krascheninnikovia Gueldenst. (Eurotia Adans.) [in Russian]', *Izv. Akad. Nauk Kazakh. S.S.R.*, (Ser. Biol. 6), pp. 4–6.

Albert, A. *et al.* (2015) 'Using basic plant traits to predict ungulate seed dispersal potential', *Ecography*, 38, pp. 440–449. doi: 10.1111/ecog.00709.

Arkhipov, S. A. *et al.* (2005) 'Chapter 4: West Siberia', in *Cenozoic Climatic and Environmental Changes in Russia*. Geological Society of America. doi: 10.1130/0-8137-2382-5.67.

Arkhipov, S. A. and Volkova, V. S. (1994) *Geological history of Pleistocene landscapes and climate in West Siberia*. Novosibirsk.

Augusto Corrêa dos Santos, R., Goldman, G. H. and Riaño-Pachón, D. M. (2017) 'ploidyNGS: Visually exploring ploidy with Next Generation Sequencing data', *Bioinformatics*, 33(16), pp. 2575–2576. doi: 10.1093/bioinformatics/btx204.

Baldwin, B. G. and Markos, S. (1998) 'Phylogenetic utility of the external transcribed spacer (ETS) of 18S–26S rDNA: congruence of ETS and ITS trees ofCalycadenia (Compositae)', *Molecular phylogenetics and evolution*, 10(3), pp. 449–463.

Bara, I., Rugina, R. and Bara, C. (2003) 'The chromosomal number for rare species from Romania', *Journal of Experimental and Molecular Biology*, 4.

Barbolini, N. *et al.* (2020) 'Cenozoic evolution of the steppe-desert biome in Central Asia', *Science Advances*, 6(41), p. eabb8227. doi: 10.1126/sciadv.abb8227.

Barnes, M. (2009) *The effect of plant source location on restoration success: A reciprocal transplant experiment with winterfat (*Krascheninnikovia lanata*)*. University of New Mexico. Available at: https://digitalrepository.unm.edu/biol_etds/4.

Barron, E. J. *et al.* (1995) 'A "simulation" of Mid-Cretaceous climate', *Paleoceanography*, 10(5), pp. 953–962. doi: https://doi.org/10.1029/95PA01624.

Basinger, J. F., Greenwood, D. R. and Sweda, T. (1994) 'Early Tertiary Vegetation of Arctic Canada and Its Relevance to Paleoclimatic Interpretation BT - Cenozoic Plants and Climates of the Arctic', in Boulter, M. C. and Fisher, H. C. (eds). Berlin, Heidelberg: Springer Berlin Heidelberg, pp. 175–198.

Beerling, D. J. and Royer, D. L. (2011) 'Convergent Cenozoic CO2 history', *Nature Geoscience*, 4(7), pp. 418–420. doi: 10.1038/ngeo1186.

Bivand, R., Keitt, T. and Rowlingson, B. (2021) 'rgdal: Bindings for the "Geospatial" Data Abstraction Library'. Available at: https://cran.r-project.org/package=rgdal.

Bivand, R. and Rundel, C. (2020) 'rgeos: Interface to Geometry Engine - Open Source ('GEOS')'. Available at: https://cran.r-project.org/package=rgeos.

Blair, J. and Briggs, J. (2014) 'Grassland Ecology', *Ecology and the Environment*, pp. 389–423. doi: 10.1007/978-1-4614-7501-9_14.

de Bolòs, O. (1951) 'Algunas consideraciones sobre las especies esteparias en la Península Ibérica', in *Anales del Jardín Botánico de Madrid*. Real Jardín Botánico, pp. 445–453.

Bouckaert, R. *et al.* (2014) 'BEAST 2: a software platform for Bayesian evolutionary analysis', *PLoS*

Comput Biol, 10(4), p. e1003537.

Bouckaert, R. R. and Heled, J. (2014) 'DensiTree 2: Seeing Trees Through the Forest', *bioRxiv*, p. 12401. doi: 10.1101/012401.

Bradley, M. (2018) 'raxml_ascbias', *GitHub https://github.com/btmartin721/raxml_ascbias*. Available at: https://github.com/btmartin721/raxml_ascbias.

Braun-Blanquet, J. and Bolòs, O. (1957) 'Les groupements végétaux du bassin moyen de l'Ebre et leur dynamisme', *Anales de la Estación Experimental de Aula Dei*, 5, pp. 1–266.

Bredenkamp, G. J., Spada, F. and Kazmierczak, E. (2002) 'On the origin of Northern and Southern Hemisphere grasslands', *Plant Ecology*, 163, pp. 209–229. doi: 10.1023/A:1020957807971.

Briggs, J. C. (1995) 'Chapter 7 Neogene', in Briggs, J. C. (ed.) *Global Biogeography*. Elsevier (Developments in Palaeontology and Stratigraphy), pp. 147–189. doi: https://doi.org/10.1016/S0920-5446(06)80057-9.

Britton, T. *et al.* (2007) 'Estimating divergence times in large phylogenetic trees', *Systematic Biology*, 56(5), pp. 741–752. doi: 10.1080/10635150701613783.

Brummitt, R. (2001) *World geographical scheme for recording plant distributions*. 2nd edn.

Bryja, J. *et al.* (2014) 'The role of dispersal and vicariance in the pleistocene history of an east african mountain rodent, Praomys delectorum', *Journal of biogeography*, 41(1), pp. 196–208.

Büchner, S. *et al.* (1965) 'A new glycoside of Adonis Vernalis', *Life Sciences*, 4(1), pp. 37–39. doi: https://doi.org/10.1016/0024-3205(65)90029-9.

Cardoso, P. (2020) 'red: IUCN Redlisting Tools'. Available at: https://cran.r-project.org/package=red.

Castroviejo, S. and Soriano, C. (1990) '*Krascheninnikovia ceratoides* Gueldenst', *Flora Ibérica II. Madrid: Servicio de Publicaciones del CSIC*.

Catchen, J. *et al.* (2013) 'Stacks: An analysis tool set for population genomics', *Molecular Ecology*, 22(11), pp. 3124–3140. doi: https://doi.org/10.1111/mec.12354.

Caves Rugenstein, J. *et al.* (2014) 'Aridification of Central Asia and uplift of the Altai and Hangay Mountains, Mongolia: Stable isotope evidence', *American Journal of Science*, 314, pp. 1171–1201. doi: 10.2475/08.2014.01].

Cheddadi, R. *et al.* (2006) 'Imprints of Glacial Refugia in the Modern Genetic Diversity of Pinus sylvestris', *Global Ecology and Biogeography*, 15(3), pp. 271–282. Available at: http://www.jstor.org/stable/3697589.

Chen, B. *et al.* (2014) 'The impact of climate change and anthropogenic activities on alpine grassland over the Qinghai-Tibet Plateau', *Agricultural and Forest Meteorology*, 189–190, pp. 11–18. doi: https://doi.org/10.1016/j.agrformet.2014.01.002.

Chen, C. *et al.* (2014) 'Understanding the formation of Mediterranean–African–Asian disjunctions: evidence for Miocene climate-driven vicariance and recent long-distance dispersal in the Tertiary relict S milax aspera (Smilacaceae)', *New Phytologist*, 204(1), pp. 243–255.

Cheng, Y. *et al.* (2020) 'Climate-Driven Holocene Migration of Forest-Steppe Ecotone in the Tien Mountains', *Forests* . doi: 10.3390/f11111139.

Chifman, J. and Kubatko, L. (2014) 'Quartet inference from SNP data under the coalescent model', *Bioinformatics (Oxford, England)*. 2014/08/07, 30(23), pp. 3317–3324. doi: 10.1093/bioinformatics/btu530.

Cohen, K. M. and Gibbard, P. L. (2019) 'Global chronostratigraphical correlation table for the last 2.7 million years, version 2019 QI-500', *Quaternary International*, 500, pp. 20–31. doi:

10.1016/j.quaint.2019.03.009.

Coleman, M. *et al.* (2003) 'Repeat intercontinental dispersal and Pleistocene speciation in disjunct Mediterranean and desert Senecio (Asteraceae)', *American Journal of Botany*, 90(10), pp. 1446–1454.

Costa Tenorio, M., Morla-Juaristi, C. and Sáinz-Ollero, H. (2000) 'Fitoecología y corología de Krascheninnikovia ceratoides en el valle del Ebro', *Memorias del Congreso de Botánica en homenaje a Francisco Loscos. Instituto de Estudios Turolenses, Teruel*.

Crane, P. R., Friis, E. M. and Pedersen, K. R. (1995) 'The origin and early diversification of angiosperms', *Nature*, 374(6517), pp. 27–33. doi: 10.1038/374027a0.

Crawford, K. M. and Whitney, K. D. (2010) 'Population genetic diversity influences colonization success', *Molecular Ecology*, 19(6), pp. 1253–1263. doi: 10.1111/j.1365-294x.2010.04550.x.

Darriba, D. *et al.* (2012) 'jModelTest 2: more models, new heuristics and parallel computing', *Nature methods*, 9(8), p. 772.

Davis, P. H. (1988) *Flora of Turkey and the east Aegean islands*. Edinburgh: Edinburgh University Press.

Dengler, J. *et al.* (2014) 'Biodiversity of Palaearctic grasslands: A synthesis', *Agriculture, Ecosystems & Environment*, 182, pp. 1–14. doi: 10.1016/j.agee.2013.12.015.

Denisow, B., Wrzesien, M. and Cwener, A. (2014) 'Pollination and floral biology of Adonis vernalis L.(Ranunculaceae)-a case study of threatened species', *Acta Societatis Botanicorum Poloniae*, 83(1).

Devyatkin, E. V. (1993) 'Meridional distribution of Pleistocene ecosystems in Asia: Basic problems', *Stratigraphy and Geological Correlation*, 1, pp. 77–83.

Dietz, R. S. and Holden, J. C. (1970) 'Reconstruction of Pangaea: Breakup and dispersion of continents, Permian to Present', *Journal of Geophysical Research (1896-1977)*, 75(26), pp. 4939–4956. doi: https://doi.org/10.1029/JB075i026p04939.

Dobeš, C. H., Hahn, B. and Morawetz, W. (1997) 'Chromosomenzahlen zur Gefässpflanzenflora Österreichs', *Linzer Biol. Beitr*, 29(1), pp. 5–43.

Dolan, A. M. *et al.* (2015) 'Modelling the enigmatic Late Pliocene Glacial Event — Marine Isotope Stage M2', *Global and Planetary Change*, 128, pp. 47–60. doi: https://doi.org/10.1016/j.gloplacha.2015.02.001.

Doležel, J. *et al.* (1998) 'Plant Genome Size Estimation by Flow Cytometry: Inter-laboratory Comparison', *Annals of Botany*, 82(suppl_1), pp. 17–26. doi: 10.1093/oxfordjournals.aob.a010312.

Doležel, J. and Greilhuber, J. (2010) 'Nuclear genome size: Are we getting closer?', *Cytometry Part A*, 77(7), pp. 635–642.

Dolukhanov, P. M. *et al.* (2009) 'Late Quaternary Caspian: Sea-levels, environments and human settlement', *The Open Geography Journal*, 2(1), pp. 1–15. doi: 10.2174/1874923200902010001.

Domínguez, F. *et al.* (2001) '*Krascheninnikovia ceratoides* (L.) Gueldenst. (Chenopodiaceae) en Aragón (España): algunos resultados para su conservación', *Bol. R. Soc. Esp. Hist. Nat. (Sec. Biol.)*, 96, pp. 15–26.

Eaton, D. A. R. and Overcast, I. (2020) 'ipyrad: Interactive assembly and analysis of RADseq datasets', *Bioinformatics*, 36(8), pp. 2592–2594. doi: 10.1093/bioinformatics/btz966.

eFloras (2008) *Published on the Internet http://www.efloras.org*.

Elias, S. and Brigham-Grette, J. (2013) 'Late Pleistocene Glacial Events in Beringia', *Encyclopedia of Quaternary Science*, 2, pp. 191–201. doi: 10.1016/B978-0-444-53643-3.00116-3.

Erdős, L. *et al.* (2018) 'The edge of two worlds: A new review and synthesis on Eurasian forest-steppes',

Applied Vegetation Science, 21(3), pp. 345–362. doi: https://doi.org/10.1111/avsc.12382.

Eronen, J. *et al.* (2010) 'Precipitation and large herbivorous mammals II: Application to fossil data', *Evolutionary Ecology Research*, 12, pp. 235–248.

Eronen, J. T. *et al.* (2009) 'Distribution history and climatic controls of the Late Miocene Pikermian chronofauna', *Proceedings of the National Academy of Sciences*, 106(29), pp. 11867 LP – 11871. doi: 10.1073/pnas.0902598106.

Farmer, G. T. and Cook, J. (2013) 'Pleistocene Glaciations', in Farmer, G. T. and Cook, J. (eds) *Climate Change Science: A Modern Synthesis*. Dordrecht: Springer Netherlands, pp. 407–427. doi: 10.1007/978-94-007-5757-8_21.

Fedeneva, I. N. and Dergacheva, M. I. (2003) 'Paleosols as the basis of environmental reconstruction in Altai mountainous areas', *Quaternary International*, 106–107, pp. 89–101. doi: 10.1016/S1040-6182(02)00164-7.

Feurdean, A. *et al.* (2015) 'Origin of the forest steppe and exceptional grassland diversity in Transylvania (central-eastern Europe)', *Journal of Biogeography*, 42(5), pp. 951–963. doi: https://doi.org/10.1111/jbi.12468.

Fokuhl, G. (2008) *Ants and plants*. Stuttgart, Germany: Schweizerbart Science Publishers. Available at: http://www.schweizerbart.de//publications/detail/isbn/9783443643218/Dissertationes_Botanicae_408_Gerriet_Fok.

Fordham, D. A. *et al.* (2017) 'PaleoView: a tool for generating continuous climate projections spanning the last 21 000 years at regional and global scales', *Ecography*, 40(11), pp. 1348–1358. doi: https://doi.org/10.1111/ecog.03031.

Franzke, A. *et al.* (2004) 'Molecular signals for Late Tertiary/Early Quaternary range splits of an Eurasian steppe plant: *Clausia aprica* (Brassicaceae)', *Molecular Ecology*, 13(9), pp. 2789–2795. doi: 10.1111/j.1365-294x.2004.02272.x.

Frenzel, B. (1968) 'Grundzüge der Pleistozänen Vegetationsgeschichte Nord-Euroasiens', *The Geographical Journal*, 136(2), p. 291. doi: 10.2307/1796333.

Frichot, E. and François, O. (2015) 'LEA: An R package for landscape and ecological association studies', *Methods in Ecology and Evolution*, 6(8), pp. 925–929. doi: 10.1111/2041-210x.12382.

Friesen, N. *et al.* (2015) 'Dated phylogenies and historical biogeography of *Dontostemon* and *Clausia* (Brassicaceae) mirror the palaeogeographical history of the Eurasian steppe', *Journal of Biogeography*, 43(4), pp. 738–749. doi: 10.1111/jbi.12658.

Friesen, N., Smirnov, S. V, *et al.* (2020) '*Allium* species of section *Rhizomatosa*, early members of the Central Asian steppe vegetation', *Flora*, 263, p. 151536. doi: 10.1016/j.flora.2019.151536.

Friesen, N., Zerdoner Calasan, A., *et al.* (2020) 'Evolutionary history of the Eurasian steppe plant *Schivereckia podolica* (Brassicaceae) and its close relatives', *Flora*, 268, p. 151602. doi: 10.1016/j.flora.2020.151602.

Ghaffari, S. M. *et al.* (2014) 'Cytology of SW Asian Chenopodiaceae: New data from Iran and a review of previous records and correlations with life forms and C4 photosynthesis', *Plant Systematics and Evolution*, 301(2), pp. 501–521. doi: 10.1007/s00606-014-1109-6.

Gibbard, P. L. *et al.* (2010) 'Formal ratification of the Quaternary System/Period and the Pleistocene Series/Epoch with a base at 2.58 Ma', *Journal of Quaternary Science*, 25(2), pp. 96–102.

Gostin, I. (2011) 'Anatomical and micromorphological peculiarities of Adonis vernalis L. (Ranunculaceae)', *Pakistan Journal of Botany*, 43.

Groucutt, H. S. *et al.* (2015) 'Rethinking the dispersal of Homo sapiens out of Africa', *Evolutionary*

Anthropology: Issues, News, and Reviews, 24(4), pp. 149–164. doi: https://doi.org/10.1002/evan.21455.

Gruber, B. *et al.* (2018) 'dartr : An R package to facilitate analysis of SNP data generated from reduced representation genome sequencing', *Molecular Ecology Resources*, 18(3), pp. 691–699. doi: 10.1111/1755-0998.12745.

Grubov, V. I. (1999) *Plants of Central Asia, Vol. 2*. Enfield (New Hampshire, USA), Plymouth (UK): Science Publisher.

Guindon, S. *et al.* (2010) 'New algorithms and methods to estimate maximum-likelihood phylogenies: Assessing the performance of PhyML 3.0', *Systematic Biology*, 59(3), pp. 307–321. doi: 10.1093/sysbio/syq010.

Hais, M. *et al.* (2015) 'Modelling the Last Glacial Maximum environments for a refugium of Pleistocene biota in the Russian Altai Mountains, Siberia', *Palaeogeography, Palaeoclimatology, Palaeoecology*, 438, pp. 135–145. doi: 10.1016/j.palaeo.2015.07.037.

Hamilton, W. (1968) 'Cenozoic climatic change and its cause', in Billings, D. E. et al. (eds) *Causes of climatic change*. Boston, MA: American Meteorological Society, pp. 128–133. doi: 10.1007/978-1-935704-38-6_12.

Hartmann, H. (1997) 'Zur Flora und Vegetation der Halbwüsten, Steppen und Rasengesellschaften im südöstlichen Ladakh (Indien)', in *Jahrbuch des Vereins zum Schutz der Bergwelt*. 62nd edn, pp. 129–188.

Hay, W. W. (2017) 'Toward understanding Cretaceous climate—An updated review', *Science China Earth Sciences*, 60(1), pp. 5–19. doi: 10.1007/s11430-016-0095-9.

Heiberger, R. M. and Robbins, N. B. (2014) 'Design of Diverging Stacked Bar Charts for Likert Scales and Other Applications', *Journal of Statistical Software*, 57(5), pp. 1–32. Available at: https://www.jstatsoft.org/v57/i05/.

Hejcman, M. *et al.* (2013) 'Origin and history of grasslands in Central Europe - a review', *Grass and Forage Science*, 68(3), pp. 345–363. doi: 10.1111/gfs.12066.

Heklau, H. (2006) '(1749) Proposal to conserve the name *Kraschenninnikovia* against *Ceratoides* (Chenopodiaceae)', *TAXON*, 55(4), pp. 1044–1045. doi: 10.2307/25065713.

Heklau, H. and Röser, M. (2008) 'Delineation, taxonomy and phylogenetic relationships of the genus *Kraschenninnikovia* (Amaranthaceae subtribe Axyridinae)', *Taxon*, 57(2), pp. 563–576. doi: 10.2307/25066022.

Heklau, H. and von Wehrden, H. (2011) 'Wood anatomy reflects the distribution of *Kraschenninnikovia ceratoides* (Chenopodiaceae)', *Flora - Morphology, Distribution, Functional Ecology of Plants*, 206(4), pp. 300–309. doi: 10.1016/j.flora.2010.05.007.

Hijmans, R. . *et al.* (2011) 'Package "dismo". Available online at: http://cran.r-project.org/web/packages/dismo/index.html'.

Hill, D. J. (2015) 'The non-analogue nature of Pliocene temperature gradients', *Earth and Planetary Science Letters*, 425, pp. 232–241. Available at: http://eprints.whiterose.ac.uk/87717/.

Hirsch, H. *et al.* (2015) 'High genetic diversity declines towards the geographic range periphery of Adonis vernalis, a Eurasian dry grassland plant', *Plant Biology*, 17(6), pp. 1233–1241. doi: https://doi.org/10.1111/plb.12362.

Hoekstra, J. M. *et al.* (2005) 'Confronting a biome crisis: global disparities of habitat loss and protection', *Ecology Letters*, 8(1), pp. 23–29. doi: https://doi.org/10.1111/j.1461-0248.2004.00686.x.

Hsiao, C. *et al.* (1994) 'Phylogenetic relationships of 10 grass species: an assessment of phylogenetic

utility of the internal transcribed spacer region in nuclear ribosomal DNA in monocots', *Genome*, 37(1), pp. 112–120.

Hurka, H. *et al.* (2012) '"Missing link" species *Capsella orientalis* and *Capsella thracicaelucidate* evolution of model plant genus *Capsella* (Brassicaceae)', *Molecular Ecology*, 21(5), pp. 1223–1238. doi: 10.1111/j.1365-294x.2012.05460.x.

Hurka, H. *et al.* (2019) 'The Eurasian steppe belt: Status quo, origin and evolutionary history', *Turczaninowia*, 22(3), pp. 5–71. doi: 10.14258/turczaninowia.22.3.1.

Huson, D. H. and Bryant, D. (2005) 'Application of Phylogenetic Networks in Evolutionary Studies', *Molecular Biology and Evolution*, 23(2), pp. 254–267. doi: 10.1093/molbev/msj030.

Imperatorskaia akademiia nauk (1771) *Novi commentarii Academiae Scientiarum Imperialis Petropolitanae.* Petropolis: Typis Academiae Scientarum. Available at: https://www.biodiversitylibrary.org/item/38631.

IPNI (2020) *International Plant Names Index. Published on the Internet*, *The Royal Botanic Gardens, Kew, Harvard University Herbaria & Libraries and Australian National Botanic Gardens.* Available at: http://www.ipni.org (Accessed: 1 March 2021).

Ivanov, D. *et al.* (2011) 'Miocene vegetation and climate dynamics in Eastern and Central Paratethys (Southeastern Europe)', *Palaeogeography, Palaeoclimatology, Palaeoecology*, 304(3), pp. 262–275. doi: https://doi.org/10.1016/j.palaeo.2010.07.006.

Janis, C. M. (1993) 'Tertiary mammal evolution in the context of changing climates, vegetation, and tectonic events', *Annual Review of Ecology and Systematics*, 24(1), pp. 467–500. doi: 10.1146/annurev.es.24.110193.002343.

Jombart, T. (2008) 'adegenet: A R package for the multivariate analysis of genetic markers', *Bioinformatics*, 24(11), pp. 1403–1405. doi: 10.1093/bioinformatics/btn129.

Kadereit, G. *et al.* (2003) 'Phylogeny of Amaranthaceae and Chenopodiaceae and the evolution of C4', 164(July).

Kadereit, G. *et al.* (2005) 'Origin and age of Australian Chenopodiaceae', 5, pp. 59–80. doi: 10.1016/j.ode.2004.07.002.

Kadereit, G. *et al.* (2010) 'Molecular phylogeny of Atripliceae (Chenopodioideae, Chenopodiaceae): Implications for systematics, biogeography, flower and fruit evolution, and the origin of C4 photosynthesis', *American Journal of Botany*, 97(10), pp. 1664–1687. doi: 10.3732/ajb.1000169.

Kadereit, G. and Emre Yaprak, A. (2008) '*Microcnemum coralloides* (Chenopodiaceae- Salicornioideae): an example of intraspecific East-West disjunctions in the Mediterranean region', *Anales del Jardín Botánico de Madrid*, 65(2). doi: 10.3989/ajbm.2008.v65.i2.303.

Kadereit, G., Mucina, L. and Freitag, H. (2006) 'Phylogeny of Salicornioideae (Chenopodiaceae): diversification, biogeography, and evolutionary trends in leaf and flower morphology', *Taxon*, 55(3), pp. 617–642.

Kalinowski, S. T. (2005) 'hp-rare 1.0: A computer program for performing rarefaction on measures of allelic richness', *Molecular Ecology Notes*, 5(1), pp. 187–189. doi: 10.1111/j.1471-8286.2004.00845.x.

Karger, D. N. *et al.* (2017) 'Climatologies at high resolution for the earth's land surface areas', *Scientific Data*, 4. doi: 10.1038/sdata.2017.122.

Karger, D. N. *et al.* (no date) 'Data from: Climatologies at high resolution for the earth's land surface areas', *Dryad Digital Repository*.

Katoh, K., Rozewicki, J. and Yamada, K. D. (2019) 'MAFFT online service: multiple sequence alignment, interactive sequence choice and visualization', *Briefings in bioinformatics*, 20(4), pp. 1160–1166.

Kirschner, P. *et al.* (2020) 'Long-term isolation of European steppe outposts boosts the biome's conservation value', *Nature communications*, 11(1), p. 1968. doi: 10.1038/s41467-020-15620-2.

Komarov, V. (1964) *Flora of the U.R.S.S, Volume VI*. Leningrado: Academiae Sciencitarum U.R.S.S.

Kraudzun, T., Vanselow, K. A. and Samimi, C. (2014) 'Realities and myths of the Teresken Syndrome – An evaluation of the exploitation of dwarf shrub resources in the Eastern Pamirs of Tajikistan', *Journal of Environmental Management*, 132, pp. 49–59. doi: 10.1016/j.jenvman.2013.10.019.

Kropf, M. *et al.* (2020) 'Phylogeographical structure and genetic diversity of Adonis vernalis L. (Ranunculaceae) across and beyond the Pannonian region', *Flora*, 262, p. 151497. doi: https://doi.org/10.1016/j.flora.2019.151497.

Kühne, G. *et al.* (2017) 'Extra-Mediterranean glacial refugia in a Mediterranean faunal element: the phylogeography of the chalk-hill blue Polyommatus coridon (Lepidoptera, Lycaenidae)', *Scientific Reports*, 7(1), p. 43533. doi: 10.1038/srep43533.

Kurban, N. (1984) 'Karyotype analysis of three species of *Ceratoides* (Chenopodiaceae)', *J. Syst. Evol.*, 22, pp. 466–468.

Landis, M. J. *et al.* (2013) 'Bayesian analysis of biogeography when the number of areas is large', *Systematic biology*, 62(6), pp. 789–804.

Lang, G. (1994) *Quartäre vegetationsgeschichte Europas: methoden und ergebnisse*. Springer.

Lenton, T. M. *et al.* (2012) 'First plants cooled the Ordovician', *Nature Geoscience*, 5(2), pp. 86–89. doi: 10.1038/ngeo1390.

Lewis, P. O. (2001) 'A likelihood approach to estimating phylogeny from discrete morphological character data', *Systematic Biology*, 50(6), pp. 913–925. doi: 10.1080/106351501753462876.

Li, H. (2011) 'A statistical framework for SNP calling, mutation discovery, association mapping and population genetical parameter estimation from sequencing data', *Bioinformatics (Oxford, England)*. 2011/09/08, 27(21), pp. 2987–2993. doi: 10.1093/bioinformatics/btr509.

Li, H. and Durbin, R. (2009) 'Fast and accurate short read alignment with Burrows-Wheeler transform', *Bioinformatics (Oxford, England)*. 2009/05/18, 25(14), pp. 1754–1760. doi: 10.1093/bioinformatics/btp324.

Li, L. *et al.* (2018) 'Current challenges in distinguishing climatic and anthropogenic contributions to alpine grassland variation on the Tibetan Plateau', *Ecology and Evolution*, 8(11), pp. 5949–5963. doi: https://doi.org/10.1002/ece3.4099.

Li, Q. Q. *et al.* (2010) 'Phylogeny and biogeography of *Allium* (Amaryllidaceae: Allieae) based on nuclear ribosomal internal transcribed spacer and chloroplast rps16 sequences, focusing on the inclusion of species endemic to China', *Annals of Botany*, 106(5), pp. 709–733. doi: 10.1093/aob/mcq177.

Linder, H. P. *et al.* (2017) 'Global grass (Poaceae) success underpinned by traits facilitating colonization, persistence and habitat transformation', *Biological Reviews*, 93(2), pp. 1125–1144. doi: 10.1111/brv.12388.

Lindhuber, L. (2020) 'Phylogeny and biogeography of the conservation related genus Adonis'. [Wien], pp. 94 Blätter, Illustrationen. Available at: https://permalink.obvsg.at/bok/AC16050949.

Liu, Z. *et al.* (2009) 'Global Cooling During the Eocene-Oligocene Climate Transition', *Science*, 323(5918), pp. 1187 LP – 1190. doi: 10.1126/science.1166368.

Lomonosova, M. N. and Krasnikov, A. A. (1993) 'Chromosome numbers in some members of the Chenopodiaceae', *Bot. Zurn. (Moscow & Leningrad)*, 78, pp. 158–159.

Magallón, S. and Castillo, A. (2009) 'Angiosperm diversification through time', *American Journal of*

Botany, 96(1), pp. 349–365. doi: https://doi.org/10.3732/ajb.0800060.

Magyari, E. K. *et al.* (2010) 'Holocene persistence of wooded steppe in the Great Hungarian Plain', *Journal of Biogeography*, 37(5), pp. 915–935. doi: https://doi.org/10.1111/j.1365-2699.2009.02261.x.

Matzke, N. J. (2013) 'Probabilistic historical biogeography: New models for founder-event speciation, imperfect detection, and fossils allow improved accuracy and model-testing', *Frontiers of Biogeography*, 5(4). doi: 10.21425/f5fbg19694.

Matzke, N. J. (2014) 'Model selection in historical biogeography reveals that founder-event speciation is a crucial process in island clades', *Systematic Biology*, 63(6), pp. 951–970. doi: 10.1093/sysbio/syu056.

Matzke, N. J. (2018) 'BioGeoBEARS: BioGeography with Bayesian (and likelihood) evolutionary analysis with R scripts. Version 1.1. 1, published on GitHub on 6 November 2018'.

Metlesics, H. J. R. (1969) 'Adonis vernalis x volgensis'. Romania.

Meusel, H. *et al.* (1978) *Vergleichende Chronologie der zentraleuropäischen Flora*. Jena, Germany: Gustav Fischer Verlag.

Minh, B. Q. *et al.* (2020) 'IQ-TREE 2: New models and efficient methods for phylogenetic inference in the genomic era', *Molecular Biology and Evolution*, 37(5), pp. 1530–1534. doi: 10.1093/molbev/msaa015.

Minh, B. Q., Nguyen, M. A. T. and von Haeseler, A. (2013) 'Ultrafast approximation for phylogenetic bootstrap', *Molecular Biology and Evolution*, 30(5), pp. 1188–1195. doi: 10.1093/molbev/mst024.

Mirarab, S. *et al.* (2015) 'PASTA: ultra-large multiple sequence alignment for nucleotide and amino-acid sequences', *Journal of Computational Biology*, 22(5), pp. 377–386.

Morris, J. L. *et al.* (2018) 'The timescale of early land plant evolution', *Proceedings of the National Academy of Sciences*, 115(10), p. E2274 LP-E2283. doi: 10.1073/pnas.1719588115.

Muscarella, R. *et al.* (2014) 'ENMeval: An R package for conducting spatially independent evaluations and estimating optimal model complexity for ecological niche models', *Methods in Ecology and Evolution*, 5(11), pp. 1198–1205.

Muster, C. and Berendonk, T. U. (2006) 'Divergence and diversity: lessons from an arctic–alpine distribution (Pardosa saltuaria group, Lycosidae)', *Molecular Ecology*, 15(10), pp. 2921–2933. doi: https://doi.org/10.1111/j.1365-294X.2006.02989.x.

Novenko, E. Y. *et al.* (2016) 'Mid- and late-Holocene vegetation history, climate and human impact in the forest-steppe ecotone of European Russia: new data and a regional synthesis', *Biodiversity and Conservation*, 25(12), pp. 2453–2472. doi: 10.1007/s10531-016-1051-8.

Otto-Bliesner, B. L. *et al.* (2006) 'Simulating Arctic Climate Warmth and Icefield Retreat in the Last Interglaciation', *Science*, 311(5768), pp. 1751 LP – 1753. doi: 10.1126/science.1120808.

Parrish, J. T. (1993) 'Climate of the Supercontinent Pangea', *The Journal of Geology*, 101(2), pp. 215–233. doi: 10.1086/648217.

Pavelková Řičánková, V., Robovský, J. and Riegert, J. (2014) 'Ecological Structure of Recent and Last Glacial Mammalian Faunas in Northern Eurasia: The Case of Altai-Sayan Refugium', *PLOS ONE*, 9(1), p. e85056. Available at: https://doi.org/10.1371/journal.pone.0085056.

Perez-Collazos, E. and Catalan, P. (2007) 'Genetic diversity analysis and conservation implications for the Iberian threatened populations of the irano-turanian relict Krascheninnikovia ceratoides (Chenopodiaceae)', *Biological Journal of the Linnean Society*, 92(3), pp. 419–429.

Pérez-Collazos, E. *et al.* (2009) 'The phylogeographical history of the Iberian steppe plant Ferula loscosii

(Apiaceae): a test of the abundant-centre hypothesis', *Molecular Ecology*, 18(5), pp. 848–861.

Pfadenhauer, J. S. and Klötzli, F. A. (2020) *Fundamentals towards understanding global vegetation*. Edited by J. S. Pfadenhauer and F. A. Klötzli. Cham: Springer International Publishing. doi: 10.1007/978-3-030-49860-3_1.

Poland, J. A. *et al.* (2012) 'Development of high-density genetic maps for barley and wheat using a novel two-enzyme genotyping-by-sequencing approach', *PloS one*. 2012/02/28, 7(2), p. e32253. doi: 10.1371/journal.pone.0032253.

Poluyanova, V. I. and Lyubarskii, E. L. (2008) 'On the ecology of seed germination in Adonis vernalis L.', *Russian Journal of Ecology*, 39(1), pp. 68–69. doi: http://dx.doi.org/10.1007/s11184-008-1011-y.

Qiu, Y.-X. *et al.* (2009) 'Did glacials and/or interglacials promote allopatric incipient speciation in East Asian temperate plants? Phylogeographic and coalescent analyses on refugial isolation and divergence in Dysosma versipellis', *Molecular Phylogenetics and Evolution*, 51(2), pp. 281–293.

R Core Team (2013) *R: A language and environment for statistical computing*, *R Foundation for Statistical Computing*. Vienna, Austria. Available at: http://www.r-project.org/.

Rambaut, A. (2010) 'FigTree v1.3.1.' Edinburgh: Institute of Evolutionary Biology, University of Edinburgh. Available at: http://tree.bio.ed.ac.uk/software/figtree/.

Rechinger, K. (1963) *Flora Iranica*. Graz, Austria: Akademische Druck- und Verlagsanstalt.

Ree, R. and Smith, S. (2008) 'Maximum likelihood inference of geographic range evolution by dispersal, local extinction, and cladogenesis', *Systematic biology*, 57, pp. 4–14. doi: 10.1080/10635150701883881.

Reed, K. E. (1997) 'Early hominid evolution and ecological change through the African Plio-Pleistocene', *Journal of Human Evolution*, 32(2), pp. 289–322. doi: https://doi.org/10.1006/jhev.1996.0106.

Ren, H. and Zhou, G. (2018) 'Measuring the impacts of anthropogenic activities on Inner Mongolian temperate grassland', *Land Degradation & Development*, 29(9), pp. 2942–2950. doi: https://doi.org/10.1002/ldr.3055.

Ribera, I. and Blasco-Zumeta, J. (1998) 'Biogeographical links between steppe insects in the Monegros region (Aragón, NE Spain), the eastern Mediterranean, and central Asia', *Journal of Biogeography*, 25(5), pp. 969–986.

Ronquist, F. (1997) 'Dispersal-Vicariance Analysis: A new approach to the quantification of historical biogeography', *Systematic Biology*, 46(1), pp. 195–203. doi: 10.1093/sysbio/46.1.195.

Rubtsov, M. *et al.* (1989) 'Natural polyploids of prostrate summer cypress and winterfat as initial material for breeding', *Sov. Agric. Sci.*, 4, pp. 20–24.

Sainz Ollero, H., Múgica, F. and Arias Torcal, J. (1996) *Estrategias para la conservación de la flora amenazada de Aragón*. Consejo de Protección de la Naturaleza de Aragón.

Sala, O. E. *et al.* (2000) 'Global Biodiversity Scenarios for the Year 2100', *Science*, 287(5459), pp. 1770 LP – 1774. doi: 10.1126/science.287.5459.1770.

Schmitt, T. (2007) 'Molecular biogeography of Europe: Pleistocene cycles and postglacial trends', *Frontiers in Zoology*, 4(1), p. 11. doi: 10.1186/1742-9994-4-11.

Schmitt, T. and Hewitt, G. M. (2004) 'Molecular biogeography of the arctic-alpine disjunct burnet moth species Zygaena exulans (Zygaenidae, Lepidoptera) in the Pyrenees and Alps', *Journal of Biogeography*, 31(6), pp. 885–893. doi: https://doi.org/10.1111/j.1365-2699.2004.01079.x.

Schulze, K., Buchwald, R. and Heinken, T. (2014) 'Epizoochory via the hooves – the European bison (Bison bonasus L.) as a dispersal agent of seeds in an open-forest-mosaic Epizoochore

Samenausbreitung durch die Klauen des Wisents (Bison bonasus L.) in einem Wald-Offenland-Mosaik', *TUEXENIA*, 34, pp. 131–143. doi: 10.14471/2014.34.016.

Seidl, A. *et al.* (2020) 'Phylogeny and biogeography of the Pleistocene Holarctic steppe and semi-desert goosefoot plant *Krascheninnikovia ceratoides*', *Flora*, 262, p. 151504. doi: 10.1016/j.flora.2019.151504.

Seidl, A. *et al.* (2021) 'The phylogeographic history of Krascheninnikovia reflects the development of dry steppes and semi-deserts in Eurasia', *Scientific Reports*, 11(1), p. 6645. doi: 10.1038/s41598-021-85735-z.

Seregin, A. P., Anačkov, G. and Friesen, N. (2015) 'Molecular and morphological revision of the *Allium saxatile* group (Amaryllidaceae): Geographical isolation as the driving force of underestimated speciation', *Botanical Journal of the Linnean Society*, 178(1), pp. 67–101. doi: 10.1111/boj.12269.

Shaw, J. *et al.* (2007) 'Comparison of whole chloroplast genome sequences to choose noncoding regions for phylogenetic studies in angiosperms: the tortoise and the hare III', *American journal of botany*, 94(3), pp. 275–288.

Shi, W. *et al.* (2017) 'Evolutionary response to the Qinghai-Tibetan Plateau uplift: Phylogeny and biogeography of *Ammopiptanthus* and tribe *Thermopsideae* (Fabaceae)', *PeerJ*, 2017(7), pp. 1–24. doi: 10.7717/peerj.3607.

Smelansky, I. and Tishkov, A. (2012) 'The Steppe Biome in Russia: Ecosystem Services, Conservation Status, and Actual Challenges', in, pp. 45–101. doi: 10.1007/978-94-007-3886-7_2.

Smoliak, S. and Bezeau, L. M. (1967) 'Chemical composition and in vitro digestibility of range forage plants of the Stipa-Bouteloua prairie', *Canadian Journal of Plant Science*, 47(2), pp. 161–167. doi: 10.4141/cjps67-028.

Sokolova, S. M., Lovkova, M. Y. and Buzuk, G. N. (2007) 'Microelements and cardiac glycosides from medicinal plants', *Doklady Biological Sciences*, 413(1), pp. 146–148. doi: 10.1134/S0012496607020160.

Solomon, D. *et al.* (2007) 'Long-term impacts of anthropogenic perturbations on dynamics and speciation of organic carbon in tropical forest and subtropical grassland ecosystems', *Global Change Biology*, 13(2), pp. 511–530. doi: https://doi.org/10.1111/j.1365-2486.2006.01304.x.

South, A. (2011) 'rworldmap: A New R package for Mapping Global Data', *The R Journal*, 3(1), pp. 35–43. Available at: http://journal.r-project.org/archive/2011-1/RJournal_2011-1_South.pdf.

Stamatakis, A. (2014) 'RAxML version 8: a tool for phylogenetic analysis and post-analysis of large phylogenies', *Bioinformatics (Oxford, England)*. 2014/01/21, 30(9), pp. 1312–1313. doi: 10.1093/bioinformatics/btu033.

Steshenko, A. P. (1956) 'Formation of the semi-shrub structure in the high mountains of Pamir', *Trans Akad Nauk Tadzhik SSR*, 50(162).

Stevanović, V. *et al.* (2009) 'Distribution and diversity of Arctic-Alpine species in the Balkans', *Plant Systematics and Evolution*, 283(3), p. 219. doi: 10.1007/s00606-009-0230-4.

Stewart, J. R. *et al.* (2010) 'Refugia revisited: Individualistic responses of species in space and time', *Proceedings. Biological sciences*. 2009/10/28, 277(1682), pp. 661–671. doi: 10.1098/rspb.2009.1272.

Strömberg, C. A. E. (2011) 'Evolution of grasses and grassland ecosystems', *Annual Review of Earth and Planetary Sciences*, 39(1), pp. 517–544. doi: 10.1146/annurev-earth-040809-152402.

Suchorukow, A. P. (2005) 'Karpologische Untersuchung der Axyris-Arten (Chenopodiaceae) im Zusammenhang mit ihrer Diagnostik und Taxonomie', *Feddes Repertorium*, 116(3-4), pp. 168–176. doi: https://doi.org/10.1002/fedr.200511070.

Swofford, D. (2002) *PAUP*. Phylogenetic Analysis Using Parsimony (*and Other Methods). Version 4.0b10*. Sinauer Associates, Sunderland. doi: 10.1111/j.0014-3820.2002.tb00191.x.

Taberlet, P. *et al.* (1991) 'Universal primers for amplification of three non-coding regions of chloroplast DNA', *Plant molecular biology*, 17(5), pp. 1105–1109.

Täckholm, V. (1974) *Students' Flora of Egypt*. Beirut: Cairo University Publishing.

Takhtajan, A. (1986) *Floristic Regions of the World*. Berkeley: University of California Press.

Takhtajan, A. (1990) *Numeri chromosomatum magnoliophytorum florae URSS. Aceraceae–Menyanthaceae*. Academis Scientiarum Rossica, Institutum Botanicum nomine VL Komarovii;" Nauka".

Tarasov, P. E. *et al.* (2000) 'Last glacial maximum biomes reconstructed from pollen and plant macrofossil data from northern Eurasia', *Journal of Biogeography*, 27(3), pp. 609–620. doi: 10.1046/j.1365-2699.2000.00429.x.

Tiffney, B. H. (1985) 'The Eocene North Atlantic land bridge: Its importance in Tertiary and modern phytogeography of the northern hemisphere.', *Journal of the Arnold Arboretum*, 66(2), pp. 243–273. Available at: http://www.jstor.org/stable/43782164.

Tomescu, A. M. (2000) 'Evaluation of Holocene pollen records from the Romanian Plain.', *Review of palaeobotany and palynology*, 109(3–4), pp. 219–233. doi: 10.1016/s0034-6667(99)00056-1.

Tremetsberger, K. *et al.* (2009) 'Pleistocene refugia and polytopic replacement of diploids by tetraploids in the Patagonian and Subantarctic plant *Hypochaeris incana* (Asteraceae, Cichorieae)', *Molecular Ecology*, 18(17), pp. 3668–3682. doi: 10.1111/j.1365-294X.2009.04298.x.

Triest, L. and Sierens, T. (2014) 'Seagrass radiation after Messinian salinity crisis reflected by strong genetic structuring and out-of-Africa scenario (Ruppiaceae)', *PLoS One*, 9(8), p. e104264.

Tudryn, A. *et al.* (2013) 'Late Quaternary Caspian Sea environment: Late Khazarian and Early Khvalynian transgressions from the lower reaches of the Volga River', *Quaternary International*, 292, pp. 193–204. doi: 10.1016/j.quaint.2012.10.032.

Tutin, T. *et al.* (1993) *Flora Europaea*. Cambridge: Cambridge University Press.

Urbanek, S. (2020) 'rJava: Low-Level R to Java Interface'. Available at: https://cran.r-project.org/package=rJava.

Utescher, T. *et al.* (2007) 'Tree diversity in the Miocene forests of Western Eurasia', *Palaeogeography, Palaeoclimatology, Palaeoecology*, 253(1), pp. 226–250. doi: https://doi.org/10.1016/j.palaeo.2007.03.041.

Van de Peer, Y., Maere, S. and Meyer, A. (2009) 'The evolutionary significance of ancient genome duplications', *Nature Reviews Genetics*, 10(10), pp. 725–732. doi: 10.1038/nrg2600.

Vanselow, K. and Samimi, C. (2014) 'Predictive mapping of dwarf shrub vegetation in an arid high mountain ecosystem using remote sensing and random forests', *Remote Sensing*, 6(7), pp. 6709–6726. doi: 10.3390/rs6076709.

Varga, Z. (2009) 'Extra-Mediterranean refugia, post-glacial vegetation history and area dynamics in eastern Central Europe', *Relict Species*. Springer Berlin Heidelberg, pp. 57–87. doi: 10.1007/978-3-540-92160-8_3.

Veith, M. *et al.* (2003) 'Palaeoclimatic changes explain Anatolian mountain frog evolution: a test for alternating vicariance and dispersal events', *Molecular Ecology*, 12(1), pp. 185–199. doi: https://doi.org/10.1046/j.1365-294X.2003.01714.x.

Di Vincenzo, V. *et al.* (2018) 'Evolutionary diversification of the African achyranthoid clade (Amaranthaceae) in the context of sterile flower evolution and epizoochory', *Annals of Botany*, 122(1),

pp. 69–85. doi: 10.1093/aob/mcy055.

Vitales, D. *et al.* (2014) 'The explosive radiation of Cheirolophus (Asteraceae, Cardueae) in Macaronesia', *BMC Evolutionary Biology*, 14(1), pp. 1–15.

Volkova, P. A., Herden, T. and Friesen, N. (2017) 'Genetic variation in *Goniolimon speciosum* (Plumbaginaceae) reveals a complex history of steppe vegetation', *Botanical Journal of the Linnean Society*, 184(1), pp. 113–121.

Waldron, B. L. *et al.* (2010) '*Forage kochia* (*Kochia prostrata*) for fall and winter grazing', *Small Ruminant Research*, 91(1), pp. 47–55. doi: 10.1016/j.smallrumres.2010.01.011.

Walter, H. (1968) *Die Vegetation der Erde in öko-physiologischer Betrachtung , Band II : Die gemäßigten und arktischen Zonen, in ökologischer Betrachtung*. Gustav Fischer Verlag.

Walter, H. (1974) *Die Vegetation Osteuropas, Nord- und Zentralasiens. Vegetationsmonographien der einzelnen Großräume*. Stuttgart: Gustav Fischer Verlag.

Walter, H. and Breckle, S.-W. (1986) *Ecological systems of the geobiosphere. 2 Tropical and subtropical zonobiomes*. Springer Berlin Heidelberg. doi: 10.1007/978-3-662-06812-0.

Wang, J. *et al.* (2013) 'Phylogenetic patterns and disjunct distribution in Ligularia hodgsonii Hook.(Asteraceae)', *Journal of Biogeography*, 40(9), pp. 1741–1754.

Wang, P. C. *et al.* (2015) 'Genetic diversity of Ceratoides arborescens, a species endemic to China, detected by inter-simple sequence repeat (ISSR)', *Genetics and Molecular Research*, 14(2), pp. 5658–5666.

Webb, S. D. (1977) 'A history of savanna vertebrates in the New World. Part I: North America', *Ann. Rev. Ecol. Syst.*, (8), pp. 355–380.

Weiß, C. L. *et al.* (2018) 'nQuire: A statistical framework for ploidy estimation using next generation sequencing', *BMC bioinformatics*, 19(1), p. 122. doi: 10.1186/s12859-018-2128-z.

Welsh, S. *et al.* (1987) 'A Utah Flora', *Gt. Basin Nat.*, 9, p. 123.

Werger, M. J. A. and van Staalduinen, M. A. (2012) *Eurasian Steppes. Ecological Problems and Livelihoods in a Changing World*. 1st ed. 20. Dordrecht: Springer Netherlands (Plant and Vegetation, 6). doi: 10.1007/978-94-007-3886-7.

White, R., Murray, S. and Rohweder, M. (2000) *Pilot analysis of global ecosystems: Grassland ecosystems*. Edited by M. EDEBURN. Washington, DC: World Resources Institute.

White, T. J. *et al.* (1990) 'Amplification and direct sequencing of fungal ribosomal RNA genes for phylogenetics', *PCR protocols: a guide to methods and applications*, 18(1), pp. 315–322.

Wick, L., Lemcke, G. and Sturm, M. (2003) 'Evidence of Lateglacial and Holocene climatic change and human impact in eastern Anatolia: high-resolution pollen, charcoal, isotopic and geochemical records from the laminated sediments of Lake Van, Turkey', *The Holocene*, 13(5), pp. 665–675. doi: 10.1191/0959683603hl653rp.

Wickham, H. (2016) *ggplot2: Elegant Graphics for Data Analysis*. Springer-Verlag New York. Available at: https://ggplot2.tidyverse.org.

Willis, K. J., Rudner, E. and Sümegi, P. (2000) 'The full-glacial forests of Central and Southeastern Europe', *Quaternary Research*, 53(2), pp. 203–213. doi: 10.1006/qres.1999.2119.

Willis, K. J. and Vanandel, T. (2004) 'Trees or no trees? The environments of central and eastern Europe during the Last Glaciation', *Quaternary Science Reviews*, 23(23–24), pp. 2369–2387. doi: 10.1016/j.quascirev.2004.06.002.

Willis, K. and McElwain, J. (2014) *The evolution of plants*. Oxford University Press.

Willkomm, M. (1896) *Grundzüge der Pflanzenverbreitung auf der iberischen Halbinsel*. W. Engelmann.

Willkomm, M. and Lange, J. (1870) *Prodromus Florae Hispanicae 1–3*. Stuttgart.

Wróblewska, A. (2008) 'From the center to the margins of geographical range: molecular history of steppe plant *Iris aphylla* L. in Europe', *Plant Systematics and Evolution*, 272(1–4), pp. 49–65. doi: 10.1007/s00606-007-0630-2.

Wróblewska, A. D. A. and Brzosko, E. (2006) 'The genetic structure of the steppe plant *Iris aphylla* L. at the northern limit of its geographical range', *Botanical Journal of the Linnean Society*, 152(2), pp. 245–255. doi: 10.1111/j.1095-8339.2006.00568.x.

Xu, D. H. *et al.* (2000) 'Sequence variation of non-coding regions of chloroplast DNA of soybean and related wild species and its implications for the evolution of different chloroplast haplotypes', pp. 724–732.

Yan, G. *et al.* (1989) 'Chromosome numbers and geographical distribution of 68 species of forage plants', *Grassland China*, 4, pp. 53–60.

Yang, J. Y. *et al.* (1996) 'Analysis of three species of the genus *Ceratoides*', *Grassland China*, 1, pp. 67–71.

Yanina, T. *et al.* (2018) 'Late Pleistocene climatic events reflected in the Caspian Sea geological history (based on drilling data)', *Quaternary International*, 465, pp. 130–141. doi: 10.1016/j.quaint.2017.08.003.

Yurtsev, B. A. (2001) 'The Pleistocene "Tundra-steppe" and the productivity paradox: The landscape approach', *Quaternary Science Reviews*, 20(1–3), pp. 165–174. doi: 10.1016/S0277-3791(00)00125-6.

Zacharias, E. H. and Baldwin, B. G. (2010) 'A molecular phylogeny of north American Atripliceae (Chenopodiaceae), with implications for floral and photosynthetic pathway evolution', *Systematic Botany*, 35(4), pp. 839–857. doi: 10.1600/036364410X539907.

Zakharjeva, O. I. and Soskov, Y. D. (1981) 'Chromosome numbers in desert herbage plants', *Bulleten' VNII rastenievodstva imeni N.I. Vavilova*, 108, pp. 57–60.

Zakirova, R. (1999) 'Chromosome numbers of some Alliaceae, Salicaceae, Polygonaceae, and Chenopodiaceae of the South Balkhash territory', *Citologija*, 41, p. 1064.

Zalenski, O. V. and Steshenko, A. P. (1957) 'On the special features of the main species of the vegetation of the Pamir mountains', *Proc Bot Soc*, 7, pp. 9–12.

Žerdoner Čalasan, A. *et al.* (2019) 'The Eurasian steppe belt in time and space: Phylogeny and historical biogeography of the false flax (*Camelina* Crantz, Camelineae, Brassicaceae)', *Flora*, 260, p. 151477. doi: 10.1016/j.flora.2019.151477.

Zhang, M. L. *et al.* (2017) 'Insight into Central Asian flora from the Cenozoic Tianshan montane origin and radiation of *Lagochilus* (Lamiaceae)', *PLoS ONE*, 12(9), pp. 1–16. doi: 10.1371/journal.pone.0178389.

Zharkikh, A. (1994) 'Estimation of evolutionary distances between nucleotide sequences', *Journal of Molecular Evolution*, (39), pp. 315–329.

Zhou, K. *et al.* (2019) 'Evolutionary mechanism of genome duplication enhancing natural autotetraploid sea barley adaptability to drought stress', *Environmental and Experimental Botany*, 159, pp. 44–54. doi: 10.1016/j.envexpbot.2018.12.005.

List of figures and tables

Appendix A: *Krascheninnikovia* - PCR amplification conditionsfor each genomic region.

Chloroplast atpB-rbcL intergenic spacer cycling program:

Initial denaturation at 94°C for 2 min;

35 cycles of 94°C for 30 s,

56°C for 30 s,

72°C for 60 s;

and final extension at 72°C for 5 min.

Chloroplast rpl32-trnL and trnL-trnF regions cycling program:

Initial denaturation at 94°C for 2 min;

30 cycles of 94°C for 30 s,

50°C for 30 s,

72°C for 60 s;

and final extension at 72°C for 5 min.

Nuclear ITS5-ITS4 cycling program:

Initial denaturation at 94°C for 2 min;

35 cycles of 94°C for 30 s,

50°C for 30 s,

72°C for 2 min;

and final extension at 72°C for 5 min.

Nuclear ETS cycling program:

Initial denaturation at 96°C for 1 min;

35 cycles of 96°C for 10 s,

60°C for 30 s,

72°C for 20 s;

and final extension at 72°C for 7 min.

Appendix B: Krascheninnikovia - results of ipyrad analysis of GBS data set.

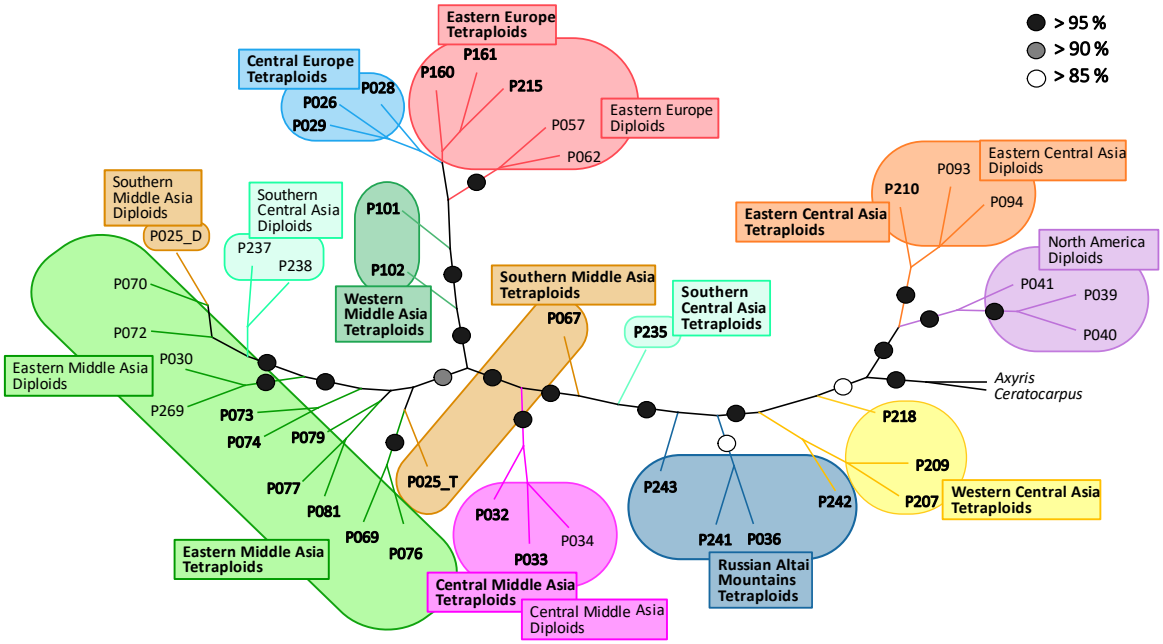

Phylogenetic network based on a coalescent method (SVDQuartets). The origin of the populations is indicated by colour. Bootstrap support is indicated by black (>95%), grey (>90%) and white (>85%) dots. The populations of Eastern Central Asia and Northern America split close to the outgroups from the populations of Western Central Asia and the Russian Altai Mountains. Tetraploids are shown in bold.

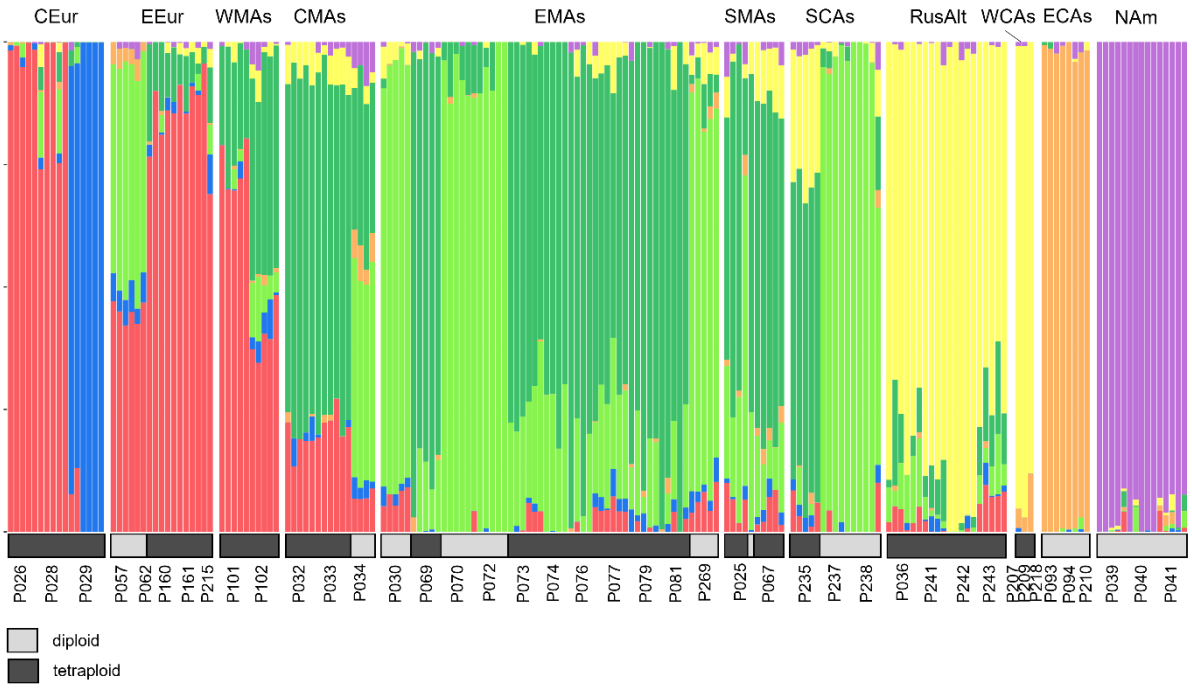

Genetic cluster membership as inferred using LEA is shown as a barplot. Vertical bars denote individuals. Seven clusters were retained, which are indicated by different colours. The samples are ordered by their assigned geographical region from west to east. Ploidy is indicated by grey (diploid) and black (tetraploid) bars.

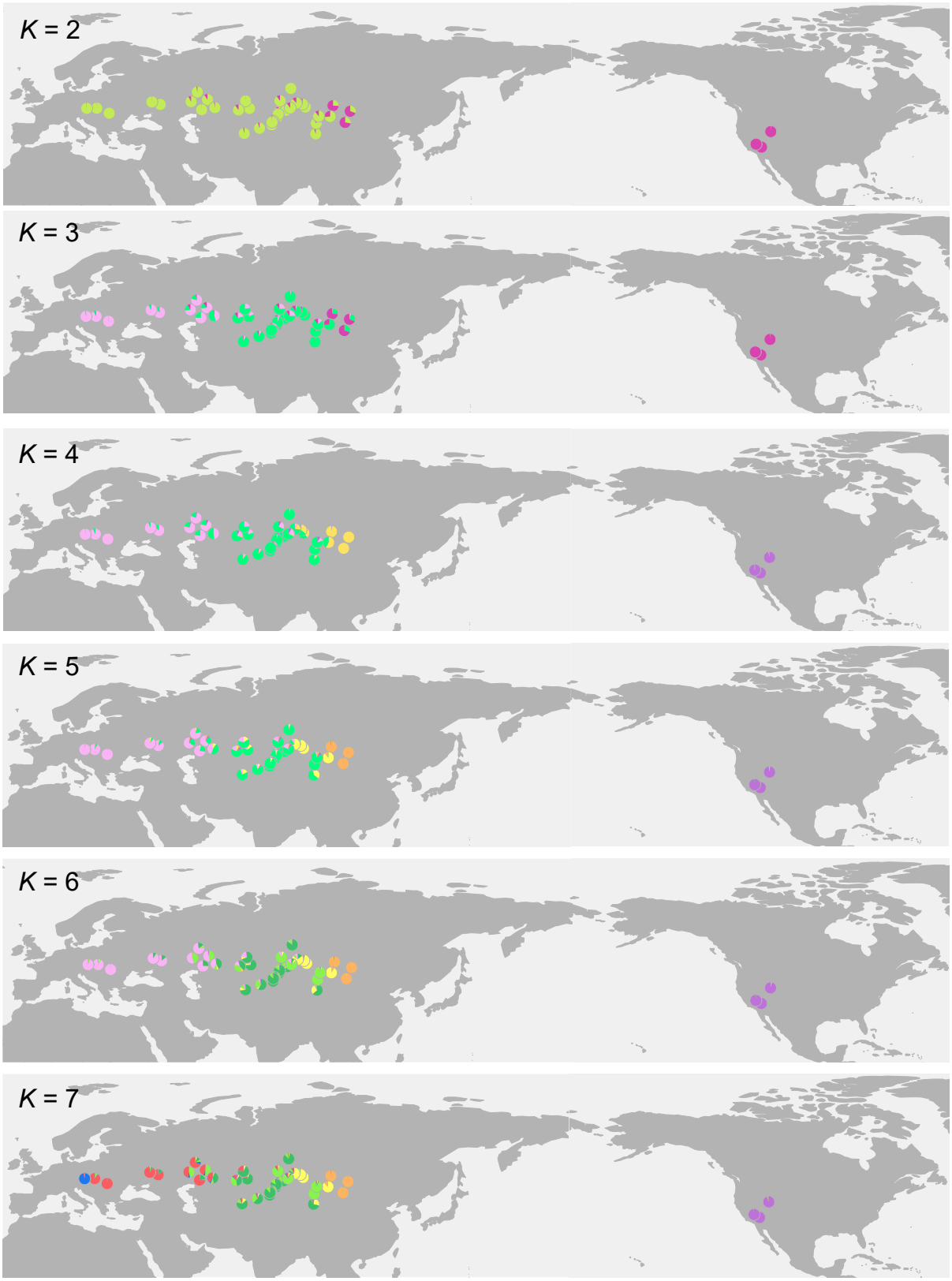

Genetic clustering of samples as revealed using LEA is shown as pie charts for *K* = 2 to *K* = 7 clusters. The first split occurred in Central Asia, dividing the populations west and east of the Khangai Mountains (*K* = 2), followed by a split in the area of the Ural Mountains (*K* = 3). At *K* = 4, the American populations separate; at *K* = 5, the populations of the Altai Mountains form their own cluster. At *K* = 6, the diploids and tetraploids of Middle Asia and adjacent areas each form their own group. The seventh cluster comprises a single population from Austria.

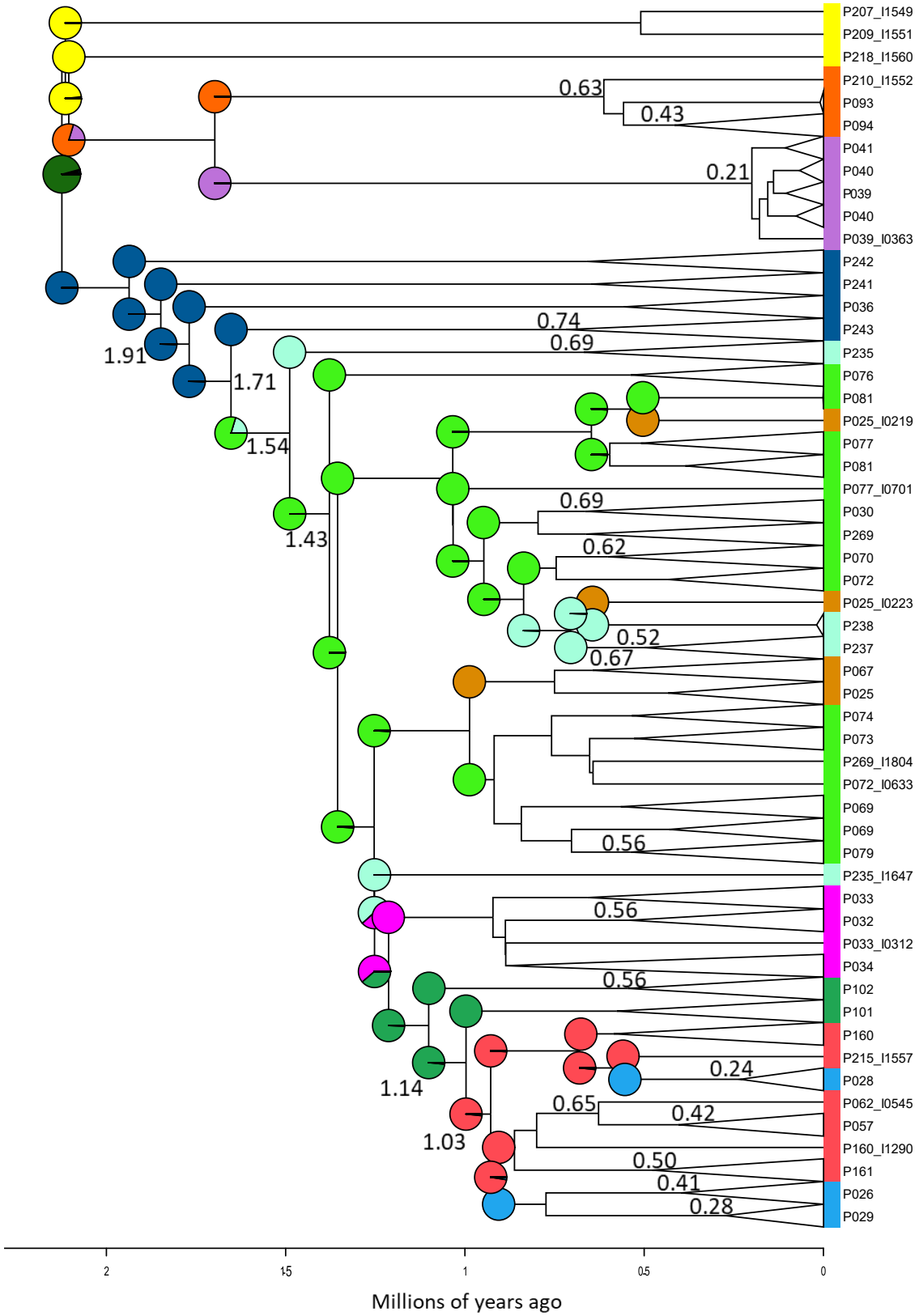

Phylogeographic analysis using the DIVALIKE model of the R package BioGeoBEARS. Colours indicate the origin of the samples (compare Appendix B: SVDQ). Branches were collapsed when several members of the same populations clustered together. Krascheninnikovia spread from the Altai Mountains to the east, reaching Eastern Central Asia and North America, and to the west, reaching Middle Asia and Europe.